THE ROLE OF GLYOXALASE I IN HYPERGLYCEMIA-INDUCED SENSORY NEURON DAMAGE AND DEVELOPMENT OF DIABETIC SENSORY NEUROPATHY SYMPTOMS

BY

Megan Marie Jack

Submitted to the graduate degree program in Anatomy and Cell Biology and the Graduate Faculty of the University of Kansas in partial fulfillment of the requirements for the degree of Doctor of Philosophy.

_____
Chairperson Douglas E. Wright, Ph.D.

_____
Dale R. Abrahamson, Ph.D.

_____
Lisa A. Stehno-Bittel, P.T., Ph.D.

_____
Russell Swerdlow, M.D.

_____
Mark A. Clements, M.D., Ph.D.

Date Defended: July 19, 2011

The Dissertation Committee for Megan Marie Jack certifies that this is the approved version of the following dissertation:

THE ROLE OF GLYOXALASE I IN HYPERGLYCEMIA-INDUCED SENSORY NEURON DAMAGE AND DEVELOPMENT OF DIABETIC SENSORY NEUROPATHY SYMPTOMS

Committee:

_____

Chairperson Douglas E. Wright, Ph.D.

Date Approved:_____

Abstract

Diabetic neuropathy is the most common and debilitating complication of diabetes mellitus with over half of all patients developing altered sensation as a result of damage to peripheral sensory neurons. Hyperglycemia results in altered nerve conduction velocities, loss of epidermal innervation, and the development of painful or painless signs and symptoms in the feet and hands. Current research has been unable to determine if a patient will develop insensate or painful neuropathy or be protected from peripheral nerve damage all together. One of the mechanisms that has been recognized to have a role in the pathogenesis of sensory neuron damage is the process of reactive dicarbonyls forming advanced glycation endproducts (AGEs) as a direct result of hyperglycemia. The glyoxalase system, composed of the enzymes glyoxalase I (GLO1) and glyoxalase II, is the main detoxification pathway involved in breaking down toxic reactive dicarbonyls before producing carbonyl stress and forming AGEs on proteins, lipids, or nucleic acids. The purpose of this study was to explore a role for GLO1 in the development, progression, and/or prevention of diabetic neuropathy in animal models of diabetic neuropathy. Initial studies characterized the pattern of expression of GLO1 in the peripheral nervous system and recognized restricted but variable expression in peptidergic C-fibers responsible for nociception. Diabetic mouse model of painful and insensate neuropathy showed reduced expression of GLO1 correlated with increased mechanical and thermal thresholds, while the strain with elevated GLO1 developed mechanical allodynia. These results suggest an imbalance of fiber types, as a direct result of hyperglycemia damage, may influence the development of signs and symptoms of

neuropathy. A study of two inbred substrains that vary in GLO1 abundance showed reduced GLO1 correlated with development of mechanical insensitivity, reduced epidermal innervation, and reduced expression of mitochondrial oxidative phosphorylation proteins. Elevated GLO1 protected from these alterations. Finally, methylglyoxal treatment of cultured adult sensory neurons resulted in reduced expression of electron transport chain proteins in certain strains. Together, these studies suggest a protective role for GLO1 in preventing reactive dicarbonyl-mediated alterations of mitochondrial oxidative phosphorylation complexes and the development of insensate neuropathy.

Dedication

To my husband, Anthony, for his willingness to take this long academic journey with me. His unwavering support and encouragement during the good times and the not-so-good times have always given me the perseverance to achieve my goals.

I could not have come this far without you.

and

To my parents Albert and Gail Dunn, for providing me with every opportunity to chase my dreams and ambitions. Your love and laughs have always kept me going.

and

To Dr. Joseph Bast for always going above and beyond for those around him. He will never know how much of an impact he has had on my career. Without him, this would not be possible.

Acknowledgments

I am eternally grateful to the many people who have been a part of my graduate career and directly or indirectly contributed to this dissertation.

I would first like to thank my research mentor, Dr. Douglas Wright, Ph.D., for his continual investment in my graduate studies. He has afforded me great freedom, much more than I ever expected as a graduate student, to design and conduct research. With his guidance and encouragement, I have learned to be an independent investigator. He has taught me to look at data with the "glass-half-full" perspective, challenge conventional views, and navigate hurdles in an academic medical setting, skills that I will carry with me throughout my own research career. Simply thank you.

A very special thanks goes out to the members of the Wright Lab for all their support, advice, and laughs throughout the years.

Janelle is truly the glue that keeps us together, especially since the lab has grown substantially over the last three years. She has been paramount at teaching me techniques, coming up with ingenious ways to get around technical problems, and always knowing the answer to the all too often question, "Hey Janelle, where can I find [insert a random piece of lab equipment]". Thank you for all of your help.

Thanks to the wonderful graduate students in the lab that have made each and every day interesting. You have each contributed so much to me both professionally and personally. Brianne, I've greatly enjoyed your company during our working weekends,

all of our laughs in Toronto, and memories at the Indianapolis German Restaurant. Caleb, I cannot thank you enough for all of your help diving into the world of culturing. Natalie, though our time in the lab only briefly overlapped, I have thoroughly enjoyed getting to know you and remember, always, always set a timer. And finally, Anna. Thank you for always being an amazing friend, "getting" my sense of humor, and helping maintain my sanity.

I would also be remiss if I did not acknowledge former members of the Wright Lab Megan Johnson, Ph.D. and Karra Muller, Ph.D. for all of their help during my rotation and their advice both during their graduate studies and after.

Thank you to all of my dissertation committee, Dr. Dale Abrahamson, Dr. Lisa Stehno-Bittel, Dr. Russell Swerdlow, and Dr. Mark Clements, for always bringing unique perspectives to my project, stimulating discussions regarding my results, and all of your support during this process. I have greatly valued each of your inputs.

I also cannot express enough gratitude to Dr. Michael Costigan, Dr. Jeffrey Mogil, and Dr. Abraham Palmer who have provided ideas, comments, and direction that have helped develop and shape this dissertation.

I cannot thank Shane Stecklein enough for his friendship, support, and advice over the past five years. You have made both medical and graduate school an enjoyable adventure. I am glad we have been able to share so many experiences that still make me

laugh hysterically when thinking about them. You truly are a brilliant scientist and I thank you for all the expertise you have shared with me.

I also owe many thanks to my friends and colleagues that I have had the pleasure of working with. Thank you for the advice and cheers along the way: Eva Selfridge, Dr. Hope Karnes-Nicely, Dr. Elizabeth Taglauer, Dr. Jill Morris, Will Messamore, Bliss Hartnett, Dr. George Thomas, Dr. Shannon Grabosch, and R. Scooter Plowman.

I have also learned so much from my interactions with the many and talented graduate students in the Anatomy and Cell Biology department particularly Chris Tanzie, Autumn Ruiz, Kim Schmidt, Ana Aleksandrova, Raul Diaz, and Ashleigh Fritz.

Other members of the Anatomy and Cell Biology Department that must be recognized for their administrative assistance that has been imperative during my graduate studies are Dr. Brenda Rongish, Helen Allensworth, Katie Bishop, and Kelly-Ann Buszek. Thank you for all that you do.

I owe many thanks to the members of the Kansas Intellectual and Developmental Disabilities Research Center (KIDDRC) particularly Beth Van Luchene, Tina Darrow, Doug Brownyard, Michelle Winter, Clark Bloomer, and Phil Shafer their help and expertise.

This dissertation would not be complete without the technical assistance and use of equipment from Dr. Hiroshi Nishimune, Dr. Tim Fields, Dr. Catherine Swenson-Fields,

Dr. John Stanford, Dr. Michael Werle, Dr. Ken McCarson, Lindsay Blick, Connie Windsor, and The Jenson Laboratory.

I also cannot thank the M.D./Ph.D. Program and Executive Committee enough for their support over the past 5 years. I extend my gratitude to Dr. Joseph Bast, Dr. Tim Fields, and Janice Fletcher for continuing to help me along the way.

I also must acknowledge those that have had an impact on my early career including both Josh Danke and Dr. Michael Henry who took me under their wings and with their tremendous mentoring and teaching abilities showed me how much I love science. Their efforts provided me with the skills to successfully hit the ground running in graduate school.

I cannot express enough gratitude to my family – Mom, Dad, and Allison. Thank you for all your love and support and especially for understanding when the phone calls home became sparse at times. While not always understanding what I do on a day-to-day basis, you are always the biggest cheerleaders in my corner. Thank you for always being there for me.

My deepest gratitude goes to my husband, Anthony. You have always made me believe I can do anything I put my mind to and never let me settle for anything less. Your patience, support, and insistence we talk about something non-science related have kept me grounded and are always appreciated. I love you.

Table of Contents

List of Figures

Chapter 1

Chapter 2

Chapter 3

Chapter 4

Chapter 5

CHAPTER 1

Introduction

Diabetes Mellitus

Diabetes mellitus is a chronic, multi-system metabolic disorder caused by a combination of environmental and genetic factors and characterized by hyperglycemia. Elevated blood glucose occurs due to either loss of insulin production by the pancreas or loss of peripheral utilization of insulin. Though disordered glucose metabolism and altered insulin functionality are hallmarks of both types of diabetes mellitus, differences do underlie the development and clinical presentation each type. Type I diabetes mellitus is an autoimmune disease that destroys insulin-producing pancreatic beta cells and typically manifests in either early childhood or young adulthood (van Belle, Coppieters et al. 2011). On the other hand, Type II diabetes mellitus results from peripheral insulin resistance and relative insulin deficiency that typically manifests during middle or old age (Casey 2011). Type II diabetes is often associated with obesity, reduced physical activity, and an unhealthy diet.

The World Health Organization estimates that 220 million people worldwide currently have diabetes. Type II diabetes mellitus is the most prevalent form and accounts for 90-95% of these cases. According to the Center for Disease Control and Prevention, 25.8 million children and adults currently suffer from diabetes mellitus in the United States. Importantly, 35% of the adult population is estimated to have prediabetes or metabolic syndrome, a condition with higher than normal blood glucose and impaired insulin sensitivity that has yet to reach diagnostic criteria for diabetes mellitus (Centers for Disease Control and Prevention 2011). Individuals with prediabetes are at a higher

potential for developing type II diabetes mellitus. Hence, a staggering 79 million adults are at risk for developing type II diabetes mellitus. Though type I diabetes mellitus accounts for a far smaller percentage, 5-10% of cases, the incidence has been steadily rising in the past decades to nearly 5% annually in the United States (van Belle, Coppieters et al. 2011). Hence, both type I and type II diabetes mellitus remain growing problems.

Diabetic Neuropathy

Classification and Prevalence

Despite the differences in etiology, clinical presentation, and disease prevalence, secondary complications, such as heart disease, stroke, retinopathy, nephropathy, and neuropathy, occur in both type I and II diabetes mellitus. Due to the continual rise in diabetes mellitus, secondary complications continue to be a large economic burden in the United States and across the world (Said 2007). Of these, diabetic neuropathy is the most common complication of long-term diabetes mellitus (Vinik, Park et al. 2000; Said 2007; Edwards, Vincent et al. 2008). The Center for Disease Control and Prevention estimates 60-70% of diabetic patients will develop diabetic neuropathy symptoms with the prevalence increasing with the duration of diabetes mellitus (Figure 1) (Centers for Disease Control and Prevention 2011). Patients with diabetic neuropathy are at an increased risk for developing ulcers, recurrent foot infections, and Charcot joints, bony destruction and deformation due to repetitive, traumatic injury, often associated with reduced sensation in the feet (Vinik, Park et al. 2000; Little, Edwards et al. 2007).

Figure 1: The prevalence of diabetic peripheral neuropathy as a consequence of both Type I and Type II diabetes mellitus suggests at least half of all diabetic patients will develop sensory signs and symptoms. The development of diabetic neuropathy is thought to be a direct consequence of hyperglycemia. Consequently, the incidence of diabetic neuropathy also increases with the duration of diabetes. Adapted from Edwards J.L., et al., 2008, *Pharmacol Ther* 120(1):1-34.

Figure 1

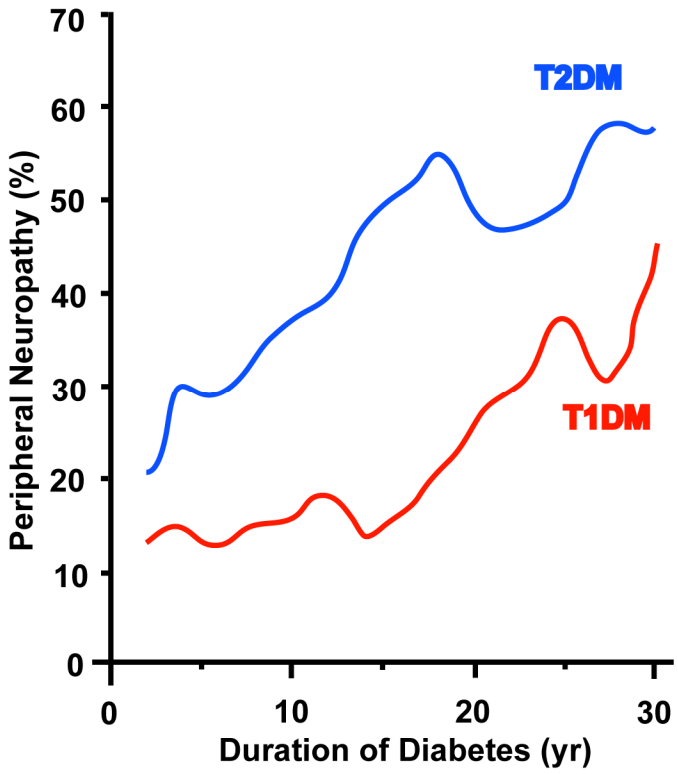
70
60
50
40
30
20
10
0
Peripheral Neuropathy (%)
T2DM
T1DM
0
10
20
30
Duration of Diabetes (yr)

Consequently, diabetic neuropathy is the cause of 50-75% of non-traumatic amputations (Vinik, Park et al. 2000). Diabetic neuropathy has a profound impact on patients' quality of life and is responsible for majority of diabetes-associated morbidity and mortality.

Diabetic neuropathy is a collection of syndromes, either focal or diffuse in nature, affecting sensory, motor, and/or autonomic peripheral neurons (Vinik, Park et al. 2000; Edwards, Vincent et al. 2008). These disorders can range from clinical to subclinical and differ in their anatomical distribution, clinical course, and spectrum of symptoms. The most prevalent of the syndromes is distal symmetrical sensorimotor polyneuropathy, often referred to as diabetic peripheral neuropathy, that results from damage to peripheral sensory nerves and accounts for nearly 80% of diabetic neuropathy cases (Said 2007). Diabetes-induced nerve damage causes a dying-back of distal axons that begins in the feet and progresses proximally in a stocking-and-glove distribution (DCCT 1993; Zochodne, Ramji et al. 2008). Diabetic peripheral neuropathy has an insidious onset and is chronic and progressive in nature; therefore, often results in severe, irreversible symptoms after longstanding diabetes mellitus.

Clinical and Pathological Features

The hallmark of diabetic neuropathy is the symmetrical loss of distal skin innervation due to dying-back of small cutaneous nerve fibers. Sural nerve biopsies from diabetic patients also demonstrate loss of unmyelinated C-fibers and small myelinated Aδ fibers in early stages of diabetic neuropathy with progressive involvement of large myelinated Aβ fibers with duration of disease (Said, Slama et al. 1983; Yagihashi,

Yamagishi et al. 2007). Despite histological and ultrastructural findings of axonal regeneration, collateral sprouting, and remyelination within peripheral nerves (Malik, Tesfaye et al. 2005), impaired nerve regeneration has been documented (Kennedy and Zochodne 2000; Kennedy and Zochodne 2005). However, regeneration is ultimately unable to compensate for the continued vicious cycle of damage and neurodegeneration of sensory neurons (Vincent, Russell et al. 2004; Kennedy and Zochodne 2005).

While neurons are clear targets of diabetes-induced damage, other cell types present in the nerve do not escape the insult. Distal axonopathy and neuronal loss are accompanied by segmental demyelination, the loss of myelinating Schwann cells over segments of the axon (Sima, Nathaniel et al. 1988). Other prominent features of diabetic nerves are abnormalities and degeneration of the nodal and paranodal apparatus. Marked paranodal swelling precedes demyelination which alters the nodes of Ranvier and normal saltatory conduction (Sima, Nathaniel et al. 1988). Endoneurial capillaries are also susceptible to the damaging effects of diabetes. As a result, it has been suggested that neuronal ischemia may be a contributing factor to diabetic polyneuropathy. Biopsies from diabetic patients show thickening of the endothelial basement membrane, endothelial cell hyperplasia, and narrowing of the capillary lumen (Malik, Tesfaye et al. 2005).

Diabetes-induced damage results in peripheral nerve pathology that correlates with clinical signs and symptoms. Nerve injury that results in structural changes can be measured through clinical neurological assessment, quantitative sensory testing, nerve

conduction studies, and peripheral nerve biopsies that are often used in combination to diagnose diabetic neuropathy. Diabetic patients are routinely screened with a battery of clinical tests, including responses to a pinprick, tuning fork vibration, and 10 g monofilament and evaluation of ankle reflexes, each of which access various sensory modalities (Pambianco, Costacou et al. 2011). The gold standard for diagnosing diabetic polyneuropathy is electrophysiological studies that include sensory (SNCV) and motor nerve conduction velocity (MNCV) as well as compound sensory nerve action potentials (SNAPs) and motor action potentials (CMAPs) (Arezzo and Zotova 2002; England, Gronseth et al. 2005). Structural alterations typically result in mild to moderate slowing of motor and sensory nerve conduction velocities as well as reduced amplitudes of evoked potentials indicative of both Schwannopathy and myelinated fiber axonopathy (Zochodne 1999; Kles and Bril 2006). More in-depth, quantitative sensory testing that measures vibration, thermal, and pain perception thresholds can also be used to detect and monitor the progression of diabetic neuropathy, particularly small fiber dysfunction (Gibbons and Freeman 2004).

The clinical features of diabetic neuropathy can be divided based on the type of fibers that are damaged and lost. Impairment of small, myelinated Aδ fibers and unmyelinated C-fibers results in altered mechanical, thermal, and pain sensation. Deficits in vibration, proprioception, and balance are often a consequence of large, myelinated Aβ fiber damage. Sensory symptoms usually predominate in diabetic peripheral neuropathy (Sinnreich, Taylor et al. 2005), although with progression of the disease, motor dysfunction may also be present (Zochodne 1999).

The majority of patients experience insensate neuropathy characterized by painless symptoms including reduced vibratory perception, numbness, and insensitivity to touch and pain. However, others have painful diabetic neuropathy that manifests as positive symptoms of hyperalgesia, tactile allodynia, paresthesias, abnormal sensitivity to temperature, and unremitting pain (Sugimoto, Murakawa et al. 2000; Obrosova 2009). Data on the prevalence of painful diabetic has varied widely with some reporting a prevalence rate of 7-20% (Tesfaye and Kempler 2005) and others reporting 40-50% of those with diabetic neuropathy having neuropathic complications. The European Diabetes (EURODIAB) prospective study found approximately 25% of type I diabetic patients developed painful symptoms throughout the course of the 7-year investigation (Tesfaye and Kempler 2005).

Although there is a considerable understanding of the molecular and pathological process responsible for damage to the peripheral nervous system that will be discussed in detail below, the mechanisms that produce painful versus insensate signs and symptoms are not known. Furthermore, neurophysiological and histological findings do not distinguish between patients suffering with positive and negative symptoms (Malik, Veves et al. 2001). The mechanisms underlying the development of these dichotomous symptoms remain a significant question that must be addressed to enable the development of improved and targeted therapies for diabetic neuropathy.

Pathogenesis

Though the precise reason the peripheral nervous system is targeted in diabetes mellitus remains unclear, sensory neurons appear particularly susceptible to prolonged hyperglycemia potentially due to a number of inherent anatomical, physiological, and structural characteristics. First, the peripheral nervous system exists outside the relatively protective blood-nerve and blood-brain barrier rendering them more vulnerable to the metabolic insults of diabetes mellitus (McHugh and McHugh 2004). Due to their high energy requirements, neurons do not rely on insulin stimulation for glucose uptake (Tomlinson and Gardiner 2008); hence, glucose concentrations in sensory neurons mirror plasma concentrations (McHugh and McHugh 2004). Consequently, dorsal root ganglion (DRG) neurons are continually exposed to damaging levels of glucose, particularly in uncontrolled diabetes mellitus (Tomlinson and Gardiner 2008). Furthermore, the unique structure of peripheral neurons, particularly in the feet and hands, may render these cells more vulnerable to metabolic alterations and diabetes-induced structural damage. Majority of the cellular mass exists in the axon that can stretch several meters from the soma. Peripheral neurons are heavily reliant on transport of cellular components for maintenance and normal functioning of peripheral processes. Consequently, damage to the neuronal cell body and/or axons hinders cellular transport and compromises support and maintenance of peripheral innervation (Zochodne, Ramji et al. 2008).

Though the pathogenesis of diabetic neuropathy is likely multifactorial, all the mechanisms that have been implicated in nerve damage are a direct or indirect

consequence of prolonged hyperglycemia (Figure 2). In fact, the only effective treatment at reducing the risk and/or delaying progression of diabetic neuropathy is maintenance of near-normal blood glucose levels (DCCT 1993). Consequently, animal and *in vitro* experiments have focused on identifying metabolic pathways involved in the development of diabetic neuropathy in the peripheral nervous system. It is also important to highlight dysfunction of these biochemical pathways also occurs in endothelial cells and Schwann cells that can cause nerve ischemia and altered nerve function, which have been implicated in the disease process.

As glucose levels rise within sensory neurons due to hyperglycemia, normal metabolic pathways become overwhelmed and excess glucose is shunted into other ancillary pathways that under these conditions become damaging. Excess glucose is initially converted to sorbitol by the enzyme aldose reductase. Increased sorbitol is thought to promote osmotic stress within the neuron itself and also by depleting other intracellular osmolytes that have secondary roles as cell signaling molecules (Tomlinson and Gardiner 2008). On the other hand others think sorbitol does not pose an osmotic challenge to the neuron because levels are far lower than other glucose metabolites (Sheetz and King 2002; Duby, Campbell et al. 2004). While some debate exists about the role of sorbitol as an osmolyte, increased flux through the polyol pathway does deplete NADPH, a reducing agent necessary for the production of glutathione, which results in reduced antioxidant defenses and increased oxidative stress (Vincent, Russell et al. 2004).

Figure 2: A schematic outlining the proposed pathogenic mechanisms that have been implicated in the development of diabetic neuropathy. Hyperglycemia produces glucose toxicity by shunting glucose and its metabolites into other metabolic pathways. These include increased polyol pathway flux, elevated protein kinase C activation, increased hexosamine pathway signaling, heightened protein glycation, and oxidative stress. These metabolic derangements can impact all of the components of the peripheral nerve including sensory and motor neurons, endothelial cells in the vasculature, and Schwann cells. . Adapted from Edwards J.L., et al., 2008, *Pharmacol Ther* 120(1):1-34 and Brownlee, M., 2005, *Diabetes* 54(6): 1615-25.

Figure 2

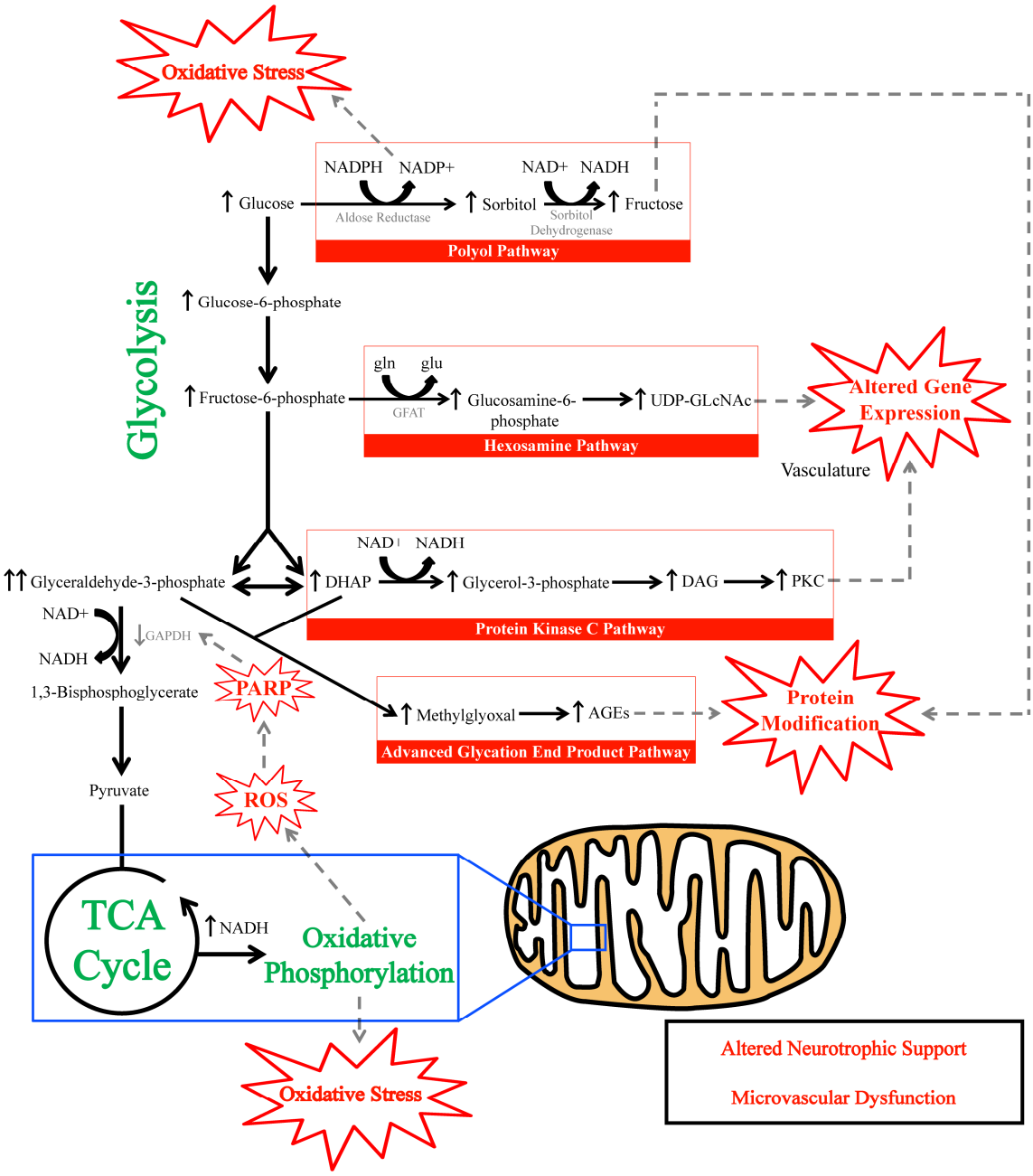
Oxidative Stress
NADPH
NADP+
NAD+
NADH
Glucose
Aldose Reductase
Sorbitol
Sorbitol Dehydrogenase
Fructose
Polyol Pathway
Glycolysis
Glucose-6-phosphate
Fructose-6-phosphate
gln
glu
GFAT
Glucosamine-6-phosphate
UDP-GLcNAc
Hexosamine Pathway
Altered Gene Expression
Vasculature
Glyceraldehyde-3-phosphate
DHAP
Glycerol-3-phosphate
DAG
PKC
Protein Kinase C Pathway
NAD+
NADH
GAPDH
1,3-Bisphosphoglycerate
PARP
Methylglyoxal
AGEs
Advanced Glycation End Product Pathway
Protein Modification
Pyruvate
ROS
TCA Cycle
NADH
Oxidative Phosphorylation
Oxidative Stress
Altered Neurotrophic Support
Microvascular Dysfunction

Two other pathways that have been implicated in the development of diabetic neuropathy are the hexosamine and protein kinase C (PKC) pathways (Figure 2). Their pathological role has been primarily investigated in endothelial cells and microvascular complications (Das Evcimen and King 2007). It is important to note that reduced endoneurial blood flow has also been implicated in the development of diabetic complications highlighting that dysfunction also occurs in the vasculature (Das Evcimen and King 2007; Geraldes and King 2010). Both of these pathways result in altered gene expression that promotes contractility, reduced flow, and inflammation resulting in nerve ischemia (Das Evcimen and King 2007; Edwards, Vincent et al. 2008; Madonna and De Caterina 2011).

Due to a combination of increased glycolysis and reduced activity of glyceraldehyde 3-phosphate dehydrogenase (GAPDH), both glyceradehyde 3-phosphate and dihydroxyacetone phosphate (DHAP) build up in the neuron. Under normal conditions, low levels of these metabolites are converted to methylglyoxal. However, under hyperglycemic conditions, concentrations of methylglyoxal increase within the neuron due to the nonezymatic breakdown of these two glycolytic intermediates (Phillips and Thornalley 1993; Thornalley 1996). Elevated levels of methylglyoxal as well as other sugars, such as fructose, lead to the formation of advanced glycation endproducts (AGEs). AGEs modify cellular components, signal through the receptor for advanced glycation endproducts (RAGE), and compromise normal neuronal function. This pathway and its role in the pathogenesis of diabetic neuropathy will be covered in more detail.

Oxidative stress has become an emerging theme that has been suggested to incorporate dysfunction in the seemingly discrete metabolic pathways discussed above and unify them into a common pathogenic mechanism (Brownlee 2001; Vincent, Russell et al. 2004; Brownlee 2005). Increased glycolysis ultimately results in excess products from the citric acid cycle, NADH and $FADH_2$. This increase in energy-substrate overloads and slows the electron transfer chain which allows for escape of electrons and the production of reactive oxygen species (ROS) (Vincent, Russell et al. 2004). Oxidative damage and reduced antioxidant capacity critically impair sensory neurons' function and is purported to contribute to signs and symptoms of diabetic neuropathy (Zochodne 1999; Duby, Campbell et al. 2004; Vincent, Russell et al. 2004).

Rodent Models of Type I Diabetic Neuropathy

Rodents have become the principal animal models to study neuropathic changes, investigate mechanisms that underlie diabetic neuropathy, and test preclinical disease-modifying therapies. Both genetic and drug-induced models exist which mimic a type I etiology (Calcutt 2004). Streptozocin (STZ) is a naturally occurring carcinogen with selective pancreatic beta cell toxicity produced by *Streptomycetes achromogenes* that is commonly used to induce experimental diabetes mellitus (Szkudelski 2001). STZ is transported by GLUT2 receptors into beta cells where its potent alkylating properties result in toxic DNA damage (Szkudelski 2001). Shortly after injection, pancreatic insulin production is severely reduced to critical levels without affecting glucagon secretion and rodents develop elevated plasma glucose levels (Portha, Blondel et al. 1989). STZ is a

conventional method for inducing diabetes mellitus in experimental animals to study secondary complications (Rossini, Like et al. 1977; Szkudelski 2001).

Existing rodent models of diabetic neuropathy vary in their presentation of symptoms and potentially offer insight into alternative pathogenic mechanisms or genetic differences that underlie symptom variability. Behavioral responses to noxious and non-noxious stimuli are used to assess the development of diabetic neuropathy in rodents. Increased responses to thermal, mechanical, or chemical stimuli are interpreted as either hyperalgesia or allodynia, while decreased responses are indicative of hypoalgesia or insensitivity.

Several strains of rats with STZ-induced diabetes develop hyperalgesia to mechanical, thermal, and chemical stimuli and tactile and thermal allodynia (Courteix, Eschalier et al. 1993). However, rat models fail to develop fiber loss and neuronal degeneration seen in human disease despite prolonged hyperglycemia (Sima and Sugimoto 1999; Zochodne 2007). As well, rats only exhibit the painful aspect of diabetic neuropathy while majority of human patients experience sensory loss.

The STZ-induced diabetes mouse model may better represent human diabetic neuropathy because this rodent model shows mild structural changes including myelin thinning, electrophysiological changes, and loss of distal innervation that may be similar to early pathology seen in human diabetic patients (Calcutt 2004; Zochodne 2007). Also, depending on the strain, either painful or insensate neuropathy can develop in diabetic mice. For instance, diabetic C57BL/6 mice develop progressive mechanical hypoalgesia

with reduced intraepidermal nerve density (Christianson, Ryals et al. 2007; Johnson, Ryals et al. 2008). Conversely, diabetic A/J mice develop mechanical allodynia. Ideally, different strains of mice would be used to better understand the dichotomous symptoms experienced by human diabetic patients. This would enable us to study related models to investigate potential mechanisms that determine the development of positive versus negative symptoms.

Advanced Glycation Endproducts and Reactive Dicarbonyls

Introduction

As previously discussed, advanced glycation endproducts (AGEs) have been shown to have a role in the pathogenesis of diabetic neuropathy. AGEs are a heterogeneous group of molecules that form from the non-enzymatic addition of sugar moieties onto arginine and lysine residues of proteins, free amino groups on lipids, or guanine nucleic acids (Peppa, Stavroulakis et al. 2009). The process of non-enzymatic glycation was first described by L.C. Maillard in the early 1900's and even at that time, he speculated it may be an important process in diabetes (Ulrich and Cerami 2001). It has subsequently become apparent that non-enzymatic glycation and AGEs have a role in many disease processes such as aging, neurological disorders like Alzheimer's disease, and diabetic complications.

Formation of AGEs

The classical AGE pathway involves the rearrangement of glucose or another reducing sugar, such as fructose, galactose, mannose, or ribose, that reacts with a free amino group of a protein, which forms a Schiff base (Nass, Bartling et al. 2007) (Figure 3). The Schiff base is highly unstable and degrades into the Amadori product or fructosamine (Nass, Bartling et al. 2007). Fructosamine is relatively stable, although levels tend to fluctuate with glucose concentrations (Huijberts, Schaper et al. 2008). The most well-known example of an Amadori product is hemoglobin A1c (HbA1c), a naturally occurring modification to the N-terminal valine amino group of the β chain of hemoglobin (Ulrich and Cerami 2001). HbA1c is elevated in diabetic patients and gives an indication of glucose levels over the previous 120 days (Koenig, Peterson et al. 1976). It is often used to monitor glucose control and has value at predicting risk of complications (DCCT 1993; Kankova 2008). With further rearrangement, oxidation, and elimination, fructosamine produces an AGE. Considerable progress has been made in understanding that AGEs form from specific metabolites despite the complexity of the glycation process. While intermediate steps in the glycation pathway are reversible, AGE formation is irreversible and causes modifications that result in both protease-resistant cross-linked and noncross-linked proteins (Ramasamy, Vannucci et al. 2005; Munch, Westcott et al. 2010).

Reactive Dicarbonyls: Methylglyoxal, Glyoxal, and 3-Deoxyglucose

Besides monosaccharides, reactive dicarbonyls or α-oxoaldehydes contribute to the production of AGEs. Reactive dicarbonyls, such as 3-deoxyglucose, glyoxal, and methylglyoxal, are highly potent and reactive species that can also modify proteins, lipids, and nucleic acids and may contribute more significantly in the glycation process than the classical pathway described above. In fact, reactive dicarbonyls are 20,000-fold more reactive than glucose (Turk 2010). Consequently, reactive dicarbonyls have gained increasing acceptance as one of the main mechanisms that drive the production of AGEs, produce carbonyl stress, and underlie the development of diabetic complications (Figure 3).

The longstanding view of glycation as a relatively long process that only resulted in AGE accumulation on long-lived extracellular proteins was revolutionized with the discovery of dicarbonyl metabolites (Huijberts, Schaper et al. 2008). Methylglyoxal and other α-oxoaldehydes form inside cells over a relatively short time period as a byproduct of many metabolic pathways (Xue, Rabbani et al. 2011) (Figure 4). Methylglyoxal is formed from spontaneous decomposition of triosephosphates, DHAP and glyceraldehyde-3-phosphate, fragmentation of other sugars, and amino acid and ketone body degradation (Oya, Hattori et al. 1999; Beisswenger, Howell et al. 2003; Thornalley 2008). Glyoxal is also a consequence of degradation of saccharides, but also of lipid peroxidation and degradation of glycated proteins (Thornalley 2008).

Figure 3: A schematic illustrating the pathways that lead to the production of reactive dicarbonyls and AGEs and the mechanisms by which AGEs cause to sensory neuron dysfunction. The most well characterized pathway that produces AGEs includes undergoing rearrangement and reacting with a protein to form a Schiff base. This is a highly unstable molecule then degrades to the Amadori product leading to AGE formation. Reactive dicarbonyls, such as glyoxal and methylglyoxal, are highly reactive compounds that also produce AGEs. Each is formed as a byproduct of many metabolic pathways that are all upregulated in diabetes mellitus. AGEs produce altered sensory function via signaling through the RAGE and by modifying intra- and extra-cellular proteins. The glyoxalase system is critical at preventing the formation of AGEs by breaking down reactive dicarbonyls.

Figure 3

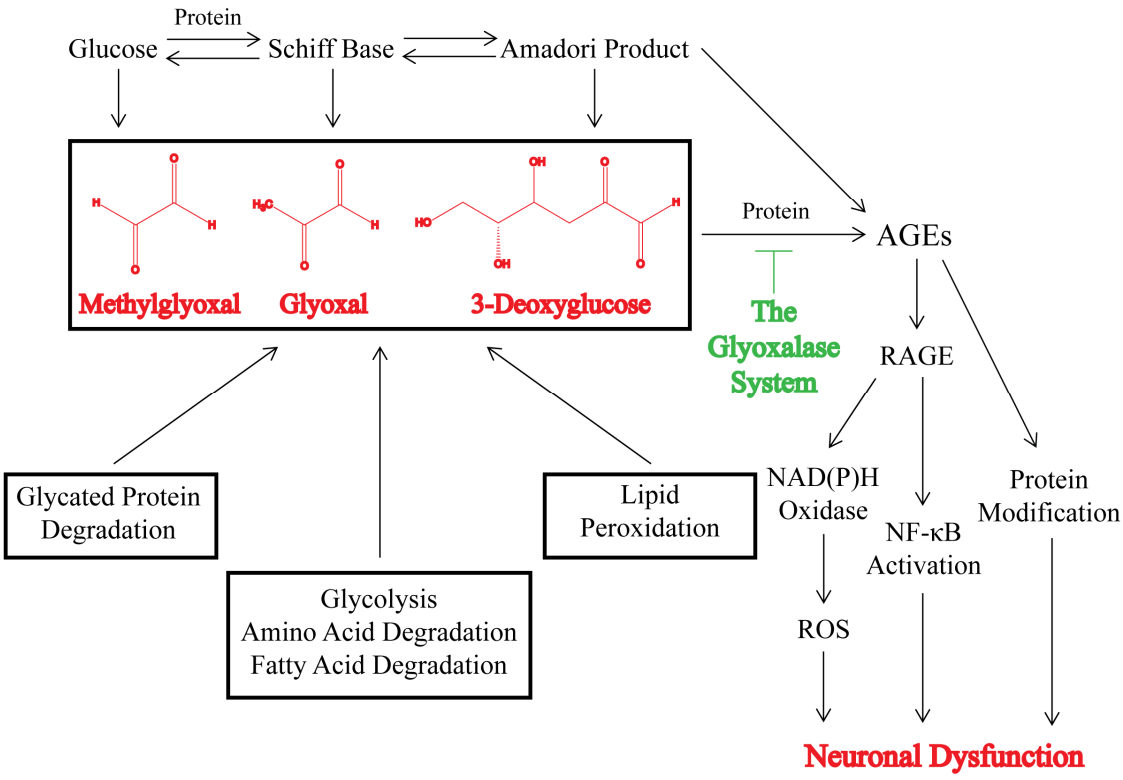
Protein
Glucose
Schiff Base
Amadori Product
Methylglyoxal
Glyoxal
3-Deoxyglucose
Protein
AGEs
The Glyoxalase System
RAGE
Glycated Protein Degradation
Lipid Peroxidation
NAD(P)H Oxidase
NF-κB Activation
Protein Modification
Glycolysis
Amino Acid Degradation
Fatty Acid Degradation
ROS
Neuronal Dysfunction

Cellular concentrations of methylglyoxal and glyoxal range from 1-5 µM and 0.1-1 µM, respectively (Fleming, Humpert et al. 2010). The biogenesis of 3-deoxyglucose results from the breakdown of fructose-3-phosphate from the polyol pathway (Turk 2010). It is important to note that all of these metabolic processes are enhanced in diabetes mellitus, which leads to a significant increase in the production of reactive dicarbonyls and AGEs.

Role in Diabetic Neuropathy

While only 0.089% of triosephosphates are converted to methylglyoxal, several studies have shown levels reactive dicarbonyls are higher in diabetic patients due to hyperglycemia (Beisswenger, Drummond et al. 2005; Mirza, Kandhro et al. 2007; Han, Randell et al. 2009). Consequently, reactive dicarbonyl-derived AGEs are elevated in plasma and accumulate in tissues prone to secondary complications including the lens, retina, kidney, and endothelial vessels of both diabetic humans and rodents (Karachalias, Babaei-Jadidi et al. 2003; Ahmed 2005; Ahmed, Babaei-Jadidi et al. 2005; Bohlender, Franke et al. 2005; Stitt 2010). Indeed, the concentration of AGEs in the sciatic nerve of diabetic rats is higher than nondiabetic rodents (Karachalias, Babaei-Jadidi et al. 2003; Thornalley 2005). Extensive accumulation of AGEs also occurs in peripheral nerves of diabetic patients particularly in the axoplasm of myelinated and unmyelinated neurons, Schwann cells, endoneurial and epineurial microvessels, perineurial basal lamina, and perineurium, suggesting AGEs have a role in the development and/or progression of neuropathies (Ryle and Donaghy 1995; Sugimoto, Nishizawa et al. 1997; Haslbeck, Schleicher et al. 2002; Misur, Zarkovic et al. 2004; Lukic, Humpert et al. 2008). A recent

study investigated skin autofluorescence as a measure of AGE deposition in nondiabetic and diabetic subjects with or without neuropathy and found a correlation between slowing of SNCV and increased autofluorescence (Meerwaldt, Links et al. 2005). Similarly, levels of serum CML or skin autofluorescence were significantly higher in type I diabetic patients with microvascular complications, like neuropathy, compared to those without complications (Hwang, Shin et al. 2005; Araszkiewicz, Naskret et al. 2011).

The pathophysiological consequences of AGE accumulation have been investigated in normal aging and in disease states such as Alzheimer's disease, renal failure, inflammation, and some diabetic complications (Ahmed and Thornalley 2007; Morcos, Du et al. 2008; Ramasamy, Yan et al. 2008; Chougale, Bhat et al. 2011). Several mechanisms are thought to mediate AGE-damage in disease. In tissues, AGE modification of structural and cellular proteins, lipids, and nucleic acids results in dysfunction of vital cellular processes with limited proteasomal degradation, increased aggregation, and enhanced half-life of glycated proteins (Nass, Bartling et al. 2007; Vincent, Perrone et al. 2007). While a number of proteins, which differ in structure and function, are known targets of the glycation process that impairs their structure and function, many more likely exist that have yet to be discovered (Mendez, Xie et al. 2010; Rabbani and Thornalley 2010). GAPDH activity was significantly reduced following methylglyoxal treatment (Lee, Howell et al. 2005), which causes a compensatory increase of the toxic metabolite (Beisswenger, Howell et al. 2003). Insulin and other key insulin-signaling molecules, such as insulin receptor substrate 1, were also susceptible to

dicarbonyl glycation, which may alter the neurotrophic support for sensory neurons (Riboulet-Chavey, Pierron et al. 2006; Schalkwijk, Brouwers et al. 2008). Methyglyoxal-modification of extracellular matrix reduced neurite outgrowth of sensory neurons, suggesting reactive dicarbonyls could impair the regenerative capacity of DRG neurons in diabetic neuropathy. Methylglyoxal has also been shown to alter the activity and expression of the 26S proteasome, as well as other chaperones involved with protein control (Schalkwijk, van Bezu et al. 2006; Bento, Marques et al. 2010; Queisser, Yao et al. 2010).

Beyond the effects of protein modification, AGEs also interact with cell surface receptors, particularly RAGE, to induce a cascade of intracellular signaling. Transient activation of PI-3K/AKT and MAPK pathways leads to nuclear translocation of NF-κB (Vincent, Perrone et al. 2007; Lukic, Humpert et al. 2008). Continual activation of NF-κB leads to altered gene expression and upregulation of RAGE creating a positive feedback loop that enhances sensory neuron damage (Toth, Martinez et al. 2007). RAGE also stimulates NAD(P)H oxidase, a potent producer of reactive oxygen species (ROS). Like glycating agents, excessive ROS alter proteins, lipids, and DNA causing cellular damage (Vincent, Perrone et al. 2007). However, as will be covered later, the source of oxidative stress in diabetic neuropathy remains contentious.

The Glyoxalase System

The glyoxalase system, which is composed of the enzymes glyoxalase I (GLO1) and glyoxalase II (GLO2), is responsible for detoxifying reactive dicarbonyls (Figure 3).

The glyoxalase system was discovered independently by Dakin, Dudley, and Neuberg in 1913. At that time, its function of catalyzing the conversion of methylglyoxal to lactate was also described (Nass, Bartling et al. 2007; Xue, Rabbani et al. 2011). Future studies revealed that reactive dicarbonyls, like methylglyoxal, react with reduced glutathione forming a hemithioacetal (Racker 1951; Mannervik 2008) (Figure 4). GLO1 converts the hemithioacetal to *S*-2-hydroxyacetylglutathione. GLO2 then catalyzes this intermediate to the corresponding α-hydroxyacid and releases reduced glutathione (Thornalley 2003).

GLO1 is considered the key enzyme in anti-glycation defense because it is the rate-limiting step in the glyoxalase pathway and prevents the accumulation of reactive dicarbonyls (Thornalley 1990; Kuhla, Boeck et al. 2006). GLO1 is highly conserved with the enzyme being described in humans, mice, yeast, plants, insects, protozoa, fungi, and many bacterial strains (Thornalley 2003). Due to its critical function, GLO1 has been reported to be ubiquitously expressed in the cytosol of all cells (Thornalley 1998; Thornalley 2003; Rabbani and Thornalley 2011; Xue, Rabbani et al. 2011)

While the role GLO1 in diabetic neuropathy has received limited attention, many studies related to other secondary complications have developed a clear understanding of the protective role of GLO1 in these tissues. *In vitro* overexpression of GLO1 in endothelial cells under hyperglycemic conditions reduced reactive dicarbonyls (Shinohara, Thornalley et al. 1998) and corrected defects in angiogenesis (Ahmed, Dobler et al. 2008) and relaxation (Brouwers, Niessen et al. 2010). Overexpression in the lens and retinal capillary pericytes protected against hyperglycemia-induced protein

Figure 4: Schematic illustrating of the glyoxalase system. The glyoxalase system is composed of two enzymes, glyoxalase I (GLO1) and glyoxalase II. Reactive dicarbonyls, like methylglyoxal, are effectively detoxified via this metabolic pathway. The glyoxalase enzyme pathway catalyzes the conversion of reactive α-oxoaldehydes into the corresponding α-hydroxyacids. In this schematic, methylglyoxal reacts with glutathione and is converted to S-D-Lactoylglutathione by GLO1. This intermediate is then broken down into D-lactate by glyoxalase II and reduced glutathione is recycled. Adapted from Thornalley P.J., 2008, *Drug Metabol Drug Interact* 23(1-2):125-50.

Figure 4

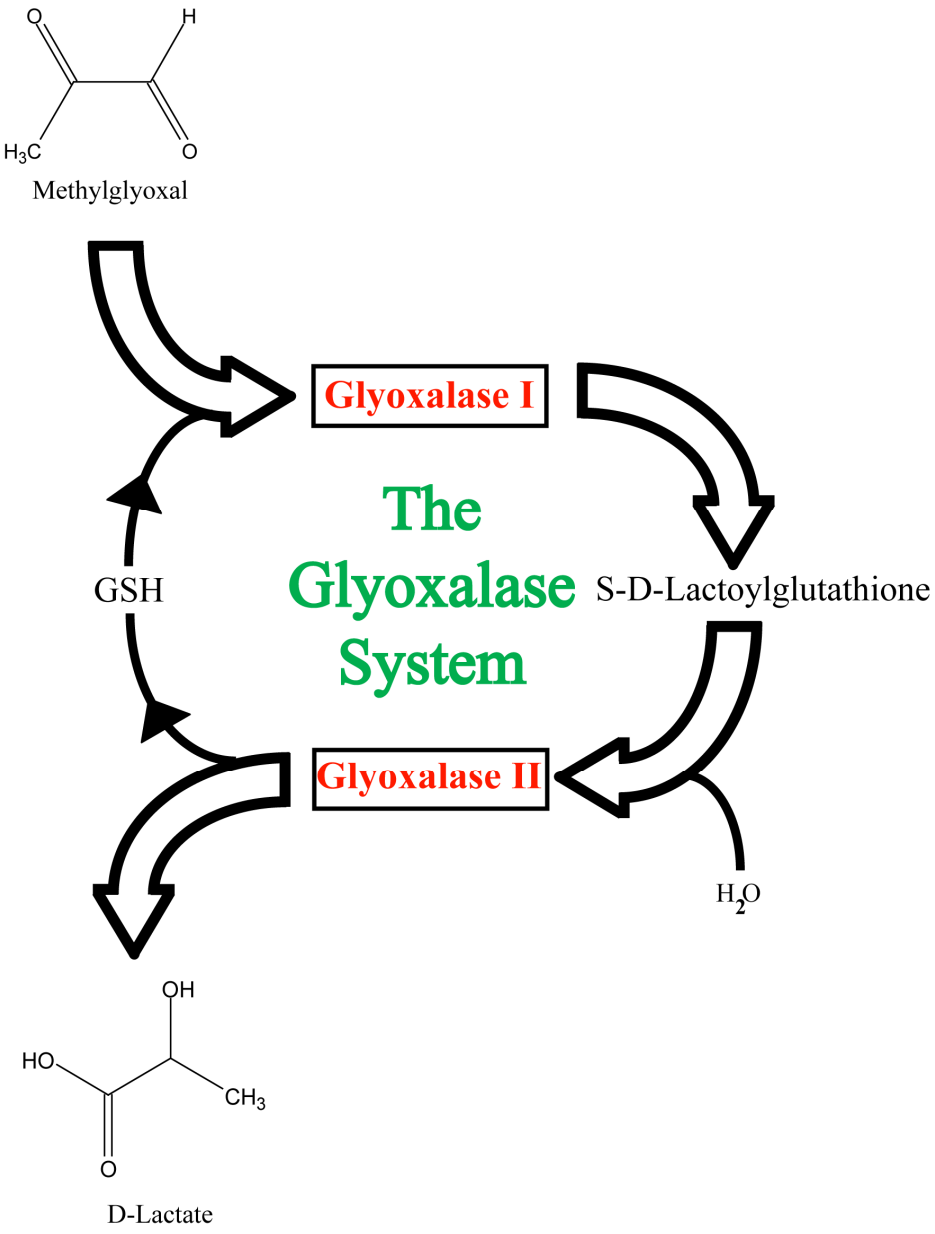
O
H
H3C
O
Methylglyoxal
Glyoxalase I
The
Glyoxalase
System
GSH
S-D-Lactoylglutathione
Glyoxalase II
H2O
OH
HO
CH3
O
D-Lactate

modification (Gangadhariah, Mailankot et al. 2010) and apoptosis (Miller, Smith et al. 2006), respectively. Similarly, markers of oxidative damage were reduced in kidneys from diabetic transgenic rats overexpressing GLO1 (Brouwers, Niessen et al. 2010).

Mitochondrial Dysfunction

Introduction

Mitochondrial dysfunction is purported to be one of the mechanisms underlying the development of diabetic neuropathy. Among a variety of functions, mitochondria are the powerhouse of the cell. Mitochondria are responsible for producing energy that cells harness for all cellular processes such as protein production, cellular transport, and cell growth and maintenance. This is particularly important for neurons given their relatively high reliance on energy production due to their increased metabolic demands (Han, Tomizawa et al. 2011). Consequently, mitochondrial damage and dysfunction have been linked to common neurological disorders (Mattson, Gleichmann et al. 2008; Lu 2009).

Mitochondria, Oxidative Phosphorylation, and ATP Production

Mitochondria function in a wide range of biochemical reactions including fatty acid oxidation, nutrient production in the citric acid cycle, oxidative phosphorylation, and ATP production. Oxidation of NADH and $FADH_2$ from glycolysis, beta oxidation, and citric acid cycle releases electrons that are passed through a coordinated series of enzyme complexes located in the mitochondrial inner membrane and are finally transferred to oxygen (Figure 5). NADH dehydrogenase or Complex I, cytochrome c reductase or

Figure 5: Schematic illustrating the molecular machinery responsible for energy production in neurons. The electron transport chain consists of five complexes that transfer electrons from complex to complex. Three complexes, Complexes I, II, and IV, create an electrochemical gradient of protons across the inner mitochondrial membrane. ATP synthase or Complex V utilizes this energy gradient to generate ATP. Adapted from Brownlee, M., 2005, *Diabetes* 54(6): 1615-25.

Figure 5

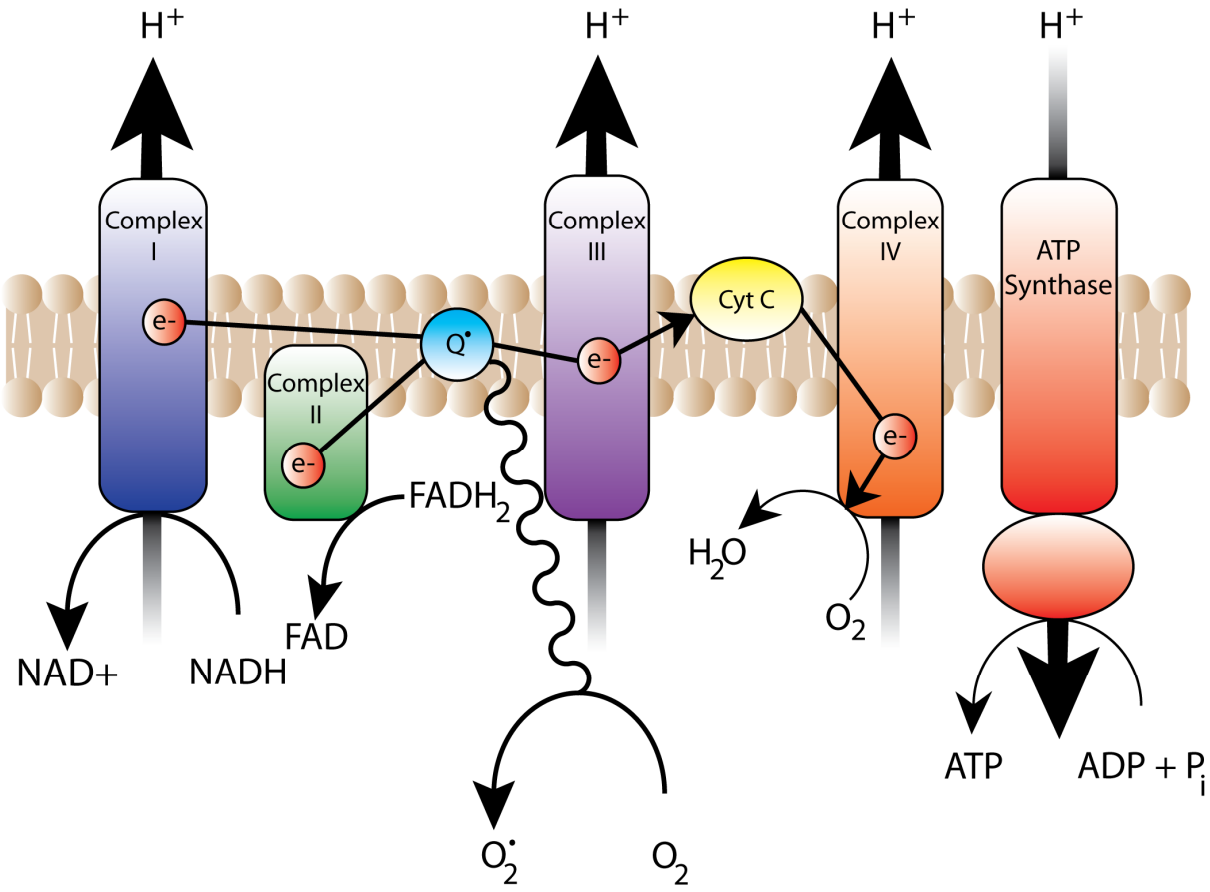
H+
H+
H+
H+
Complex I
Complex II
Complex III
Complex IV
ATP Synthase
Cyt C
e-
e-
e-
e-
Q•
FADH2
FAD
NAD+
NADH
H2O
O2
O2•
O2
ATP
ADP + Pi

Complex III, and cytochrome c oxidase or Complex IV use the redox energy released during electron transfer to pump protons from the mitochondrial matrix into the intermembrane space which creates an electrochemical gradient across the inner mitochondrial membrane (Scheffler 2001). ATP Synthase or Complex V utilizes the electrochemical gradient to produce ATP (Scheffler 2001).

Reactive Dicarbonyls and Mitochondrial Dysfunction

While mitochondrial dysfunction has been suggested to be one of the main pathogenic mechanisms in diabetic neuropathy, little is known about the nature and extent of mitochondrial damage resulting from chronic hyperglycemia. One mechanism by which elevated intracellular glucose clearly alters mitochondrial function is through glycation of mitochondrial proteins. Multiple studies have shown that reactive dicarbonyls form AGEs on mitochondrial oxidative phosphorylation proteins and produce changes in mitochondrial respiration, activity of oxidative phosphorylation proteins, and leakage of electrons from these complexes (Rosca, Mustata et al. 2005; Morcos, Du et al. 2008; Brouwers, Niessen et al. 2010). However, some dispute remains if mitochondrial dysfunction results in the production of reactive oxygen species and oxidative stress in sensory neurons. A large body of evidence supporting the idea that reactive dicarbonyl damage to mitochondria results in oxidative stress comes from studies in tissues other than the peripheral nervous system (Rosca, Monnier et al. 2002; Rosca, Mustata et al. 2005; Morcos, Du et al. 2008; Rabbani and Thornalley 2008; Schlotterer, Kukudov et al. 2009). While the axons of DRG neurons from diabetic rats

exhibited increased ROS and oxidative stress (Zherebitskaya, Akude et al. 2009), impaired respiratory function and reduced expression of certain mitochondrial oxidative phosphorylation proteins resulted in reduced production of superoxide (Chowdhury, Zherebitskaya et al. 2010; Akude, Zherebitskaya et al. 2011).

Study Significance

Diabetic neuropathy is clearly a significant burden on patients and the healthcare system, which will only be growing in the future. Peripheral sensory neurons are damaged by a variety of metabolic insults as a result of hyperglycemia. Consequently, 60-70% of diabetic patients develop diabetic peripheral neuropathy. However, 30-40% of patients remain symptom free. A genetic basis for the susceptibility or resistance to developing diabetic neuropathy complications has been suggested. Developing an understanding of the protective mechanisms that exist in these patients would allow for the development of better screening tools and more efficacious therapeutics.

Elevated reactive dicarbonyls are a consequence of diabetes-induced hyperglycemia. Reactive dicarbonyls are highly potent producers of AGEs that have been shown to have a direct role in the development of diabetic peripheral neuropathy. However, the glyoxalase system, particularly the enzyme GLO1, is an important pathway involved in reducing levels of reactive dicarbonyls by efficiently breaking them down. Consequently, GLO1 may have a role in protecting sensory neurons against hyperglycemia-induced damage. Therefore, the goal of this study was to determine the relationship between differential GLO1 expression in sensory neurons, the development

and/or progression of diabetic neuropathy, and pathological mechanisms which may result from hyperglycemia-induced sensory neuron dysfunction with reduced protective mechanisms in diabetes mellitus.

In the first study, ("Characterization of Glyoxalase I in the Nervous System"), we examined the expression and localization of GLO1throughout the peripheral nervous system. We discovered GLO1 abundance is highly variable in various inbred strains of mice. In addition, we showed GLO1 expression to be highly expressed in a subset of DRG neurons responsible for pain transmission suggesting that certain populations of sensory neurons may be more or less vulnerable reactive dicarbonyls.

In the next two studies, we measured the behavioral responses following diabetes induction of inbred strains of mice. In the first, ("Characterization of Glyoxalase I in Mouse Models of Painful and Insensate Diabetic Neuropathy") we investigated the expression of GLO1 following diabetes induction in mouse models that develop dichotomous systems of neuropathy. C57BL/6 mice with lower levels of GLO1 expression developed mechanical and thermal insensitivity, while A/J mice with higher levels of GLO1 developed mechanical allodynia. GLO1 expression may lead do an imbalance of sensory fiber types that could produce symptoms of neuropathy. In the next study, ("Elevated Glyoxalase I Expression Provides Protection From Diabetes-Induced Peripheral Neuropathy") we used two inbred substrains of BALB/c mice that have related genetic backgrounds but express very different amounts of GLO1. As in the previous study, diabetic BALB/cJ mice showed a correlation between reduced GLO1 expression

and the development of increased mechanical thresholds, reduced intraepidermal nerve fiber density, and impaired expression of mitochondrial oxidative phosphorylation proteins, a known target of reactive dicarbonyls.

Finally, in "Mitochondrial Oxidative Phosphorylation Proteins Are Reduced Following *In Vitro* Methylglyoxal Treatment of Sensory Neurons" cultured adult DRG neurons were treated with methylglyoxal *in vitro* to determine if similar reductions of oxidative phosphorylation proteins shown *in vivo* could be caused by elevated reactive dicarbonyls. We found that cultured sensory neurons had reduced expression of electron transport chain components following methylglyoxal treatment from certain strains. This study, in part, corroborated that elevated levels of reactive dicarbonyls can result in mitochondrial dysfunction.

CHAPTER 2

Characterization of glyoxalase I in the peripheral nervous system

1. Abstract

The glyoxalase system, particularly the enzyme GLO1protects cells against reactive dicarbonyl damage termed carbonyl stress. Since hyperglycemia leads to an accelerated production of α-oxoaldehydes and AGEs, the glyoxalase system has been recognized as an important pathway in diabetes mellitus and diabetic complications including retinopathy, nephropathy, and microvascular dysfunction. Previous reports have suggested that GLO1 is found in all cells primarily due to its critical function in detoxifying methylglyoxal, glyoxal, and 3-deoxyglucose; however, investigation of this pathway in the peripheral nervous system has been limited. Current studies were undertaken to characterize GLO1 expression and abundance in the peripheral nervous system. C57BL/6 mice were used to detect the pattern of distribution of GLO1 in the nervous system by immunofluorescence. GLO1immunoreactivity was found throughout the nervous system, but selectively in small, unmyelinated peptidergic DRG neurons that are involved in pain transmission. The expression of *GLO1*, assessed by quantitative real-time PCR, was highly variable in the DRG from different inbred mice strains. Two strains showing the largest differences in expression, A/J and C57BL/6 mice, also exhibited differences in *GLO1* mRNA in the sciatic nerve and brain. These results demonstrate that inbred strains of mice exhibit differential *GLO1* expression in both the central and peripheral nervous system, but are only heavily expressed in a subpopulation of DRG neurons that are responsible for nociception.

2. Introduction

The peripheral nervous system is composed of primary sensory neurons that vary in their anatomical, neurochemical, and, importantly, functional modalities that they transmit. Aβ fibers are heavily myelinated, large diameter neurons that primarily transmit information about balance and proprioception from a variety of specialized receptors that detect pressure, vibratory, and tactile stimuli. Aδ fibers are smaller in diameter and lightly myelinated, which relay information regarding discriminative touch, temperature, and pain. C-fibers are small, unmyelinated neurons that convey tactile, temperature, and noxious information. Two discrete subpopulations of C-fibers exist, peptidergic and nonpeptidergic, which have clear differences in their phenotypes and anatomical locations, suggesting the existence of parallel pain pathways (Braz, Nassar et al. 2005).

These distinct fiber types function to convey normal peripheral sensation, which can be altered in disease states. Therefore, determining differences in these cell types that may render certain populations vulnerable to damage would be beneficial. The glyoxalase system, as discussed in Chapter 1, is a critical enzyme in anti-glycation defense, which is likely punitive mechanism underlying neurodegeneration in many neurological disorders (Munch, Westcott et al. 2010). Here, we began by investigating the expression of GLO1 in the peripheral nervous system. Our results suggest that high GLO1 abundance is restricted to a subpopulation of C-fibers. Moreover, *GLO1* expression is highly variable in a group of inbred strains of mice. These findings suggest

certain DRG neurons are better able to protect against AGE-induced damage, while others are more susceptible to toxic effects of reactive dicarbonyls.

3. Experimental Procedure

Animals

Male C57BL/6 (Charles River, Sulzfeld, Germany), A/J, BALB/cJ, 129P3/J, C3H/HeJ, and DBA/2J mice (Jackson, Bar Harbor, Maine) were purchased at 7 weeks, one week prior to beginning experiments. The MrgD mouse line was generated by D. Anderson (California Institute of Technology) and maintained as a breeding colony at the University of Kansas Medical Center. Genotypes were confirmed as previously described (Johnson, Ryals et al. 2008). The animals were housed two mice per cage in 12/12-h light/dark cycle under pathogen free conditions. Mice were given free access to standard rodent chow (Harlan Teklad 8,604, 4% kcal derived from fat) and water. All animal use was in accordance with NIH guidelines and conformed to principles specified by the University of Kansas Medical Center Animal Care and Use Protocol.

Western Blot

Brain, lumbar spinal cord, sciatic nerve and DRG were rapidly isolated and excised, immediately frozen in liquid nitrogen, and stored at -80^{o}C. Tissue was homogenized for 2 min in 50 μl Cell Extraction Buffer (Invitrogen, Carlsbad, CA) with protease inhibitor cocktail (Sigma, St. Louis, MO), 200 mM NaF, and 200 mM Na_3VO_4. The homogenates were incubated on ice for 30 mins before centrifugation at 7000 rpm

for 10 mins at 4^{o}C. Protein concentrations were determined using the Bio-Rad protein assay based on the Bradford assay (Bio-Rad, Sydney, NSW, Australia). Samples containing 100 μg of protein were separated by electrophoresis through 4-20% SDS-PAGE gels (125 V, 1.5 h, 4^{o}C) and transferred onto nitrocellulose paper (35 mA, overnight, 4^{o}C). Nitrocellulose membranes were blocked with blocking buffer (3% non-fat milk and 0.05% Tween-20 in phosphate buffered saline) for 1 hour at room temperature to block non-specific binding sites. This was followed by overnight incubation with a goat anti-GLO1 primary antibody (R&D Systems, Minneapolis, MN) diluted 1:5000 in blocking buffer at 4^{o}C. The donkey anti-goat IgG-HRP secondary antibody (Santa Cruz, Santa Cruz, CA) was used diluted 1:2500 in blocking buffer at RT for 1 hour. The chemiluminescent signal was acquired using Supersignal West Femto Maximum Sensitivity Substrate (Pierce, Rockford, IL) and a CCD camera (BioSpectrum Imaging System, UVP, Upland, CA).

Immunohistochemistry

Unfixed lumbar DRG, sciatic nerve, and spinal cord were dissected, frozen, sectioned in 16-20 μm cross-sectional serial sections, and mounted on Superfrost Plus slides (Fisher Scientific, Chicago, IL) then stored at -20^{o}C. After thawing 5 min at room temperature, slide-mounted tissue was circled with a Pap Pen (Research Products International, Mt. Prospect, Illinois) to create a hydrophobic ring. Tissue sections were then covered with a blocking solution (0.5% porcine gelatin, 1.5% normal donkey serum, 0.5% Triton-X, Superblock buffer; Pierce, Rockford, IL) for 1 h at room temperature.

Primary antibodies were incubated overnight at 4^{o}C. For GLO1 immunohistochemistry, a mouse anti-glyoxalase I primary antibody (1:100; Abcam, Cambridge, MA) and a donkey anti-mouse secondary antibody (Alexa 488; 1:2000; Molecular Probes, Eugene, OR) were used to label positive cells in the L4/5/6 DRG, sciatic nerve, and spinal cord. Primary rabbit anti-neurofilament H (1:2500; Chemicon, Billerica, MA) or rabbit anti-peripherin (1:1000; Chemicon, Billerica, MA) with donkey anti-rabbit secondary antibody (Alexa 555; 1:2000; Molecular Probes, Eugene, OR) were used to label and counterstain cell populations in lumbar DRG. Sections were washed 2 x 5 min with PBST followed by incubation for 1 h with fluorochrome-conjugated secondary antibody diluted in PBST and Superblock (Pierce, Rockford, IL). Following three washes with PBS, slides were coverslipped and stored at 4^{o}C until viewing. For quantification, positive cells were counted in 3 sections from each lumbar DRG from 3 animals.

Quantitative Real-Time PCR

RNA was isolated from sciatic nerve, DRG, and brain using Trizol reagent (Ambion, Austin, TX) and RNeasy Mini Kit (Qiagen, Valencia, CA). The concentration and purity were determined using a 2100 Bioanalyzer (Agilent Technologies, Santa Clara, CA). Total RNA (0.63 μg) was synthesized directly into cDNA using the iScript cDNA Synthesis Kit (Bio-Rad, Hercules, CA). qRT-PCR was performed using iScript One-Step RT-PCR Kit with SYBR green (Bio-Rad, Hercules, CA). The primers were as follows:

GAPDH: Forward: 5'-AGGTCGGTGTGAACGGATTTG-3'

Reverse: 5'-TGTAGACCATGTAGTTGAGGTCA-3'

GLO1: Forward: 5'-GATTTGGTCACATTGGGATTGC-3'

Reverse: 5'-TTCTTTCATTTTCCCGTCATCAG

All reactions were performed in triplicate. The mRNA levels for GLO1 were normalized to GAPDH. ΔCT values and fold changes were calculated using the Pfaffl analysis method (Pfaffl, Horgan et al. 2002).

4. Results and Figures

Characterization of GLO1 Expression in the Nervous System

To characterize the GLO1-immunoreactivity was detected throughout the nervous system including both the central and peripheral nervous systems (Figure 1a). In the lumbar spinal cord of 8-week old nondiabetic C57BL/6 mice, GLO1 localized to lamina I and outer portions of lamina II of the dorsal horn (Figure 1b), interneurons (Figure 1b), ependymal cells of the central canal (Figure 1e) and ventral horn motor neurons (Figure 1f). In the peripheral nervous system, approximately 36% of L4/L5/L6 DRG neurons (*n* = 1984 out of 5501 neurons) expressed GLO1 at very high levels and these neurons were predominately small neurons with diameters ranging from 5-22 µm with an average diameter of 13 µm (Figure 1c and 1g). Consistent with these findings, ~96% of GLO1+ neurons expressed peripherin (*n* = 2115 out of 2198 neurons) (Figure 2e-h), a marker of small diameter, unmyelinated neurons with diameters ranging from 27-340 μm^2 and an average area of 148 μm^2. Accordingly, less than 7% of GLO1+ cells (*n* = 138 out of 1994 neurons) expressed heavy chain neurofilament H that labels medium and large

Figure 1: GLO1 expression in the nervous system

(a) Representative Western blot showing expression of GLO1 in the brain, lumbar spinal cord, DRG, and sciatic nerve of nondiabetic C57BL/6 mice (n = 3). Immunofluorescence staining of the lumbar spinal cord (b), lumbar DRG (c), and sciatic nerve (d) showing GLO1 expression and localization. Arrowheads indicate GLO1-positive interneurons and arrows indicate GLO1-positive terminals in the superficial lamina (b). Enhanced views of GLO1-positive ependymal cells of the central canal (e), anterior horn cells (f), neurons of the DRG (g), and axons of the sciatic nerve in longitudinal section counterstained with neurofilament H (red) (h) are shown. Arrowheads indicate a GLO1-positive axon, while arrows indicate a neurofilament H-positive axon (h). Scale bar, 50 µm.

Figure 1

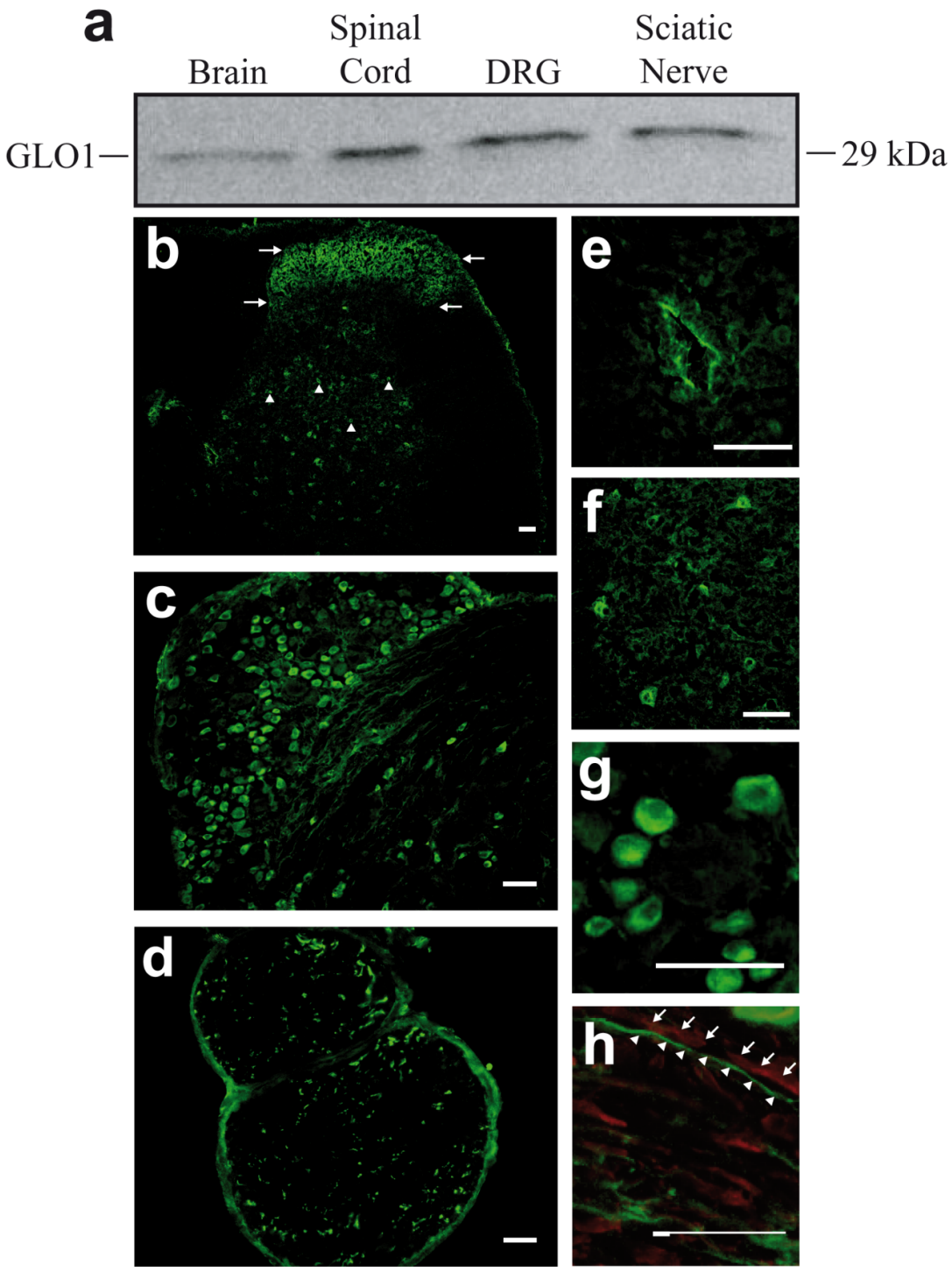

diameter, myelinated neurons with areas ranging from 126-1260 μm^2 and an average area of 552 μm^2 (Figure 2a-d). Correspondingly, GLO1 was expressed in small diameter axons in the sciatic nerve (Figure 2d). Moreover, GLO1 appears to be selective to small C-fibers based on the somal staining pattern in the DRG, the lack of co-localization of GLO1 with neurofilament H large myelinated axons (Figure 1h and 2c), and GLO1 co-localization with peripherin-positive axons (Figure 2g and 2h).

Figure 2: GLO1 expression in lumbar DRG sensory neurons

Immunofluorescence staining for GLO1 (a and e) with counterstaining for neurofilament H (b) and peripherin (f). Merged images (c and g) show GLO1 is localized to small neurons in the DRG (*n* = 3). (d and h) Enhanced views of the merged images are shown. Scale bar; 50 µm.

Figure 2

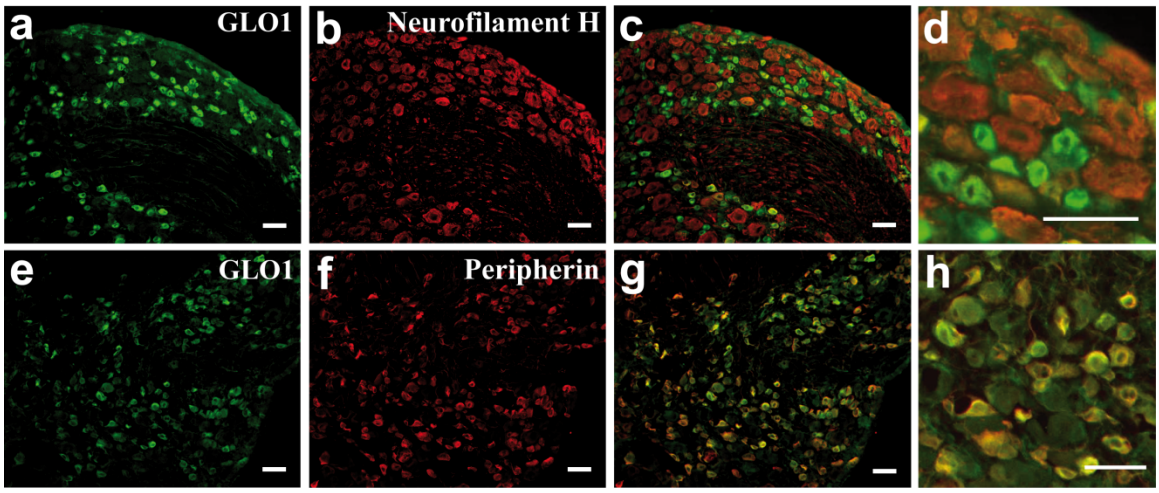

MrgD mice have previously been reported to express *EGFPf* from the *Mas-related G protein-coupled receptor D* locus that is expressed exclusively in nonpeptidergic DRG neurons innervating the epidermis (Zylka, Rice et al. 2005). Because GLO1+ neurons were predominately small, unmyelinated neurons, MrgD mice were utilized to determine whether GLO1 was expressed by peptidergic or nonpeptidergic sensory neurons. Only 8% of MrgD-GFP+ neurons (n = 93 out of 1072) expressed GLO1, suggesting GLO1 is predominately expressed by peptidergic sensory neurons in the L4/L5/L6 DRG (Figure 3).

Genetic Differences in GLO1 mRNA Expression

Quantitative analysis of *GLO1* expression in the DRG revealed variable mRNA expression in 6 different strains of inbred mice. C57BL/6, BALB/cJ, and 129P3/J showed lowest levels of mRNA expression, while C3H/HeJ and DBA/2J had intermediate *GLO1* mRNA expression (Figure 4a and 4b). A/J mice showed the highest levels of mRNA expression of the strains examined with a five-fold increase over C57BL/6 (Figure 4a and 4b). These results were also similar in the brain and sciatic nerve of A/J mice with 6.7- and 4.2-fold higher levels of GLO1 mRNA compared to C57BL/6 mice (Figure 5).

Figure 3: GLO1 expression in peptidergic C-fiber sensory neurons in the DRG.

Immunofluorescence staining for GLO1 (a) in the lumbar DRG of MrgD mice that express GFP from the MrgD locus in nonpeptidergic neurons (b) (n = 3). Merged image (c) shows GLO1 expression primarily in peptidergic C-fibers. Scale bar; 50 µm.

Figure 3

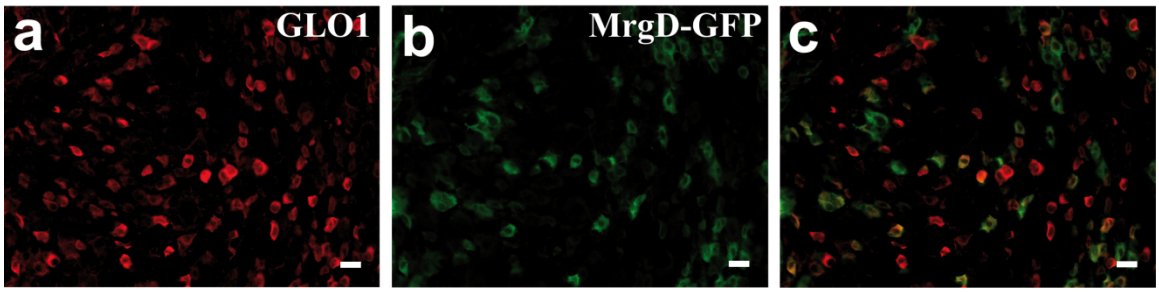

Figure 4: GLO1 mRNA expression is variable in the DRG of inbred strains of mice

(a) Comparison of *GLO1* mRNA expression in the DRG from inbred strains of nondiabetic mice (n = 3 for each strain). Levels are normalized to GAPDH. (b) Fold change in GLO1 mRNA expression relative to C57BL/6 mice. * $p<0.05$ compared to C57BL/6.

Figure 4

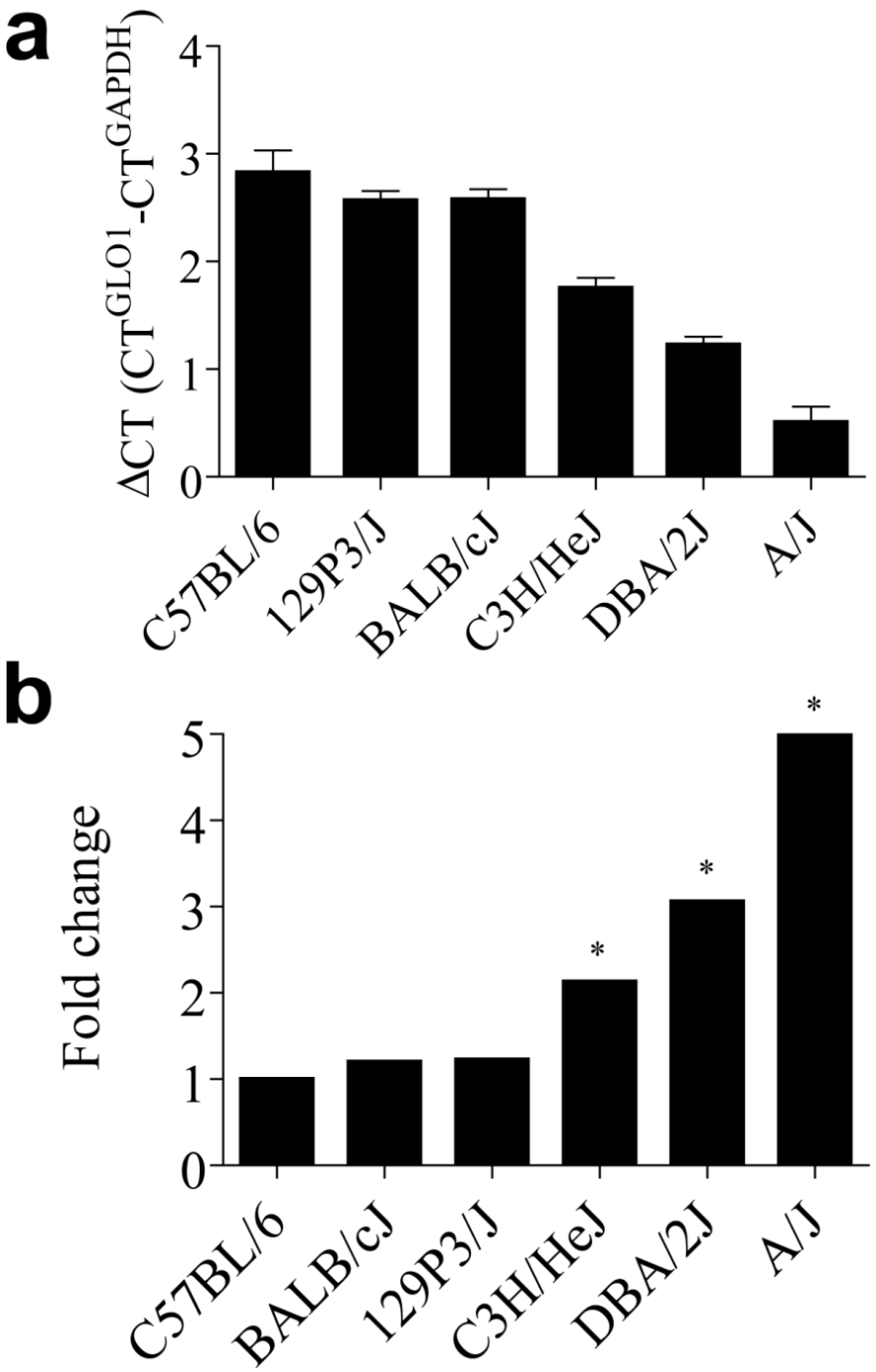
a
ΔCT (CT^GLO1-CT^GAPDH)
0
1
2
3
4
C57BL/6
129P3/J
BALB/cJ
C3H/HeJ
DBA/2J
A/J
b
Fold change
0
1
2
3
4
5
*
*
*
C57BL/6
BALB/cJ
129P3/J
C3H/HeJ
DBA/2J
A/J

Figure 5: Expression of GLO1 in the nervous system of A/J and C57BL/6 mice

(a) GLO1 and GAPDH RT-PCR products from the brain, DRG, and sciatic nerve. (b) Comparison of *GLO1* mRNA from the brain, DRG, and sciatic nerve of A/J (white bars) and C57BL/6 (black bars) mice (n = 3 for each strain). Levels were normalized to GAPDH. (c) Fold change in GLO1 mRNA expression relative to C57BL/6 (black bars) mice in the brain, DRG, and sciatic nerve. * $p<0.05$ compared to C57BL/6.

Figure 5

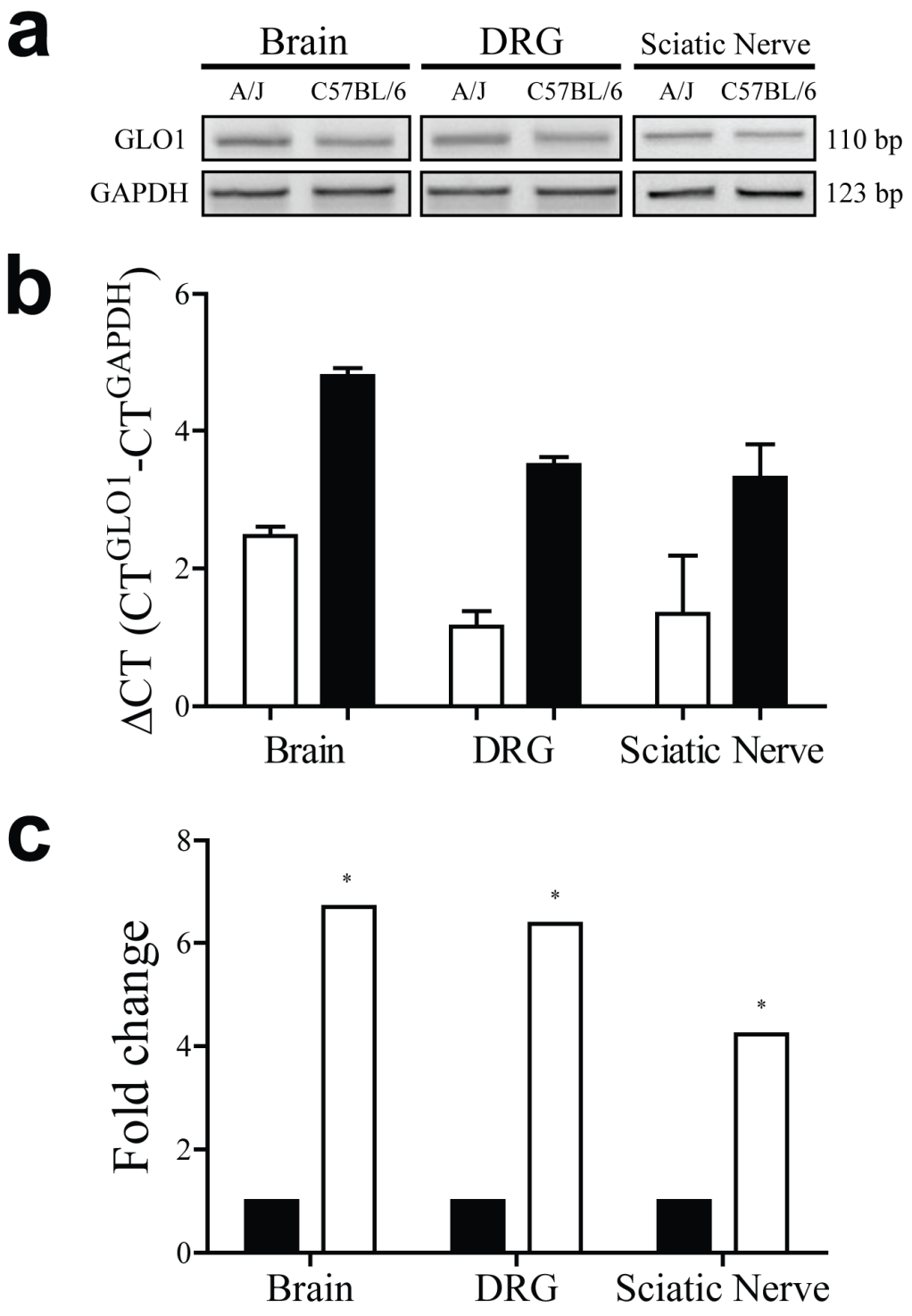
a
Brain
DRG
Sciatic Nerve
A/J
C57BL/6
A/J
C57BL/6
A/J
C57BL/6
GLO1
GAPDH
110 bp
123 bp
b
ΔCT (CT^GLO1-CT^GAPDH)
0
2
4
6
Brain
DRG
Sciatic Nerve
c
Fold change
0
2
4
6
8
*
*
*
Brain
DRG
Sciatic Nerve

5. Discussion

The present study is the first to characterize the expression of GLO1 in the peripheral nervous system. Our results reveal the expression of GLO1 is restricted to small, unmyelinated peptidergic neurons in the DRG, which are primarily responsible for transmission of noxious or painful sensory information. This was particularly interesting given the critical function, highly conserved nature, and previous reports of the ubiquitous expression of GLO1 (Thornalley 2003).

Generally this suggests that different populations of sensory neurons may rely on different pathways to detoxify reactive dicarbonyls and prevent AGE formation. Other pathways have been described; however, as mentioned in Chapter 1, the glyoxalase system has been reported to be the primary enzyme system that functions to protect cells. While other mechanisms are only minor contributors, aldose reductase, betaine aldehyde dehydrogenase and 2-oxoaldehye dehydrogenase are also recognized metabolism pathways for methylglyoxal (Thornalley 1996; Nemet, Varga-Defterdarovic et al. 2006; Turk 2010). Both betaine aldehyde dehydrogenase and 2-oxoaldehyde dehydrogenase have remained largely uninvestigated in the nervous system. However, aldose reductase has been reported to be expressed in the peripheral nervous system, particularly abundant Schwann cells (Powell, Garrett et al. 1991). Though GLO1 may have a prominent role in reducing reactive dicarbonyls in many cells, populations of sensory neurons other than peptidergic neurons may rely on other pathways to detoxify these reactive compounds.

On the other hand, if these other detoxifying pathways are not prominent features of sensory neurons, this suggests populations of neurons may be vulnerable to different types of damage, particularly in diabetes mellitus. Specifically, nonpeptidergic C-fibers and myelinated neurons may experience increased carbonyl stress and accumulation of AGEs leading to altered neuronal function. On the other hand, peptidergic neurons may be more protected from the toxic effects of elevated glucose and reactive dicarbonyls due to the expression of GLO1. This may have significant consequences on the phenotype of altered sensation in diabetic neuropathy.

In this study, *GLO1* mRNA expression was shown to be highly variable in the DRG from multiple inbred strains of mice. A previous study using Affymetrix exon arrays also reported high genetic variability of *GLO1* in the amygdala of a large panel of inbred strains of mice (Williams, Lim et al. 2009). Williams *et al.* discovered the genomic region encoding *GLO1* exists as copy number variant (CNV) in mice with certain strains undergoing duplications and others having lost the duplicated region due to nonhomologous recombination, which could explain expression differences in the DRG (Graubert, Cahan et al. 2007; Williams, Lim et al. 2009).

Interestingly, CNVs have recently been characterized in humans as a substantial source of genetic diversity and disease (Choy, Setlur et al. ; Perry, Yang et al. 2008). In fact, a single CNV encompassing *GLO1* has been described in humans (Redon, Ishikawa et al. 2006). There are also many intronic and exonic SNPs and SNPs located in regulatory 3' and 5' UTR regions have been described (Engelen, Ferreira et al. 2009). In

particular, the Ala111Glu SNP has recently been shown to reduce the activity of GLO1, which leads to an increase in methylglyoxal levels (Barua, Jenkins et al. 2011). This suggests that underlying genetic differences, alterations in regulation, or modifications in disease, particularly in diabetes, may influence the expression and activity of GLO1 (Ranganathan, Ciaccio et al. 1999; Thornalley 2008). To date, little investigation has occurred attempting to define these in humans.

Finally, the restrictive pattern of GLO1, particularly in MrgD mice, provides further evidence for differences in parallel pain pathways. The two subpopulations of C-fiber nociceptors have clear biochemical, morphological, anatomical, and developmental differences that argue for the existence of two pathways that function in normal pain sensation (Almeida, Roizenblatt et al. 2004; Braz, Nassar et al. 2005; Zylka 2005; Zylka, Rice et al. 2005). Our results reveal these two subpopulations also have different abilities and/or mechanisms by which they manage carbonyl stress. This has clear implications in disease states where pain and sensation are altered as in diabetic neuropathy. Previous work in our laboratory showed peptidergic fibers are lost early in the progression of diabetes and this loss correlated with the loss of cutaneous sensitivity in diabetic C57BL/6 mice (Johnson, Ryals et al. 2008). It is plausible to suggest that reduced GLO1 in peptidergic neurons from this strain may render them more vulnerable to the metabolic insults of diabetes mellitus.

CHAPTER 3

Characterization of Glyoxalase I in Mouse Models of Painful and Insensate Diabetic Neuropathy

1. Abstract

Diabetic peripheral neuropathy is a common complication of diabetes; however, the mechanisms producing positive or negative symptoms are not well understood. Glyoxalase I (GLO1) is an enzyme that detoxifies reactive dicarbonyls that form advanced glycation endproducts (AGEs), and GLO1 may affect how sensory neurons respond to heightened AGE levels in diabetic neuropathy. We hypothesize differential GLO1 expression levels in sensory neurons may lead to differences in AGE formation and modulate the phenotype of diabetic neuropathy. Diabetic A/J and C57BL/6 mice are two mouse strains that express divergent levels of *GLO1*. Behavioral assessments were conducted on diabetic A/J and C57BL/6 mice to determine mechanical and thermal sensitivity. Strikingly, these two strains display dramatically different behavioral responses to mechanical stimuli. Diabetic A/J mice displayed increased responses to mechanical stimuli, characteristic of painful neuropathy. Conversely, diabetic C57BL/6 mice developed mechanical and thermal hypoalgesia, which is distinguishing feature of insensate neuropathy. Both strains exhibit loss of epidermal innervation, a feature of both painful and painless neuropathy. Following diabetes induction, diabetic C57BL/6 showed reduced expression of GLO1. This may have important implications on modulation of peripheral sensitivity and lead to the development of different symptoms of neuropathy.

2. Introduction

Diabetic peripheral neuropathy is a common and debilitating complication of longstanding hyperglycemia as a consequence of diabetes mellitus (Figueroa-Romero, Sadidi et al. 2008). The majority of diabetic patients present with insensate neuropathy or negative symptoms, although, estimates have varied widely, suggesting 10-50% of diabetic patients have painful neuropathy or positive symptoms (Calcutt and Backonja 2007; Tavakoli and Malik 2008; Veves, Backonja et al. 2008). However, a clear understanding of the underlying pathological mechanisms that determine which signs and symptoms of neuropathy, either positive or negative, arise in certain patients has yet to be determined.

One of the mechanisms linked to neuronal dysfunction in diabetic neuropathy is the accumulation of advanced glycation endproducts (AGEs) (Ahmed and Thornalley 2007; Toth, Martinez et al. 2007). In clinical studies and diabetic rodent models, AGEs accumulate in sites affected by diabetic complications including the kidney, retina, and peripheral nerves (Karachalias, Babaei-Jadidi et al. 2003). In diabetic patients, the accumulation of AGEs in the skin precedes clinical neuropathy (Meerwaldt, Links et al. 2005), correlates with the severity of symptoms (Meerwaldt, Links et al. 2005), and predicts the progression of diabetic neuropathy (Genuth, Sun et al. 2005).

Reactive dicarbonyls or α-oxoaldehydes such as methylglyoxal, glyoxal, and 3-deoxyglucose have been found to be important precursors of AGEs and contribute in their own right to diabetic complications (Ulrich and Cerami 2001; de Arriba, Stuchbury

et al. 2007). As highlighted in Chapter 1, reactive dicarbonyls are formed in many metabolic pathways including glycolysis, protein breakdown, lipid peroxidation, and degradation of glycated proteins, all of which are heightened in diabetes mellitus (Thornalley 2002; Ahmed and Thornalley 2007). α-oxoaldehydes are up to 20,000-fold more reactive than glucose leading to increased carbonyl stress and accelerated production of AGEs (Turk 2010). Therefore, reactive dicarbonyls are thought to have an important role in the pathogenesis of diabetic neuropathy.

The glyoxalase enzyme system, composed of glyoxalase I (GLO1) and glyoxalase II, is a key cellular pathway that detoxifies reactive dicarbonyls and limits AGE formation. GLO1 levels and activity can be altered in disease states including diabetes (Phillips, Mirrlees et al. 1993; Miller, Smith et al. 2006; Fujimoto, Uchida et al. 2008). Thus, GLO1 has been investigated in diabetic retinopathy, nephropathy, cardiomyopathy, and endothelial dysfunction (Ahmed 2005). As our previous results have shown, GLO1 is primarily expressed in small, unmyelinated peptidergic neurons that function to transmit noxious information (Jack, Ryals et al. 2011). And, as discussed in Chapter 2, GLO1 exists as a CNV. Consequently, certain strains that have reduced expression of GLO1 in peptidergic neurons may be more vulnerable to developing sensory deficits in diabetic neuropathy. The present study was designed to better understand the potential role of GLO1 in modulating the development of diabetic neuropathy. Here we investigated GLO1 expression in two mouse models of diabetes mellitus that develop different characteristics of neuropathy.

3. Experimental Procedures

Animals

Male C57BL/6 (Charles River, Sulzfeld, Germany) and A/J mice (Jackson, Bar Harbor, Maine) were purchased at 7 weeks of age, one week prior to beginning experiments. The animals were housed in 12/12-h light/dark cycle under pathogen free conditions. Mice were given free access to standard rodent chow (Harlan Teklad 8,604, 4% kcal derived from fat) and water. All animal use was in accordance with NIH guidelines and conformed to principles specified by the University of Kansas Medical Center Animal Care and Use Protocol.

Streptozocin-induced diabetes

Diabetes was induced in 8-week-old male C57BL/6 and A/J mice. C57BL/6 mice were injected with a single intraperitoneal injection of streptozocin (STZ) (180 mg/kg body weight; Sigma, St. Louis, MO) dissolved in 10 mmol/l sodium citrate buffer, pH 4.5. A/J mice were injected with 85 mg/kg STZ followed by a second injection with 65 mg/kg STZ 24 hours later. Controls received sodium citrate buffer alone. Animals of either strain that did not develop hyperglycemia one week after the initial injection were re-injected with 85 mg/kg STZ. Food was removed from all cages for 3 h before and after STZ-injection. Animals did not receive insulin at any time.

Glucose measurements

Animal weight and blood glucose levels (glucose diagnostic reagents, Sigma, St. Louis, MO) were measured 1 week after STZ injection and every week thereafter. Mice were considered diabetic if their nonfasting blood glucose level, measured from tail vein sampling for intermediate measures and decapitation pool for the terminal measure, was > 12.0 mmol/l at every measurement.

Mechanical testing

Mechanical behavioral responses to a Semmes-Weinstein von Frey monofilament (1 or 1.4 g) (Stoelting, Wood Dale, Illinois) were assessed at 4, 5, and 6 weeks after STZ injection. Mice underwent a training session on the day prior to the first day of testing. Mice were placed in individual clear plastic cages (11 x 5 x 3.5 cm) on a wire mesh screen elevated 55 cm above the table and allowed to acclimate for 30 minutes. The combined mean percent withdrawal of three applications to each hindpaw was calculated for each animal for each testing session. The group means were calculated.

Thermal Testing

Thermal testing was performed using a thermal analgesiometer (UARDG, La Jolla, CA) at 4 weeks after STZ injection. Mice were placed in individual clear plastic compartments on top of a glass surface and allowed to acclimate for 30 min. A radiant heat source (4.0V) was applied to the mid-plantar surface of one hindpaw for a maximum of 20 s. The number of seconds until the animal withdrew its hindpaw was recorded as

the latency. Testing was recorded three times on alternating hindpaws with at least 10 min separating applications to the same hind paw. The combined mean withdrawal latency of six applications was calculated for each animal. The group means were calculated.

Hot and cold plate testing was done using a Hot/Cold Plate Analgesia Meter (IITC Life Science, Woodland Hills, CA). Mice were placed in the enclosure over the temperature plate. The initial temperature was set at 25^{o}C for both hot and cold testing. The temperature either increased or decreased by 0.1^{o}C/sec until the animal responded. A positive response included licking/biting paws, rearing, or jumping and the temperature and latency were recorded at that time. For hot testing, the maximum temperature was set at 55^{o}C and for cold testing the minimum temperature was set at 5^{o}C. The average temperature was calculated per group.

Immunohistochemistry

Unfixed lumbar DRG were dissected, frozen, sectioned in 16-20 μm cross-sectional serial sections, and mounted on Superfrost Plus slides (Fisher Scientific, Chicago, IL) then stored at -20^{o}C. After thawing 5 min at room temperature, slide-mounted tissue was circled with a Pap Pen (Research Products International, Mt. Prospect, Illinois) to create a hydrophobic ring. Tissue sections were then covered with a blocking solution (0.5% porcine gelatin, 1.5% normal donkey serum, 0.5% Triton-X, Superblock buffer; Pierce, Rockford, IL) for 1 h at room temperature. Primary antibodies were incubated overnight at 4^{o}C. For GLO1 immunohistochemistry, a mouse anti-

glyoxalase I primary antibody (1:100; Abcam, Cambridge, MA) and a donkey anti-mouse secondary antibody (Alexa 555; 1:2000; Molecular Probes, Eugene, OR) were used to label positive cells in the L4/5/6 DRG. Sections were washed 2 x 5 min with PBST followed by incubation for 1 h with fluorochrome-conjugated secondary antibody diluted in PBST and Superblock (Pierce, Rockford, IL). Following three washes with PBS, slides were coverslipped and stored at 4^{o}C until viewing.

Quantitative Real-Time PCR

Total RNA was isolated from DRG of diabetic and nondiabetic C57BL/6 mice using Trizol reagent (Ambion, Austin, TX) and RNeasy Mini Kit (Qiagen, Valencia, CA). The concentration and purity were determined using a 2100 Bioanalyzer (Agilent Technologies, Santa Clara, CA). Total RNA (0.63 μg) was synthesized directly into cDNA using the iScript cDNA Synthesis Kit (Bio-Rad, Hercules, CA). qRT-PCR was performed using iScript One-Step RT-PCR Kit with SYBR green (Bio-Rad, Hercules, CA). The primers were as follows:

GAPDH: Forward: 5'-AGGTCGGTGTGAACGGATTTG-3'

Reverse: 5'-TGTAGACCATGTAGTTGAGGTCA-3'

GLO1: Forward: 5'-GATTTGGTCACATTGGGATTGC-3'

Reverse: 5'-TTCTTTCATTTTCCCGTCATCAG

All reactions were performed in triplicate. ΔCT values and fold changes were calculated using the Pfaffl analysis method (Pfaffl, Horgan et al. 2002). The mRNA levels for GLO1 were normalized to GAPDH.

Western blot

DRG were rapidly isolated, frozen in liquid nitrogen, and stored at -80^{o}C. Tissue was homogenized for 2 min in 50 µl Cell Extraction Buffer (Invitrogen, Carlsbad, CA) with protease inhibitor cocktail (Sigma, St. Louis, MO), 200 mM NaF, and 200 mM Na_3VO_4. The homogenates were incubated on ice for 30 mins before centrifugation at 7000 rpm for 10 mins at 4^{o}C. Protein concentrations were determined using the Bio-Rad protein assay based on the Bradford assay (Bio-Rad, Sydney, NSW, Australia).

Samples containing 100 µg of protein were separated by electrophoresis through 4-20% SDS-PAGE gels (125 V, 1.5 h, 4^{o}C) and transferred onto nitrocellulose paper (35 mA, overnight, 4^{o}C). Nitrocellulose membranes were blocked with blocking buffer (3% non-fat milk and 0.05% Tween-20 in phosphate buffered saline) for 1 hour at room temperature to block non-specific binding sites, followed by overnight incubation with a goat anti-GLO1 primary antibody (R&D Systems, Minneapolis, MN) diluted 1:5000 in blocking buffer at 4^{o}C. The donkey anti-goat IgG-HRP secondary antibody (Santa Cruz, Santa Cruz, CA) was used diluted 1:2500 in blocking buffer at RT for 1 hour.

Nitrocellulose membranes were stripped using Restore Plus Western Blot Stripping Buffer (Pierce, Rockford, IL), followed by 1-hour incubation with an actin primary antibody (Millipore, Billerica, MA) diluted 1:100,000 in blocking buffer at RT.

The donkey anti-mouse IgG-HRP secondary antibody (Santa Cruz, Santa Cruz, CA) was used diluted 1:2500 in blocking buffer at RT for 1 hour. The chemiluminescent signal was acquired using Supersignal West Femto Maximum Sensitivity Substrate (Pierce, Rockford, IL) and a CCD camera (BioSpectrum Imaging System, UVP, Upland, CA). NIH ImageJ software was used to measure and quantify densitometry readings.

Intraepidermal Nerve Fiber Density

Cutaneous innervation of the footpad was assessed in nondiabetic and diabetic mice after seven weeks of diabetes. The right footpad skin was harvested from mice at the time of sacrifice and immersion fixed in Zamboni's fixative (4% paraformaldehyde, 14% saturated picric acid, 0.1 M phosphate buffered saline; pH 7.4) for 1 hour on ice. Footpads were washed in PBS twice and placed in PBS overnight at 4^{o}C. Footpads were then cryoprotected in 30% sucrose overnight at 4^{o}C. 30 µm serial sections were cut and placed on Superfrost Plus microscope slides (Fischer, Chicago, IL). Immunohistochemistry was performed as previous described (Christianson, Ryals et al. 2007; Johnson, Ryals et al. 2008). Small cutaneous, PGP9.5+ fibers that crossed the dermal-epidermal junction were quantified in three areas from three tissue sections from each footpad. The length of the dermal-epidermal junction was measured and intraepidermal nerve fiber density (IENFD) was expressed as the number of fibers per millimeter.

Statistics

Data are expressed as mean ± SEM. Differences were analyzed using Student's T-test or ANOVA followed by Bonferroni's test, as appropriate. Significance was defined as $p \leq 0.05$.

4. Results and Figures

STZ Induced Diabetes

Following STZ injection, C57BL/6 and A/J mice developed significantly higher blood glucose that persisted throughout the course of the 6-week study (Figure 1a). Both strains showed similar blood glucose levels after diabetes induction (Figure 1a). Diabetic A/J mice had significantly lower body weights than nondiabetic mice. Nondiabetic A/J mice gained 2.1 ± 0.7 g on average, while diabetic A/J mice lost 4.6 ± 0.5 g on average (Figure 1b). Diabetic C57BL/6 also had significantly lower body weights compared to nondiabetic C57BL/6 mice and failed to gain weight over the course of the study (Figure 1b). Both diabetic C57BL/6 and A/J mice also displayed other characteristic symptoms of type I diabetes, including polydipsia and polyuria.

Figure 1: Blood glucose and weights of diabetic A/J and C57BL/6 mice

(a) Blood glucose and (b) weights of C57BL/6 (n = 5 nondiabetic, closed circles, 9 diabetic, open circles) and A/J (n = 5 nondiabetic, closed triangles, 9 diabetic, open triangles) mice. Circles represent Blood glucose is expressed in mmol/l and weight is expressed in grams. Data represents means ± standard error of the mean. # $p<0.05$ vs. C57BL/6 nondiabetic. #### $p<0.0001$ vs. C57BL/6 nondiabetic. **** $p<0.0001$ vs. A/J nondiabetic

Figure 1

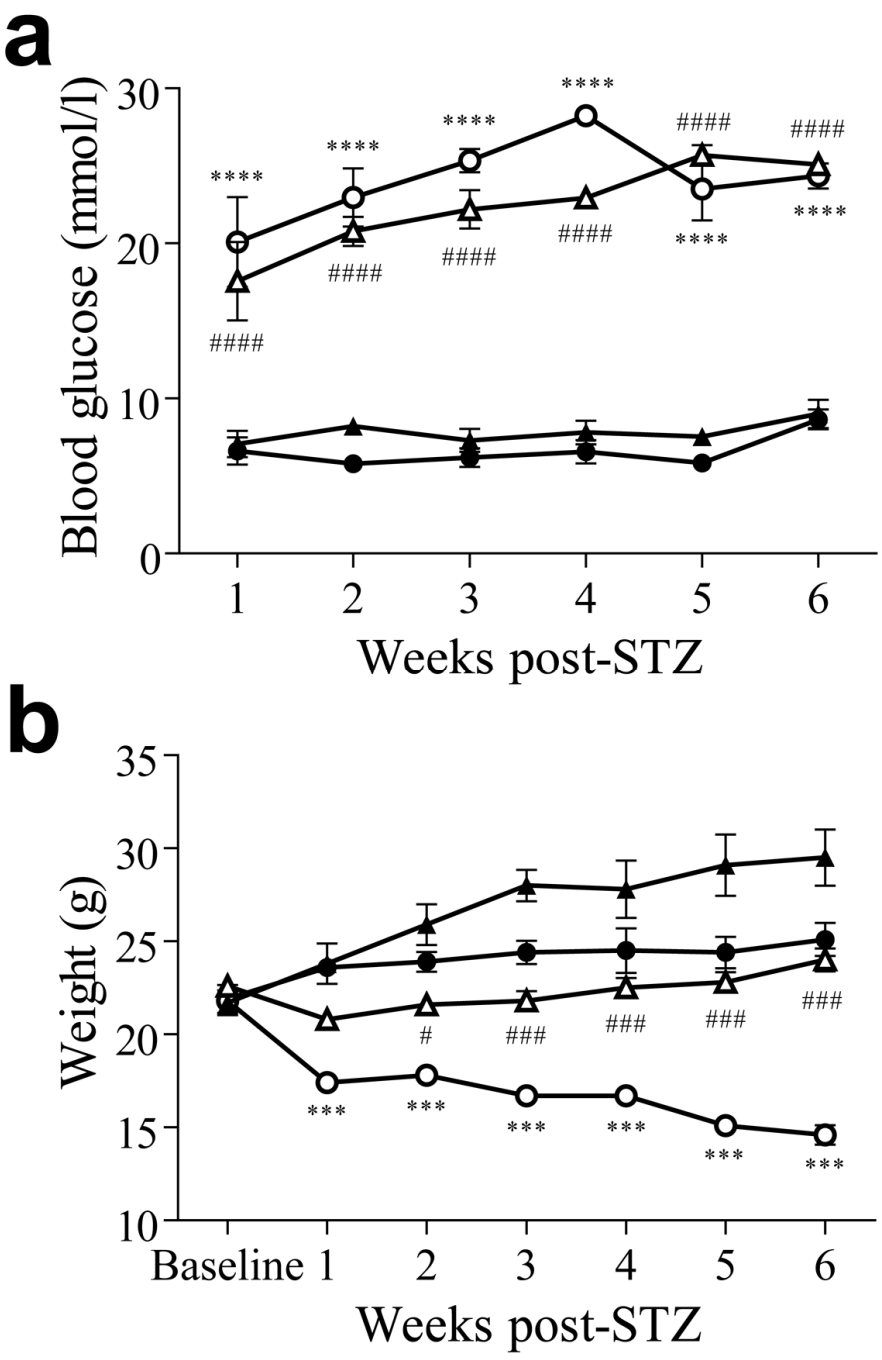
a
Blood glucose (mmol/l)
30
20
10
0
1
2
3
4
5
6
Weeks post-STZ
****
####
b
Weight (g)
35
30
25
20
15
10
Baseline
Weeks post-STZ
***
#
###

Behavioral Sensitivity to Mechanical Stimuli

Assessment of baseline behavioral responses to a 1.4 g Von Frey mechanical stimulus revealed that C57BL/6 and A/J mice displayed different mechanical sensitivity (Figure 2a). A/J mice displayed a higher average percent withdrawal following 6 applications of Von Frey monofilaments and, therefore, were more sensitive to force applied to the hindpaw than C57BL/6 (Figure 2a). Consequently, a smaller filament, 1.0 g, was chosen to test the mechanical sensitivity of A/J mice in order to detect behavioral changes following diabetes induction.

Mechanical sensitivity of the hindpaw was tested at 4, 5, and 6 weeks after STZ injection. Consistent with this strain and model, diabetic C57BL/6 mice showed reduced responses to a 1.4-g von Frey monofilament (Figure 2c) (Christianson, Ryals et al. 2003; Johnson, Ryals et al. 2008). After four weeks of diabetes, diabetic C57BL/6 mice displayed a withdrawal response to mechanical stimulation an average of 41.2% ± 5.32, while nondiabetic mice responded 64.4% ± 11.7 of the time. This mechanical insensitivity persisted and worsened with progression of the disease with diabetic mice withdrawing 23.2% ± 2.97 at 6 weeks post-STZ (Figure 6c; 4- vs. 6-week post-STZ).

Figure 2: Behavioral responses of mice to mechanical stimulation of the hind paw.

(a) Baseline behavioral measurements of nondiabetic A/J (n = 15) and C57BL/6 (n = 12) mice using a 1.4 g monofilament. The percent paw withdrawal is the percentage of responses following six repeated applications of von Frey monofilaments. Either a 1.0 g or 1.4 g were applied to the hindpaws of A/J (b, n = 4 nondiabetic, closed circles, 4 diabetic, open circles) and C57BL/6 (c, n = 7 nondiabetic, closed triangles, 34 diabetic, open triangles) mice, respectively. Data represents means ± standard error of the mean. * p<0.05 vs. nondiabetic. ** p<0.01 vs. nondiabetic.

Figure 2

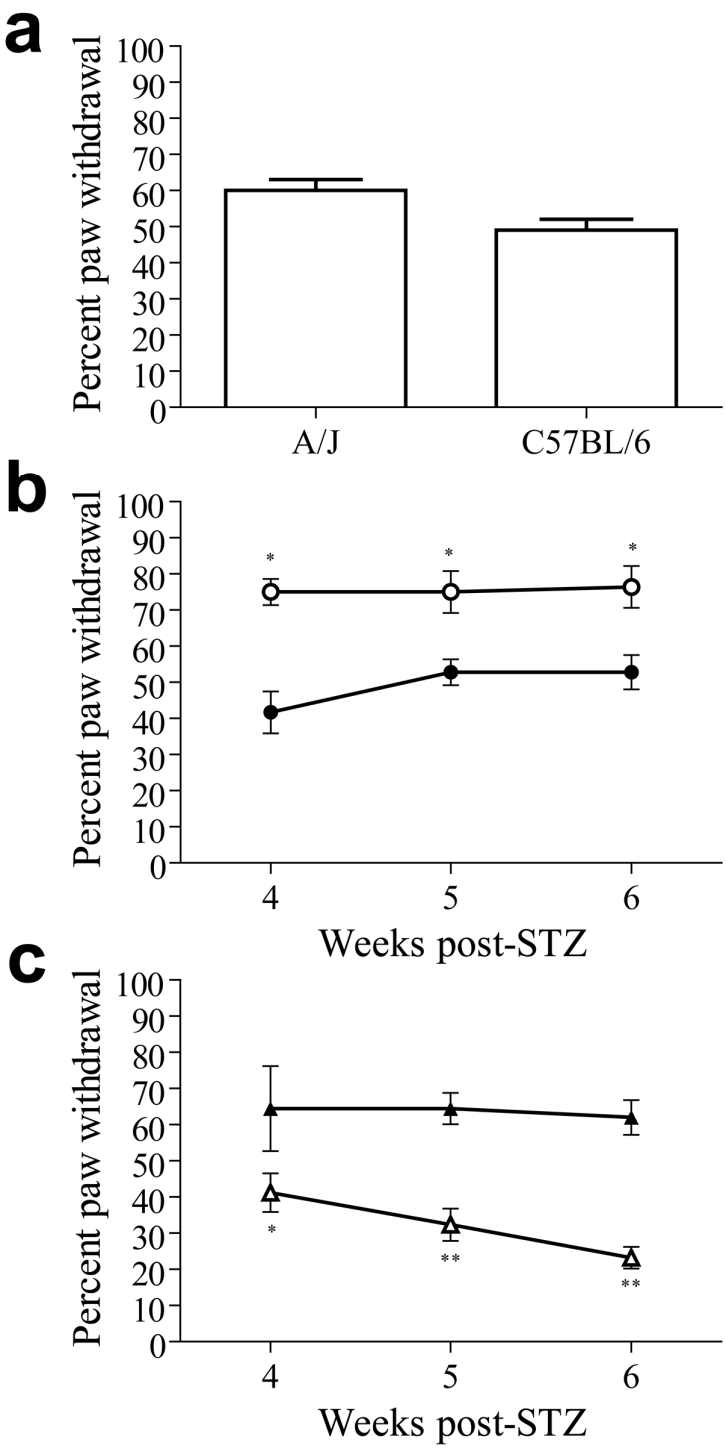
a
Percent paw withdrawal
100
90
80
70
60
50
40
30
20
10
0
A/J
C57BL/6
b
Percent paw withdrawal
*
*
*
4
5
6
Weeks post-STZ
c
Percent paw withdrawal
*
**
**
4
5
6
Weeks post-STZ

Conversely, as early as 1 week following STZ injection, diabetic A/J mice displayed increased responses to a 1-g von Frey monofilament (data not shown). Mechanical allodynia was present at 4, 5, and 6 weeks following STZ injection with diabetic A/J mice responding nearly 75% of the time (Figure 2b). Thus, diabetic C57BL/6 mice develop increased mechanical thresholds and severe mechanical insensitivity, whereas diabetic A/J mice developed reduced mechanical thresholds and mechanical allodynia after 4 weeks of diabetes.

Behavioral Sensitivity to Thermal Stimuli

Thermal sensitivity of the hindpaw was tested with a thermal analgesiometer at 4 weeks after STZ injection. Diabetic C57BL/6 mice exhibited increased latency to the time of withdrawal from a radiant heat source applied to the hindpaw (Figure 3a). However, diabetic A/J mice had similar latencies to nondiabetic mice, 13.1 s ± 0.8s vs. 14.4 s ± 1.4 s, respectively (Figure 3b).

Because thermal latencies were not different, A/J mice underwent hot and cold plate testing at 5 and 6 weeks following STZ injection to determine if either of the thermal thresholds was different at later time points. Diabetic A/J mice did not display altered sensitivity to either hot (Figure 4a and 4b) or cold (Figure 4c and 4d) temperatures. Diabetic A/J mice showed positive responses to heat at an average temperature of 46.6 ^{o}C ± 1.2 at week 5 and 45.9 ^{o}C ± 0.6 at week 6 following diabetes induction, while nondiabetic A/J mice displayed responses at average temperatures of 46.5 ^{o}C ± 0.7 and 46.8 ^{o}C ± 0.3 (Figure 4a and 4b). Again, cold thresholds were not

Figure 3: Thermal testing of nondiabetic and diabetic C57BL/6 and A/J mice 4 weeks after diabetes induction

(a) Thermal testing of nondiabetic and diabetic C57BL/6 (n = 6-7) and (b) A/J (n = 6-7) mice using a radiant light source applied to the hindpaw. The latency is the length of time until the mouse displayed a withdrawal behavior such as retracting or licking the hindpaw. Data represents means ± standard error of the mean. * $p<0.05$ vs. nondiabetic C57BL/6.

Figure 3

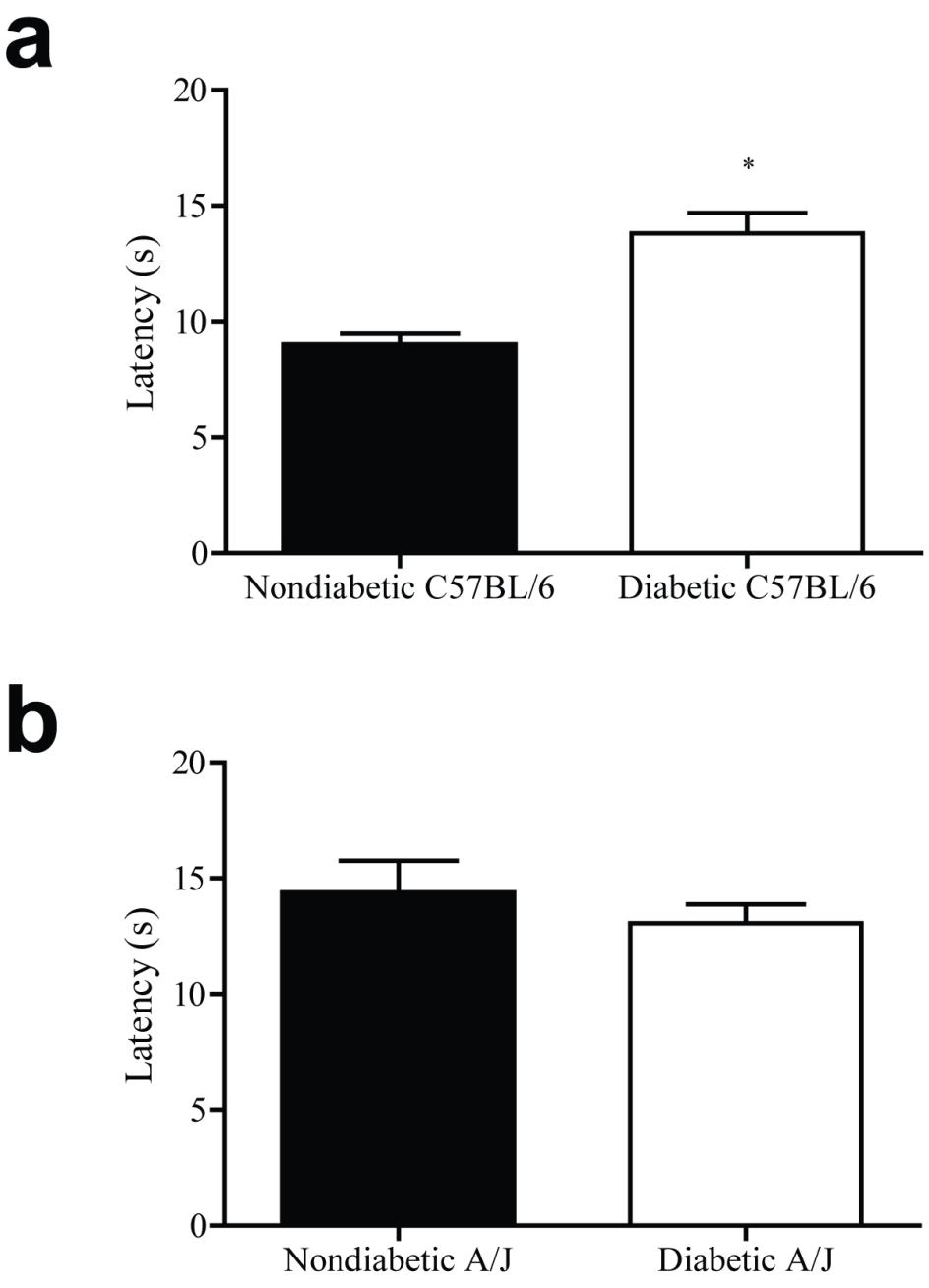
a
20
15
10
5
0
Latency (s)
*
Nondiabetic C57BL/6
Diabetic C57BL/6
b
20
15
10
5
0
Latency (s)
Nondiabetic A/J
Diabetic A/J

Figure 4: Hot and cold plate testing of nondiabetic and diabetic A/J mice at five and six weeks after STZ injection

(Top) Heat thresholds of nondiabetic and diabetic A/J (*n* = 6-7) at (a) 5 weeks and (b) 6 weeks after diabetes induction. (Bottom) Cold thresholds of nondiabetic and diabetic A/J (n = 6-7) at (c) 5 weeks and (d) 6 weeks after STZ injection. The threshold temperature was recorded when the animal displayed withdrawal activity such as biting or licking the hindpaw, jumping, or rearing. Data represents means ± standard error of the mean.

Figure 4

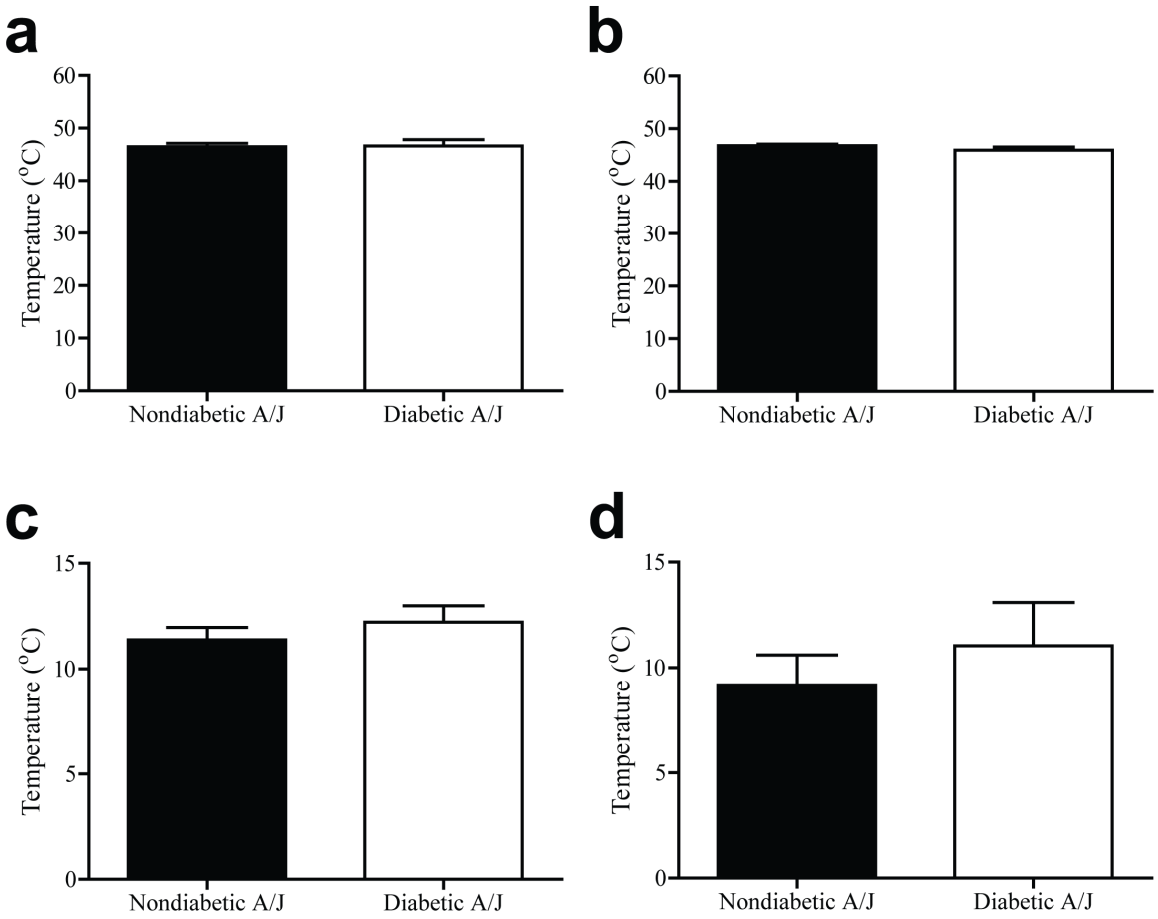
a
b
c
d
Temperature (°C)
60
50
40
30
20
10
0
15
5
Nondiabetic A/J
Diabetic A/J

different at either of the two time points tested with nondiabetic A/J mice responding at average temperatures of 11.4 ^{o}C ± 0.6 and 9.2 ^{o}C ± 1.4 and diabetic A/J mice responding at average temperatures of 12.2 ^{o}C ± 0.8 and 11.0 ^{o}C ± 2.0 (Figure 4c and 4d). Latencies to withdrawal were also not significantly different between groups at either time tested.

Intraepidermal Nerve Fiber Density

Although nondiabetic A/J mice had more than twice the number of fibers in the epidermis than nondiabetic C57BL/6, diabetic mice from both strains displayed changes in fiber density following diabetes induction. After 7 weeks of diabetes, both diabetic A/J and C57BL/6 mice displayed reduced epidermal innervation of the hindpaw (Figure 5). Diabetic C57BL/6 mice showed a 44% loss in epidermal axons, while diabetic A/J mice underwent a 30% reduction in fiber density (Figure 5).

GLO1 Expression in Diabetes

After 6 weeks of diabetes, GLO1 protein levels in the DRG of diabetic A/J mice remained similar to nondiabetic mice (Figure 6a and 6b). In contrast, diabetic C57BL/6 mice showed a 59.6% reduction in GLO1 expression in the lumbar DRG (Figure 6a and 6c). There was no difference in GLO1 mRNA levels of diabetic C57BL/6 mice compared to the nondiabetic counterparts (Figure 6d).

The pattern of GLO1 expression in the DRG did not change following diabetes induction. Small-diameter neurons predominately expressed GLO1 in both nondiabetic and diabetic mice (Figure 7a-d). The percentage of GLO1+ neurons from both diabetic

Figure 5: Effect of diabetes on intraepidermal nerve fiber density in diabetic A/J and C57BL/6 mice

Representative photomicrographs of skin from the right footpad of (a) nondiabetic C57BL/6, (b) diabetic C57BL/6, (c) nondiabetic A/J, and (d) diabetic A/J mice. Diabetic mice show a reduction in PGP9.5-positive cutaneous nerve fibers in the skin. Scale bar = 50 µm. (e) Quantification of IENFD of nondiabetic (black bars) and diabetic (white bars) C57BL/6 and A/J mice. Data plotted as means ± SEM. *$p < 0.05$ vs. nondiabetic. Scale bar; 50 µm.

Figure 5

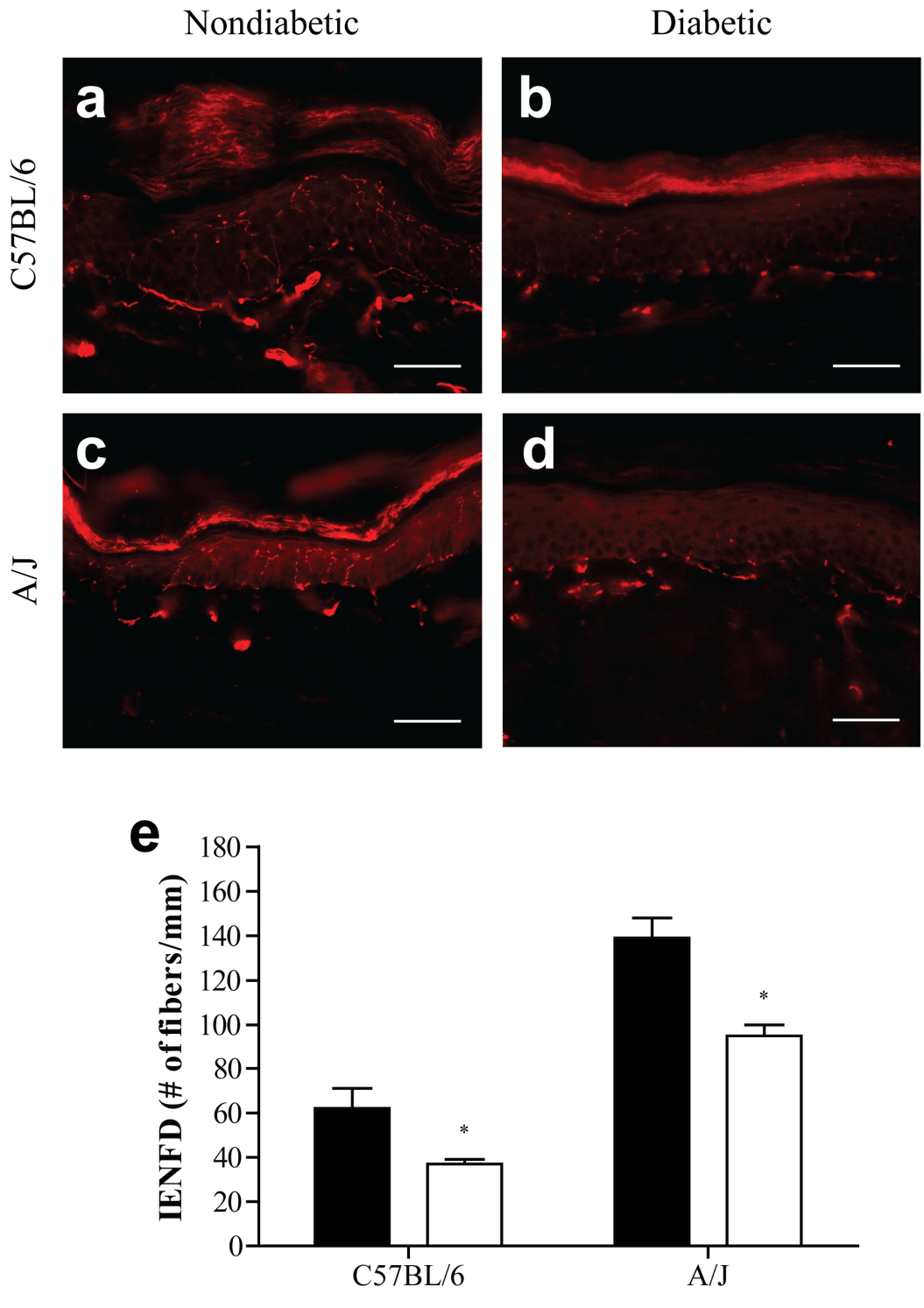
Nondiabetic
Diabetic
C57BL/6
A/J
a
b
c
d
e
IENFD (# of fibers/mm)
180
160
140
120
100
80
60
40
20
0
*
*
C57BL/6
A/J

Figure 6: Effect of diabetes on levels of GLO1 in the DRG of A/J and C57BL/6 mice.

(a) Representative Western blots from nondiabetic and diabetic A/J (left) and C57BL/6 (right) mice are shown for GLO1 and actin. Quantification of protein band intensities for A/J mice (b, n = 3 nondiabetic, 3 diabetic) and C57BL/6 mice (c, n = 3 nondiabetic, 3 diabetic). Band intensities are shown as normalized means ± standard error of the mean. (d) Comparison of GLO1 mRNA expression in the DRG from nondiabetic and diabetic C57BL/6 mice after six weeks of diabetes (n = 3). $^{**}p<0.01$ compared to nondiabetic.

Figure 6

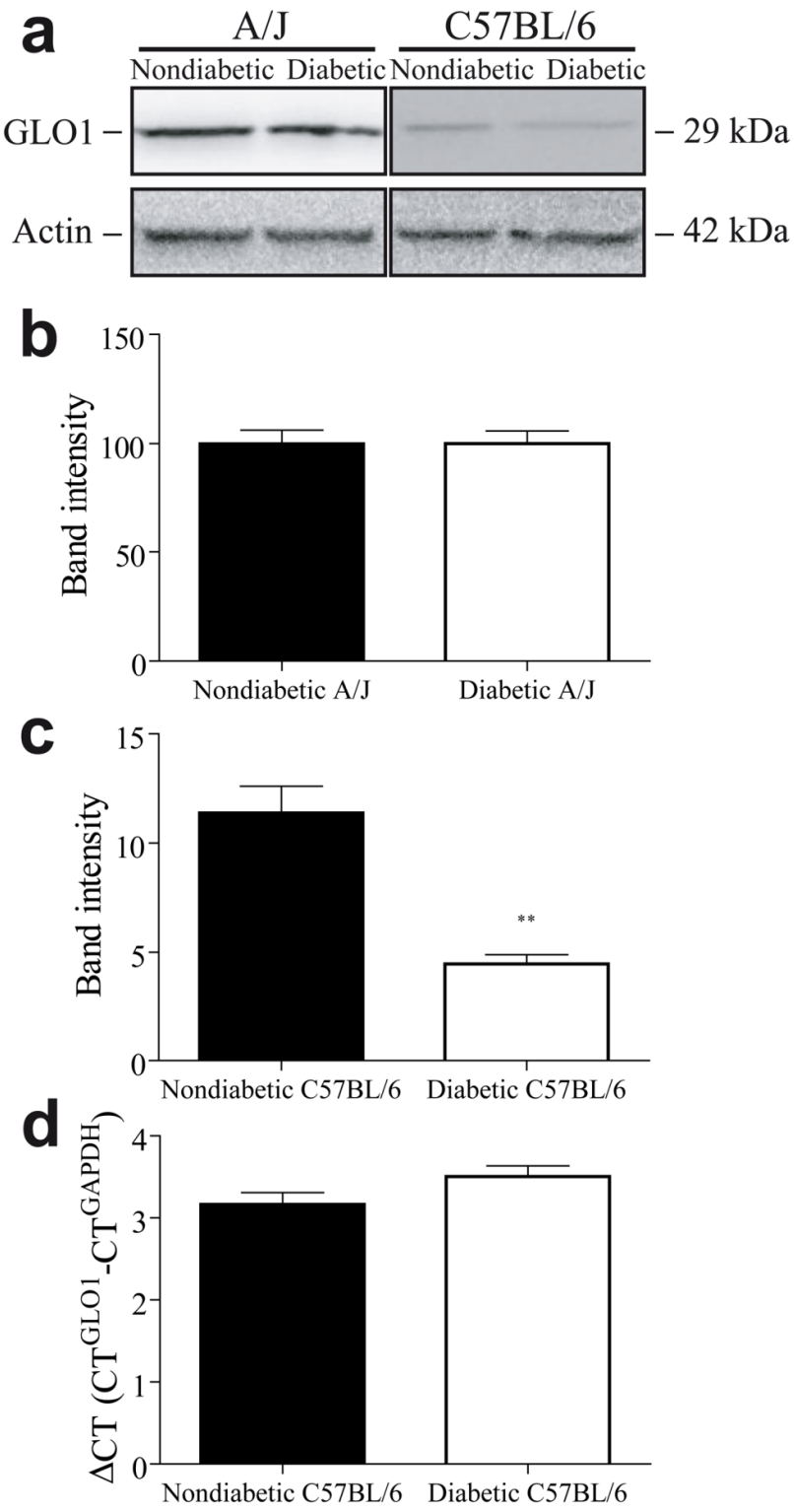
a
A/J
C57BL/6
Nondiabetic
Diabetic
Nondiabetic
Diabetic
GLO1
29 kDa
Actin
42 kDa
b
Band intensity
150
100
50
0
Nondiabetic A/J
Diabetic A/J
c
Band intensity
15
10
5
0
**
Nondiabetic C57BL/6
Diabetic C57BL/6
d
ΔCT (CT^GLO1-CT^GAPDH)
4
3
2
1
0
Nondiabetic C57BL/6
Diabetic C57BL/6

strains was similar to their nondiabetic counterparts, 30 ± 2% for nondiabetic C57BL/6 (*n* = 663 out of 2194) vs. 28 ± 2% for diabetic C57BL/6 (*n* = 756 out of 2660) and 29 ± 2% for nondiabetic A/J (*n* = 597out of 2032) vs. 26 ± 1% for diabetic A/J (*n* = 468 out of 1795) (Figure 7e). Similarly, the number of GLO1+ neurons from both diabetic C57BL/5 and A/J mice was comparable (Figure 7e).

5. Discussion

Chronic hyperglycemia is the main driving force of the development and progression of diabetic neuropathy. Elevated intra- and extra-cellular glucose concentrations lead to accelerated production of AGEs. AGEs alter the function of many proteins including tubulin, mitochondrial electron transport chain proteins, insulin, and neuronal extracellular matrix proteins (Mendez, Xie et al. ; Williams, Howarth et al. 1982; Rabbani and Thornalley 2008; Schalkwijk, Brouwers et al. 2008; Thornalley 2008; Duran-Jimenez, Dobler et al. 2009).

AGEs are elevated in peripheral nerves and skin of both diabetic patients and rodents (Chabroux, Canoui-Poitrine et al. ; Karachalias, Babaei-Jadidi et al. 2003; Meerwaldt, Links et al. 2005; Yu, Thorpe et al. 2006), and elevated levels have also been measured in plasma of type I diabetic patients without complications, suggesting AGEs may have a role in the development and/or progression of diabetic neuropathy (Han, Randell et al. 2009). GLO1, a key enzyme in anti-glycation defense, is critical to preventing this accumulation of AGEs and limiting their toxic effects by breaking down the highly reactive precursors, α-oxoaldehydes.

Figure 7: The pattern of GLO1 expression in the DRG following 6 weeks of diabetes.

Immunofluorescence staining for GLO1 in the DRG of A/J nondiabetic (a, *n* = 3) and diabetic (b, *n* = 3) and C57BL/6 nondiabetic (c, *n* = 3) and diabetic (d, *n* = 3) mice. Scale bars; 50 µm. (e) Quantification of the percentage of GLO1 positive neurons of total neurons in the DRG. Black bars represent nondiabetic mice and white bars represent diabetic mice. Data represents means ± standard error of the mean.

Figure 7

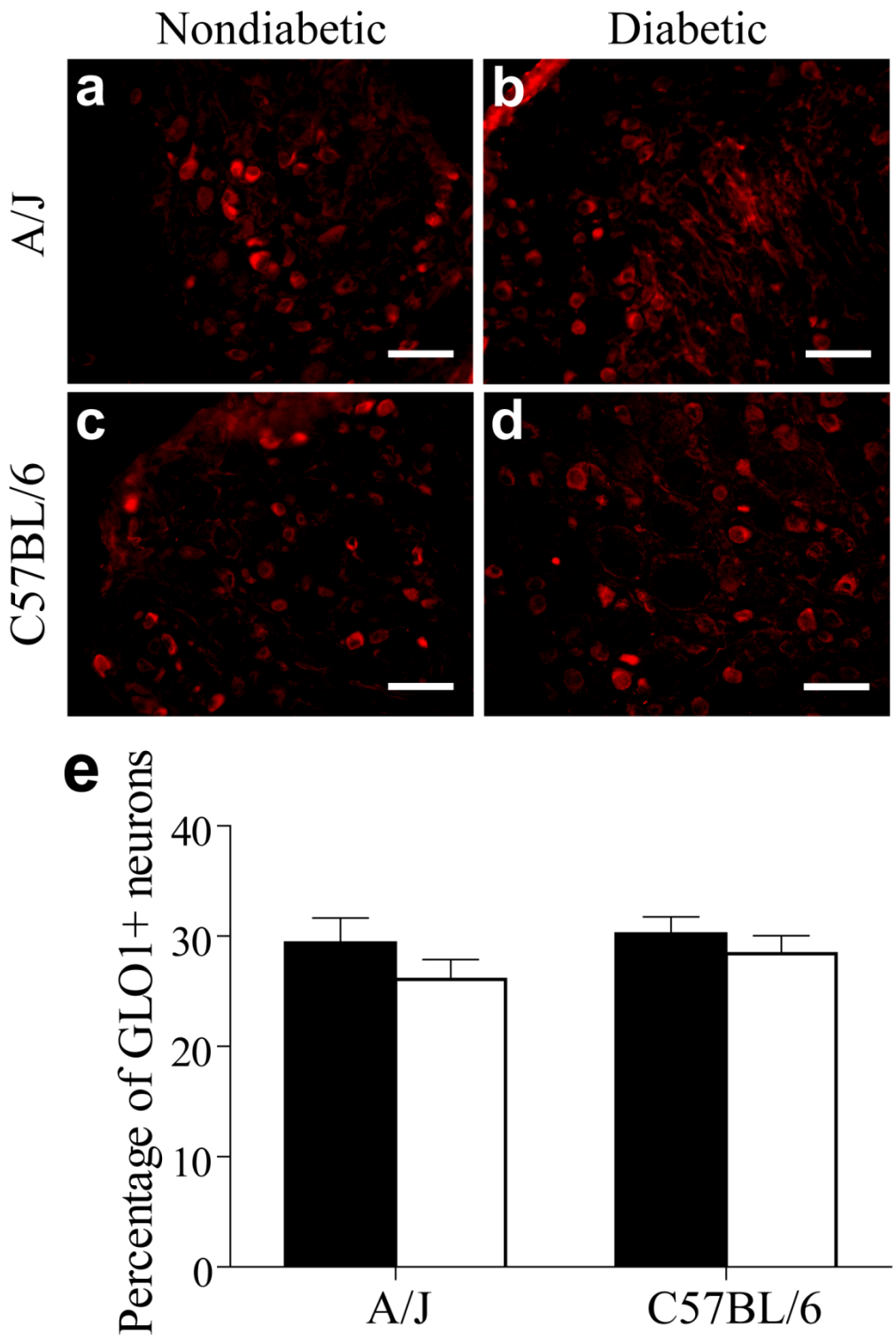
Nondiabetic
Diabetic
a
b
A/J
c
d
C57BL/6
e
Percentage of GLO1+ neurons
40
30
20
10
0
A/J
C57BL/6

In this study, diabetic mice expressing different levels of GLO1 showed variable responses to mechanical stimuli. Previous studies have also suggested a link between mechanical and thermal sensation, GLO1, and AGEs. Both Bierhaus *et al*. and Toth *et al*. showed RAGE has a role in sensory neuron dysfunction in diabetes (Bierhaus, Haslbeck et al. 2004; Toth, Rong et al. 2008). Diabetic $RAGE^{-/-}$ mice were protected from pathological, physiological, and behavior signs of DN (Bierhaus, Haslbeck et al. 2004; Toth, Martinez et al. 2007; Toth, Rong et al. 2008). Mechanical sensitivity is mediated by both unmyelinated and myelinated sensory neurons that respond to a range of sensory stimulus modalities. Indeed, most C-fibers also respond to mechanical sensitivity (Rau, McIlwrath et al. 2009). Thus, afferent information encoding mechanical information likely converges in the spinal cord to convey complex mechano-sensory information. Thus, it is plausible to suggest that a balance between fiber types is required to convey appropriate sensory information from the periphery. The ability of specific neuronal populations to be more susceptible to and/or protect against hyperglycemia-induced damage, which occurs in diabetes, may alter this balance leading to abnormal peripheral nociceptive input and produce different signs and symptoms of neuropathy.

Based on our findings, it is plausible hypothesize that an imbalance of fiber type input may underlie the development of positive or negative mechanical sensitivity. In the setting of high GLO1 expression, as in A/J mice, peptidergic neurons may be protected from extensive damage by reactive dicarbonyls and retain the ability to transmit noxious sensory information. However, A-fiber and nonpeptidergic sensory neurons have no detectable expression of GLO1 and may be more vulnerable to direct damage by reactive

dicarbonyl that leads to neuronal dysfunction in these fibers. This is supported by studies that suggest that a range of sensory afferents likely contribute to overall pain sensation, including both A and C-fibers (Shields, Cavanaugh et al. 2010). Therefore, despite protection from GLO1, it is possible that peptidergic C-fiber function may be affected by damage to other fibers which could lead to hyperexcitability and peripheral sensitization (Wu, Ringkamp et al. 2002; Ringkamp and Meyer 2005; Meyer and Ringkamp 2008).

Conversely, in the setting of low GLO1 expression, as in C57BL/6 mice, peptidergic neurons may accumulate reactive dicarbonyl-derived AGEs and experience physiological dysfunction similar to other fibers. Thus, peptidergic C-fiber mechano-thresholds may be increased due to intrinsic dysfunction stemming from reduced GLO1 expression and accumulation of reactive dicarbonyls. Previous studies in C57BL/6 mice have demonstrated that a reduction in peptidergic C-fibers following diabetes induction mirrored the loss of both mechanical and thermal sensitivity (Johnson, Ryals et al. 2008). Because this population of sensory neurons expresses GLO1 at significantly lower levels than other strains, particularly A/J mice, elevated intracellular glucose and reactive dicarbonyls could overwhelm the protective enzyme system and cause sensory dysfunction.

Nonpeptidergic fibers are by far the most prevalent C-fiber subpopulation innervating the epidermis (Lindfors, Voikar et al. 2006) with only 25-40% of the total fiber population classified as peptidergic (Zylka, Rice et al. 2005; Johnson, Ryals et al. 2008). Interestingly, the loss of cutaneous innervation is a hallmark of both painful and

painless neuropathy (Tavee and Zhou 2009). However, precise fiber-type changes in the skin have not been characterized as they have in rodents. However, overt fiber loss quantified in both diabetic C57BL/6 and A/J mice are likely nonpeptidergic fibers and peptidergic loss, in the case of C57BL/6, is masked by overall total innervation (Johnson, Ryals et al. 2008). It remains to be determined what percentage of peptidergic fibers, if any, is lost in A/J mice.

Although the present study does not directly address the mechanisms causing either positive or negative mechanical sensitivity associated with diabetic neuropathy, this issue is clearly important and relevant to humans with diabetic neuropathy. Sensory loss, including chronic numbness and insensitivity to pain or touch, develops in the majority of affected human patients. Painful symptoms, including tactile allodynia, are reported in approximately 30% of patients with DN, oftentimes present early in the disease progression, and have a slightly higher prevalence in type 2 diabetes (Sorensen, Molyneaux et al. 2002; Quattrini and Tesfaye 2003). This dichotomy in positive vs. negative symptoms is reflected in animal models of diabetic neuropathy, with some resembling the painful, and others the painless aspects of diabetic neuropathy (Christianson, Ryals et al. 2003; Walwyn, Matsuka et al. 2006; Calcutt and Backonja 2007). Our current findings in C57BL/6 and A/J mice are consistent with this feature and may provide approaches address how genetic differences, including altered GLO1 expression, may help shape the phenotype of diabetic neuropathy in diabetic patients.

Finally, our results revealed that GLO1 levels are reduced by diabetes in C57BL/6 mice, which could also play a role in determining the phenotype of the DN. Reductions in GLO1 in diabetic C57BL/6 mice could occur through increased proteosomal degradation, particularly if GLO1 itself is modified by methylglyoxal, or by RAGE-mediated reduction in GLO1 (Thornalley 2008). Both *in vivo* and *in vitro* overexpression of GLO1 has been shown to dramatically reduce the levels of reactive dicarbonyls and AGEs (Shinohara, Thornalley et al. 1998; Ahmed, Dobler et al. 2008; Morcos, Du et al. 2008). However, it remains to be seen if physiological overexpression is robust enough to produce similar reductions. Given the restricted expression pattern of GLO1 in the DRG and behavioral differences following induction of diabetes, our findings suggest that genetic variability in GLO1 could be a modifier of the spectrum of DN symptoms.

CHAPTER 4

Elevated Glyoxalase I Expression Provides Protection From Diabetes-Induced Peripheral Neuropathy

1. Abstract

Diabetic neuropathy is a common complication of diabetes mellitus with over half of all patients developing neuropathy symptoms due to sensory nerve damage. Diabetes-induced hyperglycemia leads to the accelerated production of advanced glycation end products (AGEs) that alter proteins, thereby leading to neuronal dysfunction. The glyoxalase enzyme system, specifically glyoxalase I (GLO1), is responsible for detoxifying precursors of AGEs, such as methylglyoxal and other reactive dicarbonyls. The purpose of our studies was to determine if expression differences of GLO1 play a role in the development of diabetic sensory neuropathy. BALB/cJ mice naturally express low levels of GLO1, while BALB/cByJ express approximately 10-fold higher levels on a similar genetic background due to increased copy numbers of GLO1. Five weeks following STZ injection, diabetic BALB/cJ mice developed a 68% increase in mechanical thresholds, characteristic of insensate neuropathy or loss of mechanical sensitivity. This behavior change correlated with a 38% reduction in intraepidermal nerve fiber density (IENFD). Diabetic BALB/cJ mice also had reduced expression of mitochondrial oxidative phosphorylation proteins in Complex I and V by 83% and 47%, respectively. Conversely, diabetic BALB/cByJ mice did not develop signs of neuropathy, changes in IENFD, or alterations in mitochondrial protein expression. Reduced expression of GLO1 paired with diabetes-induced hyperglycemia may lead to neuronal mitochondrial damage and symptoms of diabetic neuropathy. Therefore, AGEs, the glyoxalase system, and mitochondrial dysfunction may play a role in the development and modulation of diabetic peripheral neuropathy.

2. Introduction

As covered in Chapter 1, diabetic neuropathy is a secondary consequence of longstanding diabetes mellitus. Sensory neurons appear particularly vulnerable to elevated glucose and damage in diabetes mellitus (Zochodne, Ramji et al. 2008). Consequently, 50-70% of patients develop diabetic neuropathy signs and symptoms throughout the course of the disease (Centers for Disease Control and Prevention 2011). Moreover, diabetic neuropathy remains a growing problem in the United States and throughout the world with only limited symptomatic treatments (Edwards, Vincent et al. 2008).

Although the pathogenesis of diabetic neuropathy is likely multifactorial, one mechanism leading to sensory neuron damage and dysfunction is the accumulation of a heterogeneous group of reactive sugars known as advanced glycation endproducts (AGEs) (Ahmed 2005; Brownlee 2005). As discussed in Chapter 1, AGEs can form via a number of pathways inside and outside the neuron. In particular, reactive dicarbonyls, a potent producer of AGEs, are formed as a normal byproduct of glycolysis, lipid peroxidation, and degradation of glycated proteins (Ahmed and Thornalley 2007; Thornalley 2008). Each of these processes is enhanced in diabetes mellitus leading to an increased formation of toxic reactive dicarbonyls. Once formed, reactive dicarbonyls react with proteins, lipids, or nucleic acids forming AGEs and cause neuronal dysfunction (Thornalley 2008).

The glyoxalase system functions to detoxify reactive dicarbonyls before they react with cellular components and form AGEs (Rabbani and Thornalley 2011). The glyoxalase system is composed of two enzymes, glyoxalase I (GLO1) and glyoxalase II, that detoxify reactive dicarbonyls by converting them to lactic acid, thereby preventing the formation of AGEs (Thornalley 2003). As our previous results have shown in Chapter 2, GLO1 is primarily expressed in small, unmyelinated peptidergic neurons, a subset of DRG neurons that are responsible for pain transmission in the peripheral nervous system (Jack, Ryals et al. 2011). While GLO1 has been investigated in other diabetic complications, its role in diabetic neuropathy has remained largely uninvestigated.

GLO1 exists as a copy number variant (CNV) in many inbred strains mice (Williams, Lim et al. 2009). In particular, BALB/cByJ mice have multiple copies, while BALB/cJ mice have a single copy (Williams, Lim et al. 2009). BALB/cByJ and BALB/cJ mice originated from the same parental strain and were separated in the 1930s (Bailey 1978). Despite 80 years of segregated inbreeding, these two strains remain isogenic at all typed SNPs (Williams, Lim et al. 2009; Velez, Sokoloff et al. 2010). However, BALB/cJ have lost multiple copies of the region encompassing GLO1 (Williams, Lim et al. 2009). Thus, BALB/cByJ and BALB/cJ mice express variable levels of GLO1 on similar genetic backgrounds.

In Chapter 3, we investigated behavioral deficits in two strains that express different levels of GLO1 and develop diverse sensory deficits following diabetes

induction. However, these two strains have different genetic backgrounds. Consequently, we chose to use two substrains of BALB/c mice to determine diabetes-induced behavior deficits in mouse models that vary in their GLO1 expression.

Given the clear evidence showing GLO1 has a role in protecting against hyperglycemia-induced diabetic complications including nephropathy and endothelial dysfunction, GLO1 may also have a role in protecting sensory neurons from the damaging effects of diabetes mellitus (Wautier and Schmidt 2004; Ahmed, Dobler et al. 2008). In this study, we took advantage of the natural genetic variation in substrains of BALB/c mice to investigate sensory damage in diabetic neuropathy in strains expressing different amounts of GLO1. Our results suggest that higher expression of GLO1 protects against neuropathy-related behavior changes and sensory neuron damage associated with elevated reactive dicarbonyls.

3. Experimental Procedures

Animals

Male BALB/cJ and BALB/cByJ mice (Jackson, Bar Harbor, ME) were purchased at 7 weeks, one week prior to the onset of experimental testing. BALB/cJ mice were housed one mouse per cage, while BALB/cByJ mice were housed two per cage in 12/12-h light/dark cycle under pathogen free conditions. Mice were given free access to standard rodent chow (Harlan Teklad 8,604, 4% kcal derived from fat) and water. All

animal use was in accordance with NIH guidelines and conformed to principles specified by the University of Kansas Medical Center Animal Care and Use Protocol.

Diabetes Induction

Diabetes was induced in 8-week-old male BALB/cJ and BALB/cByJ mice. BALB/cJ and BALB/cByJ mice were injected with a single intraperitoneal injection of streptozocin (STZ) (260 mg/kg and 200 mg/kg body weight, respectively; Sigma, St. Louis, MO) dissolved in 10 mmol/L sodium citrate buffer, pH 4.5. Controls received sodium citrate buffer alone. Animals of either strain that did not develop hyperglycemia three days after the initial injection were re-injected with STZ (200 mg/kg body weight). Food was removed from all cages for 3 h before and after STZ injection. Animals did not receive insulin at any point in the study.

Glucose Measurements

Animal weights and blood glucose levels (glucose diagnostic reagents, Sigma, St. Louis, MO) were measured three days and one week after STZ injection. Both were then measured every week thereafter from tail vein sampling and decapitation blood pool for terminal measurements. Mice were considered diabetic if their fasting blood glucose level is greater than 200 mg/dl at every measurement.

Behavior Testing

Mice underwent training sessions on the four days prior to behavioral testing. Mice were placed into individual clear plastic cages on a wire mesh screen elevated 55

cm above the table. Mice were allowed to acclimate in their cages to the behavior room for 30 minutes and on the mesh grid for 15-45 minutes on the table during the training sessions, depending on the training day. Before each behavioral testing session, mice were allowed to acclimate to the behavior room in their cages for 30 minutes and to the wire mesh grid for 15 minutes. The up-down method was used to test mechanical sensitivity (Dixon 1980). Briefly, a set of standard von Frey monofilaments (0.02, 0.07, 0.16, 0.4, 1.0, 2.0, 6.0, and 10.0 g) were used. Beginning with the 0.4 g monofilament, mice received a single application to the right hindpaw. Depending on the response of the mouse to the previous application, the next smaller filament was used if there was negative response or the next larger gram filament was used if there was a positive response. This was repeated on each mouse until there was a change from either a positive response to negative response or vice versa. Four trials after the change were then conducted with 5 min intervals between applications. A positive response was considered a brisk withdrawal of the paw to which the force was applied. Five negative responses were recorded as the maximum threshold or 10 g, while 5 positive responses were recorded as the minimum threshold or 0.02 g. The 50% threshold was calculated for each mouse and group means were determined as previous described (Chaplan, Bach et al. 1994). Baseline behavior was measured before diabetes induction. Afterwards, all animals were tested weekly for 6 weeks.

Tissue Preparation

DRG were rapidly isolated and excised, immediately frozen in liquid nitrogen, and stored at -80^{o}C. DRG were sonicated for 5 intervals of 10 sec each in 50 μL Cell Extraction Buffer (Invitrogen, Carlsbad, CA) with protease inhibitor cocktail (Sigma, St. Louis, MO), 200 mM NaF, and 200 mM Na_3VO_4. The homogenates were incubated on ice for 30 mins before centrifugation at 7000 rpm for 10 mins at 4^{o}C. Protein concentrations were determined using the Bio-Rad protein assay based on the Bradford assay (Bio-Rad, Sydney, NSW, Australia).

Glyoxalase I Expression

Samples containing 100 μg of protein from total DRG homogenates were separated by electrophoresis through 4-20% SDS-PAGE gels (125 V, 1.5 h, 4^{o}C) and transferred onto nitrocellulose paper (35 mA, overnight, 4^{o}C). Nitrocellulose membranes were blocked with blocking buffer (3% non-fat milk and 0.05% Tween-20 in phosphate buffered saline) for 1 hour at room temperature to block non-specific binding sites. This was followed by overnight incubation with a goat anti-GLO1 primary antibody (R&D Systems, Minneapolis, MN) diluted 1:5000 in blocking buffer at 4^{o}C. The donkey anti-goat IgG-HRP (Santa Cruz, Santa Cruz, CA) secondary antibody was used diluted 1:2500 in blocking buffer at RT for 1 hour.

Nitrocellulose membranes were stripped using Restore Plus Western Blot Stripping Buffer (Pierce, Rockford, IL). This was followed by 1-hour incubation with

actin primary antibody (Millipore, Billerica, MA) diluted 1:100,000 in blocking buffer at RT. The donkey anti-mouse IgG-HRP secondary antibody (Santa Cruz, Santa Cruz, CA) was used diluted 1:2500 in blocking buffer at RT for 1 hour. The chemiluminescent signal was acquired using Supersignal West Femto Maximum Sensitivity Substrate (Pierce, Rockford, IL) and a CCD camera (BioSpectrum Imaging System, UVP, Upland, CA). Labworks Analysis Software (UVP, Upland, CA) was used to quantify densitometry readings.

Glutathione Assay

Total glutathione was measured using the Glutathione Assay Kit (Cayman Chemical, Ann Arbor, MI). Briefly, the entire spinal cord from 8 week-old nondiabetic BALB/cByJ and BALB/cJ mice was dissected, rinsed in PBS, immediately frozen in liquid nitrogen, and stored at -80^{o}C. Tissues were homogenized in 5 mL of cold buffer (50 mM PBS, pH 6, containing 1 mM EDTA) per gram of tissue. The samples were then deproteinated and the assay was performed according to the manufacturer's protocol.

Nerve Conduction Velocity

Nerve conduction velocity was conducted as previously described on a Viasys Healthcare TECA Synergy (Stevens, Obrosova et al. 2000; Muller, Ryals et al. 2008). Animals were deeply anesthetized with Avertin (1.25% v/v tribromoethanol, 2.5% tert-amyl alcohol, dH_2O; 200 mg/kg body weight). Corneal reflexes were checked and body temperature was monitored and maintained at 37^{o}C throughout the procedure. Motor

nerve conduction velocities (MNCVs) were obtained by measuring compound muscle action potentials using supramaximal stimulation (9.9 mA) at the ankle distally and at the sciatic notch proximally. The average of three independent recordings was obtained from the first interosseous muscle. Sensory nerve conduction velocity (SNCV) was measured behind the medial malleolus with a 0.5-ms square wave pulse using the smallest current to elicit a response (2.4 mA), stimulating at the digital nerve of the second toe. SNCV was the average of 10 recordings.

Intraepidermal Nerve Fiber Density

Cutaneous innervation of the footpad was assessed in nondiabetic and diabetic mice after six weeks of diabetes. The right footpad skin was harvested from mice at the time of sacrifice and immersion fixed in Zamboni's fixative (4% paraformaldehyde, 14% saturated picric acid, 0.1 M phosphate buffered saline; pH 7.4) for 1 hour on ice. Footpads were washed in PBS twice and placed in PBS overnight at 4^{o}C. Footpads were then cryoprotected in 30% sucrose overnight at 4^{o}C. 30 µm serial sections were cut and placed on Superfrost Plus microscope slides (Fischer, Chicago, IL). Immunohistochemistry was performed as previous described (Christianson, Ryals et al. 2007; Johnson, Ryals et al. 2008). Briefly, tissue sections were blocked in Primary Incubation Solution containing SuperBlock buffer (Pierce, Rockford, IL) with 1.5% normal donkey serum, 0.5% porcine gelatin, and 0.5% Triton X-100 for 1 hour at RT. Sections were then incubated in the primary antibody solution containing 1:1 Primary Incubation Solution and SuperBlock buffer with rabbit anti-PGP9.5 primary antibody

(1:400) overnight at 4°C. A donkey anti-rabbit secondary antibody (Alexa 555, 1:2000, Molecular Probes, Eugene, OR) in 1X PBST was incubated for 1 hour at 4°C. Small cutaneous, PGP9.5+ fibers that crossed the dermal-epidermal junction were quantified in three areas from three tissue sections from each footpad. The length of the dermal-epidermal junction was measured and intraepidermal nerve fiber density (IENFD) was expressed as the number of fibers per millimeter.

Mitochondrial Enzyme Expression

15 µg of protein from total DRG homogenates was separated by electrophoresis (150 V, 2 h, 4°C) on a 10-20% Tris-Glycine SDS-PAGE gels (Invitrogen, Carlsbad, CA) and transferred onto nitrocellulose paper (150 mA, 2 h, 4°C). Membranes were blocked in 5% non-fat milk and 0.05% Tween-20 in phosphate buffered saline either overnight at 4°C or 3 hours at RT. An antibody cocktail against mitochondrial electron transport proteins (MS601, MitoSciences, Eugene, OR) was diluted 205X in 1% milk and incubated at RT for 2 h.. The donkey anti-mouse IgG-HRP (Santa Cruz, Santa Cruz, CA) secondary antibody was used diluted 1:2000 in blocking buffer at RT for 2 hours. The chemiluminescence signal was acquired using Supersignal West Femto Maximum Sensitivity Substrate (Pierce, Rockford, IL) and a CCD camera (BioSpectrum Imaging System, UVP, Upland, CA). LabWorks Analysis Software (UVP, Upland, CA) was used to quantify densitometry readings. All bands were normalized for actin expression.

Statistics

Data are expressed as mean ± SEM. *n* is the number of animals per given experimental setting. Differences were analyzed using ANOVA followed by Bonferroni's test, as appropriate. Significance was defined as $p \leq 0.05$.

4. Results and Figures

Blood Glucose and Weights

More than 90% of mice of both strains injected with STZ developed diabetes shortly after injection. As early as 1 week following STZ injection, diabetic mice displayed markedly increased blood glucose levels. At the earliest time point, diabetic BALB/cByJ mice had an average blood glucose of 325.495 ± 15.943 mg/dl and diabetic BALB/cJ mice had an average blood glucose of 341.206 ± 19.735 mg/dl (Figure 1a). The elevated blood glucose persisted and worsened throughout the study with diabetic BALB/cByJ mice having an average blood glucose of 510.871 ± 19.737 mg/dl and diabetic BALB/cJ mice having an average blood glucose of 535.698 ± 12.120 mg/dl after 6 weeks of diabetes (Figure 1a). At all time points measured, diabetic mice from both strains had similar blood glucose levels that were not statistically different (Figure 1a).

Diabetic mice displayed other characteristic symptoms of hyperglycemia including polyuria, polydipsia, and limited weight gain. Throughout the study, nondiabetic BALB/cByJ mice gained on average 6.9 ± 0.3 g and, similarly, nondiabetic BALB/cJ mice gained 5.6 ± 0.6 g (Figure 1b). Conversely, diabetic mice had reduced

weight gain, as is characteristic of diabetic mouse models. Diabetic BALB/cByJ gained 2.1 ± 0.5 g from baseline, while diabetic BALB/cJ gained 0.2 ± 0.9 g (Figure 1b). Throughout the study, the average weight of diabetic mice was not significantly different between the two strains.

Behavioral Measures

The responses of mice to von Frey monofilaments were used to determine mechanical sensitivity of the right hindpaw by measuring the 50% gram threshold weekly. No difference existed in baseline behavioral measures between strains with thresholds of 2.429 ± 0.425 g for BALB/cByJ and 2.076 ± 0.323 g for BALB/cJ (p = 0.5110) (Figure 2). The baseline thresholds were similar for all four groups tested with nondiabetic BALB/cByJ mice, diabetic BALB/cByJ, nondiabetic BALB/cJ, and diabetic BALB/cJ having baseline thresholds of 2.152 ± 0.428 g, 3.119 ± 0.781 g, 2.975 ± 0.549 g, and 1.389 ± 0.329 g, respectively.

After five weeks of severe hyperglycemia, diabetic BALB/cJ mice develop increased mechanical thresholds that are indicative of insensate neuropathy (Figure 2). The 50% withdrawal threshold of diabetic BALB/cJ mice at five weeks after STZ injection was 5.899 ± 0.977 g, while nondiabetic BALB/cByJ and BALB/cJ mice had thresholds of 2.805 ± 0.581g and 1.888 ± 0.373 g, respectively. Decreased mechanical sensitivity was also present after six weeks of diabetes in diabetic BALB/cJ mice reaching nearly a 77% increase from baseline. Diabetic BALB/cJ mice at had

Figure 1: Diabetic BALB/cByJ and BALB/cJ mice display characteristic features of diabetes including hyperglycemia and smaller body weight.

Blood glucose (a) and weights (b) of nondiabetic and diabetic BALB/cByJ and BALB/cJ measured weekly for six weeks. (a) Diabetic BALB/cByJ (gray circles, n = 15) and BALB/cJ (red triangles, n = 15) showed similar blood glucose measures each week, which was significantly different than nondiabetic BALB/cByJ (black circles, n = 10) and BALB/cJ (black triangles, n =10) ($p < 0.0001$). (b) Diabetic BALB/cByJ (gray circles, n = 15) and diabetic BALB/cJ (red triangles, n = 15) had reduced weight gain compared to nondiabetic mice (black circles, BALB/cByJ, n =10 and black triangles, BALB/cJ, n = 10) ($p < 0.0001$). Data are presented as means ± SEM. *$p < 0.05$ vs. nondiabetic BALB/cByJ mice. ***$p < 0.001$ vs. nondiabetic BALB/cByJ mice. ****$p < 0.0001$ vs. nondiabetic BALB/cByJ mice. ##$p < 0.01$ vs. nondiabetic BALB/cJ mice. ###$p < 0.001$ vs. nondiabetic BALB/cJ mice. ####$p < 0.0001$ vs. nondiabetic BALB/cJ mice.

Figure 1

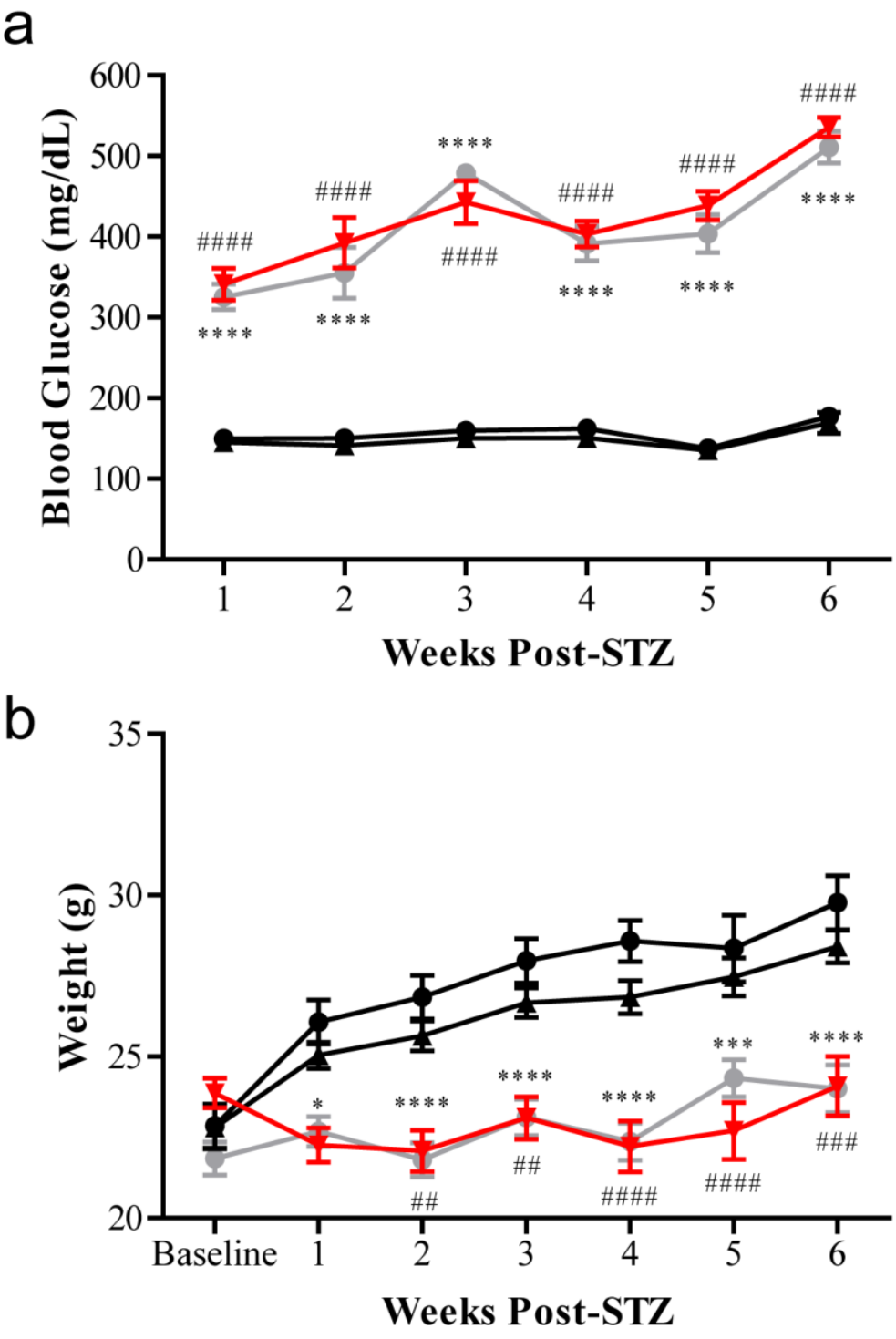
a
Blood Glucose (mg/dL)
600
500
400
300
200
100
0
1
2
3
4
5
6
Weeks Post-STZ
b
Weight (g)
35
30
25
20
Baseline
1
2
3
4
5
6
Weeks Post-STZ

Figure 2: Diabetic BALB/cByJ mice are protected from symptoms of neuropathy, while diabetic BALB/cJ mice develop symptoms insensate neuropathy.

Behavioral responses to non-noxious mechanical stimuli were evaluated weekly in nondiabetic BALB/cByJ (black circles), diabetic BALB/cByJ (gray circles), nondiabetic BALB/cJ (black triangles), and diabetic BALB/cJ (red triangles) mice. Baseline behavioral measurements were similar for all groups tested. By 5 weeks after STZ induction, diabetic BALB/cJ (red $n = 15$) mice developed increased mechanical thresholds indicative of insensate neuropathy. The mechanical thresholds of diabetic BALB/cByJ ($n = 15$) were not different from the thresholds of both nondiabetic strains ($n = 10$ each) at all time points suggesting diabetic BALB/cByJ are protected from neuropathy damage. Data plotted as means ± SEM. *$p < 0.05$ vs. nondiabetic BALB/cByJ. ***$p < 0.001$ vs. nondiabetic BALB/cByJ. ###$p < 0.001$ vs. diabetic BALB/cJ. ††$p < 0.01$ vs. diabetic BALB/cByJ. †††$p < 0.001$ vs. diabetic BALB/cByJ.

Figure 2

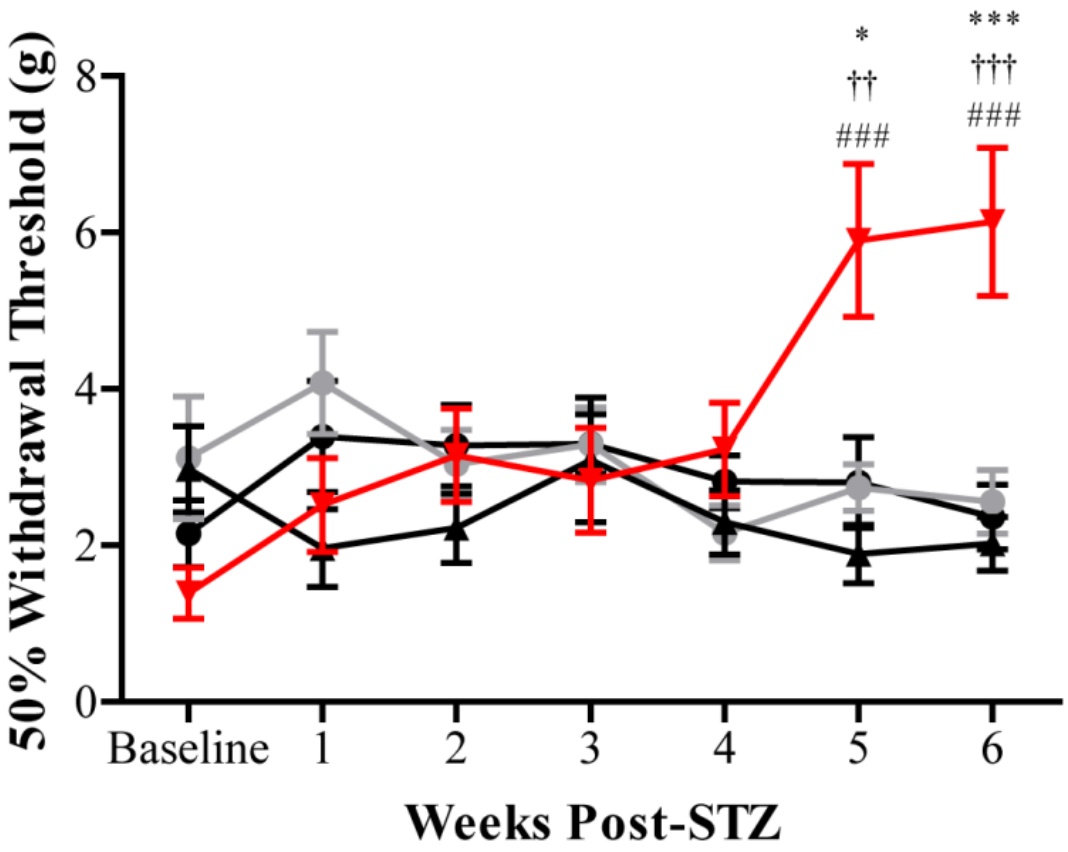
50% Withdrawal Threshold (g)
0
2
4
6
8
Baseline
1
2
3
4
5
6
Weeks Post-STZ
*
††
###
***
†††
###

mechanical thresholds of 6.138 ± 0.945 g, while nondiabetic BALB/cByJ and BALB/cJ mice had thresholds of 2.362 ± 0.415 g and 2.022 ± 0.344 g, respectively. This behavioral change is similar in time course and severity to that seen in STZ-treated C57BL/6 mice (Christianson, Ryals et al. 2007; Johnson, Ryals et al. 2008).

Despite having significant hyperglycemia for six weeks, diabetic BALB/cByJ mice do not develop thresholds significantly different from baseline (Figure 2). Mechanical thresholds of diabetic BALB/cByJ mice are also not significantly different from nondiabetic BALB/cByJ or BALB/cJ at any time point. On the other hand, diabetic BALB/cByJ mice had significantly lower thresholds compared to diabetic BALB/cJ mice at both five and six weeks post-STZ (2.739 ± 0.299 g vs. 5.899 ± 0.977g and 2.555 ± 0.408 g vs. 6.138 ± 0.945 g).

GLO1 Expression in Diabetes

After six weeks of diabetes, Western blots were used to determine GLO1 expression differences between strains and the impact of diabetes on GLO1 levels. Nondiabetic BALB/cByJ mice had significantly higher expression of GLO1 in the DRG compared to nondiabetic BALB/cJ (1.000 ± 0.084 vs. 0.132 ± 0.097) (Figure 3). Since GLO1 expression remained unchanged from nondiabetic levels following diabetes induction in both diabetic BALB/cJ and BALB/cByJ, diabetic BALB/cJ mice had significantly lower expression than diabetic BALB/cByJ mice (0.091 ± 0.001 vs. 0.852 ± 0.134) (Figure 3). Combined, BALB/cByJ mice had 8-15-fold higher GLO1 expression compared to BALB/cJ mice.

Figure 3: BALB/cByJ mice express higher levels of GLO1 compared to BALB/cJ mice.

GLO1 expression in the DRG was measured by Western blot in nondiabetic (n = 3 each) and diabetic mice (n = 4 each) following 6 weeks of diabetes. Nondiabetic BALB/cByJ mice express significantly higher levels of GLO1 compared to nondiabetic BALB/cJ mice. Similarly, diabetic BALB/cByJ mice also have significantly higher expression of GLO1 compared to diabetic BALB/cJ mice. Diabetes does not affect the expression of GLO1 in either strain. Diabetic BALB/cByJ and BALB/cJ mice show similar expression levels as their nondiabetic counterparts. Data plotted as means ± SEM. ***$p < 0.001$ vs. nondiabetic Balb/cByJ. ###$p < 0.001$ vs. diabetic Balb/cByJ.

Figure 3

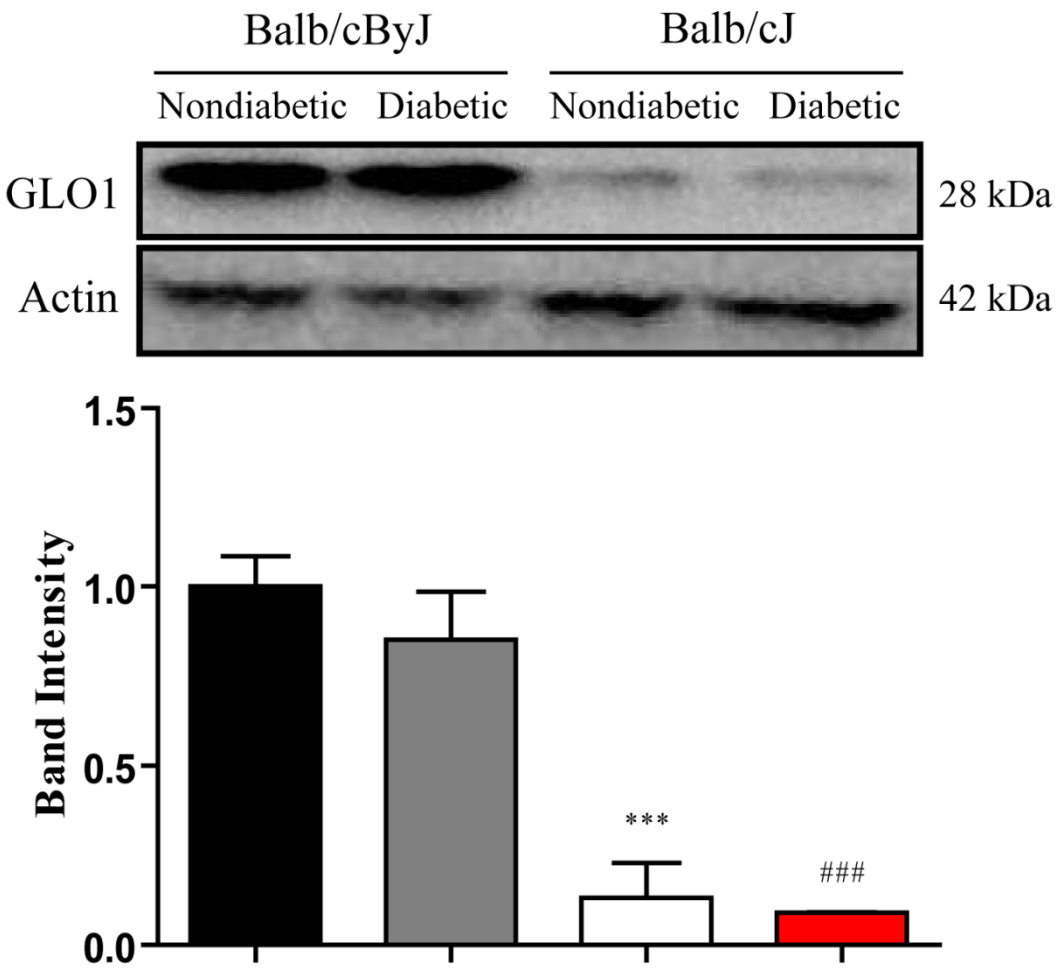
Balb/cByJ
Balb/cJ
Nondiabetic
Diabetic
Nondiabetic
Diabetic
GLO1
28 kDa
Actin
42 kDa
Band Intensity
1.5
1.0
0.5
0.0
***
###

Glutathione Measurement

Total glutathione was measured in the whole spinal cord from 8 week-old nondiabetic BALB/cByJ and BALB/cJ (Figure 4). Glutathione concentrations were not significantly different between the two strains. Nondiabetic BALB/cByJ mice had glutathione concentrations of 0.291 ± 0.128 µM/mg protein and nondiabetic BALB/cJ mice had 0.206 ± 0.102 µM/mg protein in the spinal cord.

Intraepidermal Nerve Fiber Density Following Diabetes Induction

After six weeks of diabetes, the pan-neuronal marker, PGP-9.5 was used to quantify cutaneous C-fibers in the hindpaw epidermis. IENFD was similar between strains of nondiabetic mice (Figure 5a, b, and e). Control BALB/cByJ mice had 80.3 ± 5.3 fibers/mm in the right hindpaw which was no different from control BALB/cJ mice that had 89.3 ± 4.5 fibers/mm. Conversely, diabetic BALB/cJ mice had 38% and 31% loss of cutaneous innervation compared to nondiabetic BALB/cJ and BALB/cByJ, respectively (Figure 5a, b, d, and e). On the other hand, diabetic BALB/cByJ mice, which did not display mechanical deficits, showed IENFD similar to both nondiabetic strains (Figure 5 a, b, c, and e). Thus, diabetic BALB/cJ mice also showed a 35% reduction of IENFD compared to diabetic BALB/cByJ mice.

Figure 4: Spinal cord glutathione concentration is not different between strains of diabetic mice.

Glutathione was measured in the spinal cord of 10 week old nondiabetic BALB/cByJ (black bar) and BALB/cJ (white bar) by colorimetric assay. Both strains had similar levels of glutathione (n = 3). Data expressed as µM/mg of protein and plotted as means ± SEM.

Figure 4

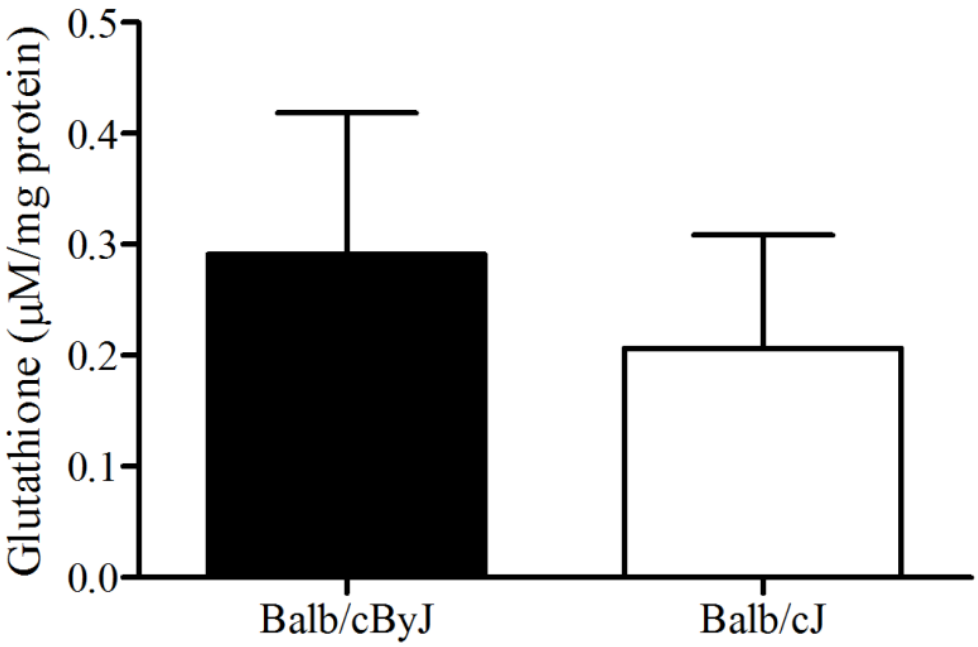

Figure 5: Intraepidermal nerve fiber density is reduced in diabetic BALB/cJ mice.

Representative photomicrographs of skin from the right footpad of (a) nondiabetic BALB/cByJ, (b) nondiabetic BALB/cJ, (c) diabetic BALB/cByJ, and (d) diabetic BALB/cJ mice. Diabetic BALB/cJ mice show a reduction in PGP9.5-positive cutaneous nerve fibers in the skin. Scale bar = 10 µm. (e) Quantification of IENFD of nondiabetic BALB/cByJ (black bar, n = 5), diabetic BALB/cByJ (gray bar, n = 5), and nondiabetic BALB/cJ (white bar, n =5). Diabetic BALB/cJ (red bar, n = 5) have a significant loss of cutaneous innervation after six weeks of diabetes. Data plotted as means ± SEM. ###p < 0.001 vs. nondiabetic BALB/cJ. *p < 0.05 vs. nondiabetic BALB/cByJ. ††p < 0.01 vs. diabetic BALB/cJ.

Figure 5

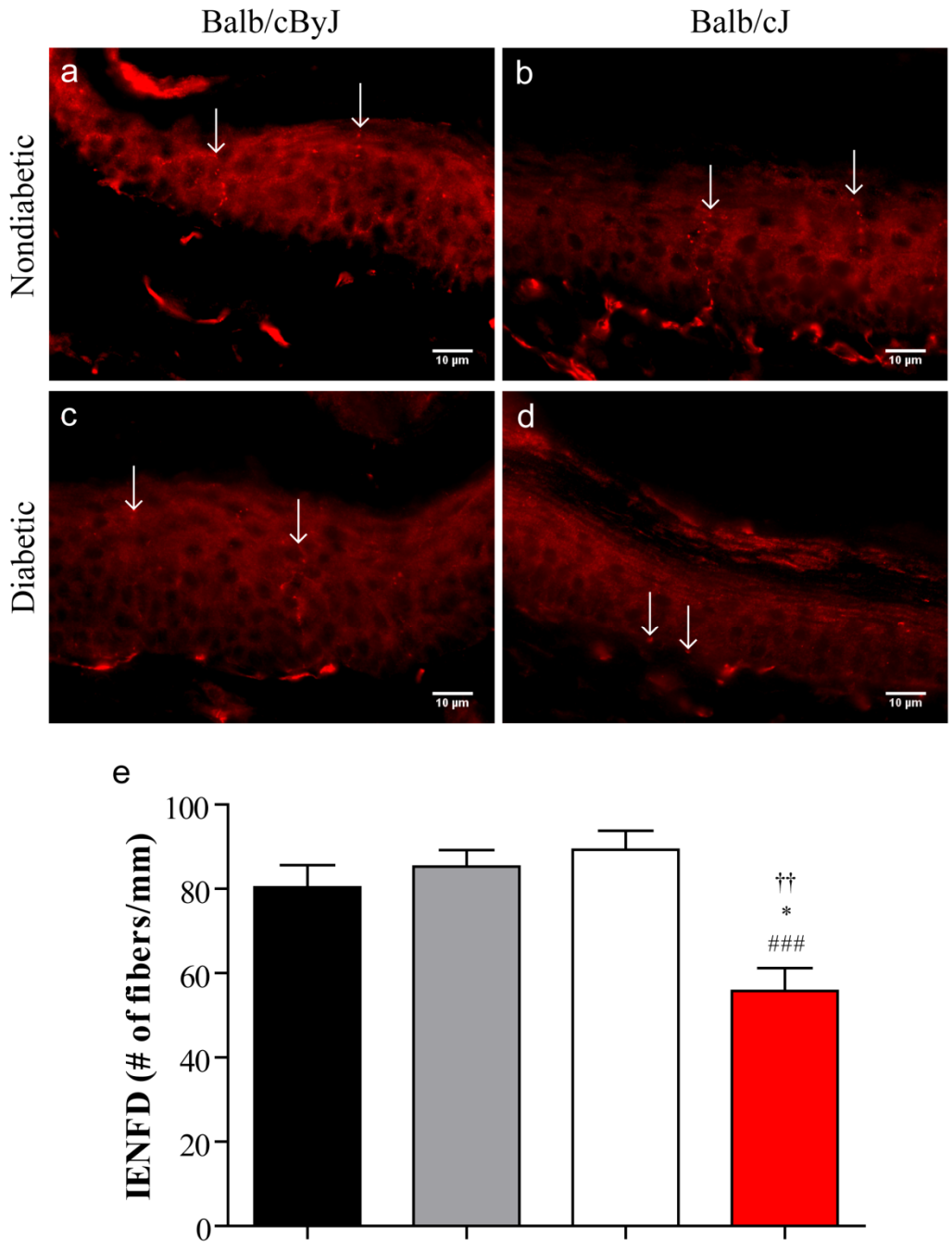
Balb/cByJ
Balb/cJ
Nondiabetic
Diabetic
a
b
c
d
10 µm
e
IENFD (# of fibers/mm)
100
80
60
40
20
0
††
*
###

Nerve Conduction Velocity

Both motor (MNCV) and sensory nerve conduction velocities (SNCV) were measured at the end of the six-week study in all four groups. SNCV was not significantly different between any groups (p=0.055) (Figure 6a). While nondiabetic BALB/cByJ and BALB/cJ mice had similar MNCV (50.825 ± 1.380 m/s vs. 55.120 ± 1.088 m/s, respectively), recordings identified motor dysfunction in both diabetic strains (Figure 6b). Diabetic BALB/cByJ mice had MNCVs of 42.456 ± 1.716 m/s, which was significantly lower compared to both nondiabetic BALB/cByJ and BALB/cJ strains. However, diabetic BALB/cJ mice only had significant slowing of MNCV when compared to nondiabetic BALB/cJ mice. The MNCV of diabetic BALB/cJ mice was similar to diabetic BALB/cByJ mice (Figure 6b).

Mitochondrial Dysfunction

The expression of mitochondrial oxidative phosphorylation proteins was measured in the DRG to determine potential mechanisms leading to neuronal dysfunction. No strain differences were apparent in the levels of Complex I subunit NDUFB8, Complex II FeS subunit, Complex III subunit Core 2, or Complex V subunit alpha between nondiabetic BALB/cByJ and BALB/cJ mice (Figure 7a, b, c, and d). Strikingly, Complex I expression was dramatically reduced in diabetic BALB/cJ compared to the other three groups (Figure 6d). The expression of the NDUFB8 subunit was 83%, 81%, and 81% lower compared to nondiabetic BALB/cJ, nondiabetic BALB/cByJ, and diabetic BALB/cByJ, respectively (Figure 7d). While Complex II and

III expression was not significantly different between groups (Figure 7b and c), Complex V was also reduced by 47% and 51% in diabetic BALB/cJ mice compared to nondiabetic BALB/cJ and diabetic BALB/cByJ mice (Figure 7a).

5. Discussion

In this study, two genetically similar strains of inbred mice that are natural genetic variants of GLO1 were used to investigate the potential role of GLO1 in development and modulation of diabetic neuropathy. We have previously shown GLO1 is predominately expressed in small, unmyelinated peptidergic neurons in the DRG, suggesting this DRG sensory neurons may be more or less vulnerable to hyperglycemia-damage depending on the level of GLO1 expression. Here, our results reveal that BALB/cByJ mice have increased expression of GLO1 and are protected from the development of neuropathy symptoms following six weeks of hyperglycemia, while BALB/cJ mice develop increased mechanical thresholds and hypoalgesia characteristic of insensate neuropathy. Other parameters of neuron dysfunction are present in both diabetic strains including slowing of MNCV, however, only diabetic BALB/cJ mice display reduced C-fiber innervation of the hindpaw. It is plausible to suggest that these anatomical and behavior changes are a consequence of differential levels of reactive dicarbonyl-derived AGEs that modify mitochondrial oxidative phosphorylation structural proteins and lead to mitochondrial dysfunction (Brownlee 2005; Brouwers, Niessen et al. 2010). Collectively, these results suggest that reduced expression of GLO1 may prevent efficient

Figure 6: Motor nerve conduction velocity (MNCV), but not sensory nerve conduction velocity (SNCV), is reduced in diabetic mice.

Quantification of (a) SNCV and (b) MNCV in nondiabetic BALB/cByJ (black bars, n = 10), diabetic BALB/cByJ (gray bars, n = 14), nondiabetic BALB/cJ (white bars, n = 10), and diabetic BALB/cJ (red bars, n = 7). SNCV is not significantly different between groups. However, MNCV is reduced in diabetic mice compared to their nondiabetic counterparts. Data plotted as means ± SEM. ***$p < 0.001$ vs. nondiabetic BALB/cByJ. #$p < 0.05$ vs. nondiabetic BALB/cJ.

Figure 6

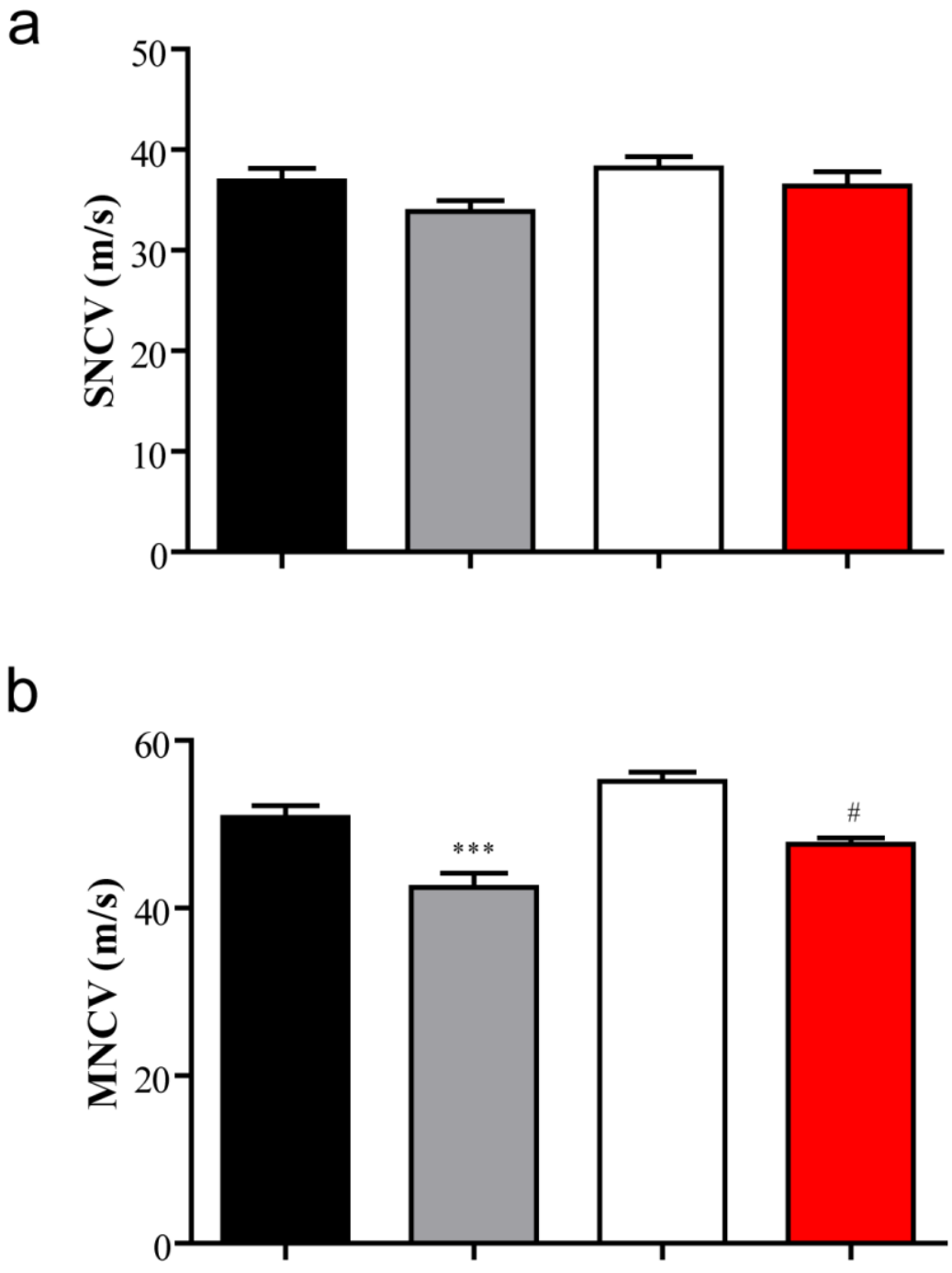

Figure 7: Mitochondrial oxidative phosphorylation proteins are reduced in diabetic BALB/cJ mice.

The expression of proteins from mitochondrial oxidative phosphorylation complexes were measured in the DRG after six weeks of diabetes. The expression of structural components of complexes V (a), III (b), II (c), and I (a) were all accessed by Western blot in nondiabetic BALB/cByJ (black bars, $n = 3$), diabetic BALB/cByJ (gray bars, $n = 3$), nondiabetic BALB/cJ (white bars, $n = 3$), and diabetic BALB/cJ (red bars, $n = 3$). Expression of both ATP synthase subunit α and Complex I subunit NDUFB8 were significantly reduced in diabetic BALB/cJ mice unlike diabetic BALB/cByJ mice. #$p < 0.05$ vs. nondiabetic BALB/cJ. ##$p < 0.01$ vs. nondiabetic BALB/cJ. *$p < 0.05$ vs. nondiabetic BALB/cByJ. †$p < 0.05$ vs. diabetic BALB/cJ.

Figure 7

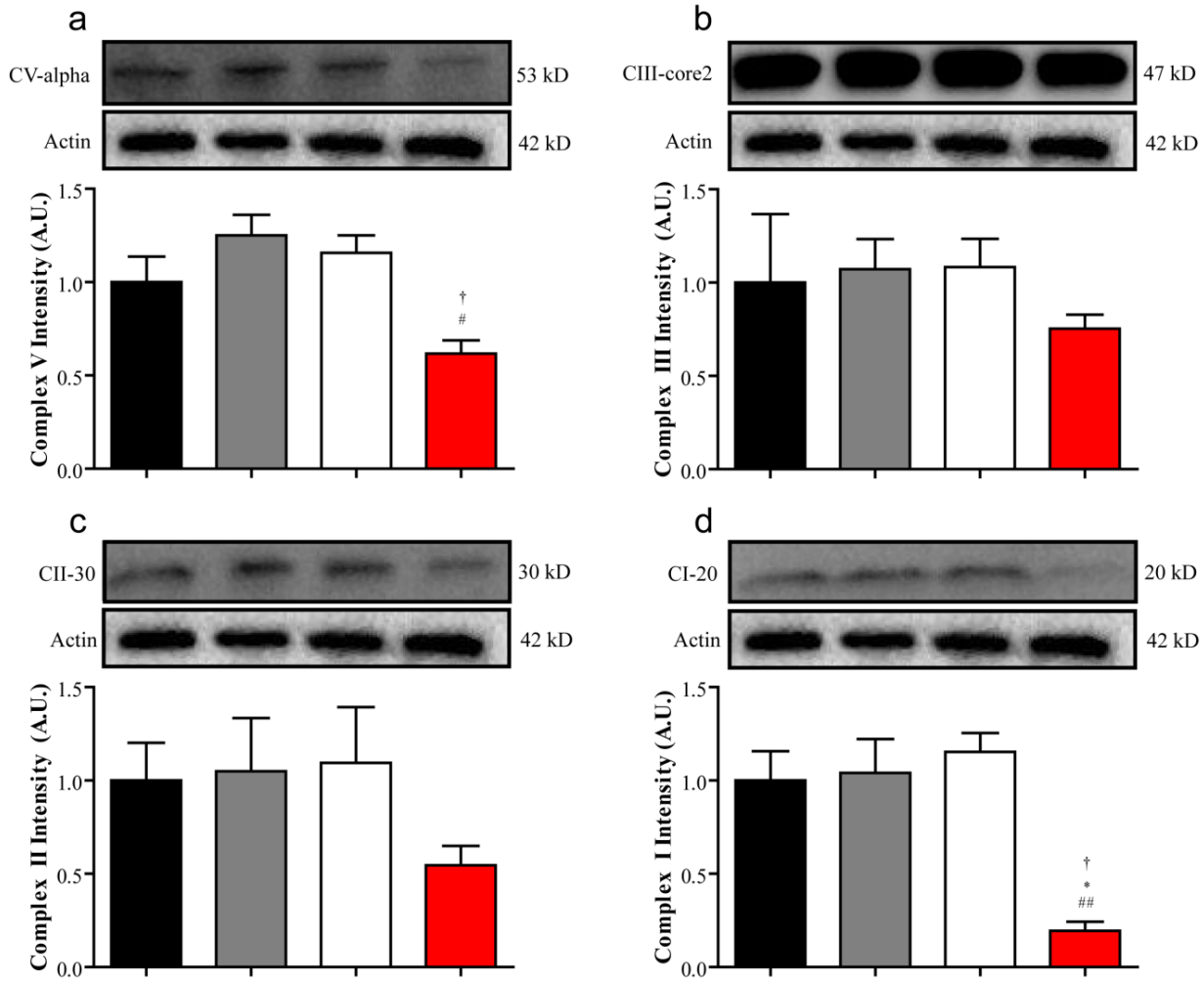
a
CV-alpha
53 kD
Actin
42 kD
Complex V Intensity (A.U.)
1.5
1.0
0.5
0.0
†
#
b
CIII-core2
47 kD
Actin
42 kD
Complex III Intensity (A.U.)
1.5
1.0
0.5
0.0
c
CII-30
30 kD
Actin
42 kD
Complex II Intensity (A.U.)
1.5
1.0
0.5
0.0
d
CI-20
20 kD
Actin
42 kD
Complex I Intensity (A.U.)
1.5
1.0
0.5
0.0
†
*
##

breakdown of reactive-dicarbonyl that cause mitochondrial damage, loss of peripheral C-fiber innervation, and the development of mechanical insensitivity in diabetic neuropathy.

Numerous studies have shown overexpression of GLO1 to be protective against reactive dicarbonyl damage (Morcos, Du et al. 2008; Schlotterer, Kukudov et al. 2009; Brouwers, Niessen et al. 2010; Brouwers, Niessen et al. 2010; Gangadhariah, Mailankot et al. 2010). However, few studies have investigated the importance of GLO1 at physiological levels. To our knowledge, this is the first to investigate variable expression in peripheral nerves and its role in the development of diabetic neuropathy. A week after the onset of reduced mechanical sensitivity, GLO1 expression in the DRG of diabetic BALB/cJ mice remains similar to that of nondiabetic mice. Although expression and activity in diabetes are likely species-, strain-, and tissue-dependent, our studies suggest that GLO1 expression is not altered by diabetes in the DRG of these two strains of inbred mice. However, due to the known CNV, GLO1 expression in both nondiabetic and diabetic BALB/cJ mice is significantly lower than either nondiabetic or diabetic BALB/cByJ mice. Higher expression of GLO1 may limit carbonyl stress and ultimately reduce AGE-mediated damage, at least early in the disease process.

The loss of cutaneous nerve fibers, nerve conduction velocity, and behavioral measures have all been used to assess the presence of sensory nerve damage characteristic of diabetic neuropathy in both rodents and human patients. Diabetic BALB/cJ mice develop loss of epidermal innervation, reduced nerve conduction velocities, and increased mechanical thresholds, as do majority of diabetic patients. At

least early in the disease course, diabetic BALB/cByJ mice are protected from developing signs of diabetic neuropathy that diabetic BALB/cJ mice develop. Similarly, a sizable percentage of patients, nearly 30-40%, do not develop classic overt neuropathy signs and symptoms even after years of diabetes mellitus. Recently, a study of Joslin Gold Medalists, patients who have survived type I diabetes mellitus for over 50 years, determined that glycemic control was unrelated to the development of diabetic complications (Sun, Keenan et al. 2011). However, those patients with higher concentrations of AGEs, including methylglyoxal-derived *N*-(carboxyethyl)lysine, were 2.5 times more likely to suffer from neuropathy (Sun, Keenan et al. 2011). Those authors and others have suggested that certain patients may have an abundance of protective mechanisms that allow them to remain complication free.

This suggests that underlying genetic differences in certain diabetic patients can protect against damage from methylglyoxal. Since GLO1 is the major detoxification system of reactive dicarbonyls, it is plausible that differences in production and activity of the enzyme influences AGE production and the development and/or modulation of diabetic neuropathy. Studies have recognized various SNPs, null alleles, and CNVs of GLO1 in humans (Sparkes, Sparkes et al. 1983; Gale, Futers et al. 2004; Gale and Grant 2004; Redon, Ishikawa et al. 2006). While a number of studies have measured increased AGEs in diabetic patients in the skin and peripheral nerve (Sugimoto, Nishizawa et al. 1997; Misur, Zarkovic et al. 2004; Meerwaldt, Links et al. 2005; Yu, Thorpe et al. 2006), limited investigation into the variability of protective mechanisms, particularly in these

tissues, has occurred and may help explain why some patients develop diabetic neuropathy and others do not.

Investigation into early signs and symptoms of neuronal dysfunction is critical to understanding the mechanisms driving the pathogenesis of diabetic neuropathy. A week after the onset of reduced mechanical sensitivity in diabetic BALB/cJ mice, the expression of structural components of mitochondrial oxidative phosphorylation proteins Complex I and V is dramatically reduced. Evidence linking reactive dicarbonyls with mitochondrial dysfunction has been mounting (Rabbani and Thornalley 2008). In a *C. elegan* model of aging, the reactive dicarbonyl-derived AGE, MG-H1, modified mitochondrial proteins leading to increased ROS which was attenuated with GLO1 overexpression (Morcos, Du et al. 2008). *In vitro* investigation utilizing a neuroblastoma cell line found ATP and mitochondrial membrane potential were both reduced following exposure to methylglyoxal (de Arriba, Stuchbury et al. 2007). Further evidence suggesting increased GLO1 expression protects against mitochondrial damage was recently published utilizing a transgenic rat model overexpressing GLO1. Diabetic transgenic rats showed increased GLO1 expression, reduced levels of plasma reactive dicarbonyls and AGEs, and higher expression of mitochondrial oxidative phosphorylation proteins compared to wild type diabetic rats (Brouwers, Niessen et al. 2010).

Mitochondrial dysfunction has also been implicated in the pathogenesis of diabetic neuropathy. Similar to our data, Chowdhury *et al.* observed reduced expression of NDUFS3, one component of the iron-sulfur protein of Complex I, in STZ-diabetic rats

(Chowdhury, Zherebitskaya et al. 2010). They have also observed alterations in other mitochondrial proteins, including components of oxidative phosphorylation including ATP synthase (Akude, Zherebitskaya et al. 2011). Functionally, rates of respiration and activity of oxidative phosphorylation complexes are reduced in in the peripheral nervous system of diabetic rats that result from proteome alterations (Chowdhury, Zherebitskaya et al. 2010). With evidence linking oxidative phosphorylation proteins modified by reactive dicarbonyls with mitochondrial dysfunction, diabetic BALB/cByJ mice could be protected from these proteome alterations due to increased GLO1 production. Thus, genetic differences in protective mechanisms, particularly of GLO1, could play a role in preventing early mitochondrial dysfunction that causes sensory neuron damage and diabetic neuropathy symptoms.

CHAPTER 5

Mitochondrial Oxidative Phosphorylation Proteins Are Reduced Following *In Vitro* Methylglyoxal Treatment of Sensory Neurons

1. Abstract

Altered mitochondrial function has been implicated in the development of many neurological disorders. Recently, mitochondrial stress and dysfunction have been recognized in sensory neurons and Schwann cells from diabetic rodents and clinically in cases of neuropathy; however the cause and implications of this dysfunction remain unknown. In this study, cultured adult sensory neurons from nondiabetic animals were treated with methylglyoxal. Methylglyoxal was not overtly to toxic sensory neurons and did not result in neuronal death. However, methylglyoxal treatment resulted in significant reduction in the expression of mitochondrial oxidative phosphorylation proteins in C57BL/6 mice. However, similar treatment did not result in altered expression of mitochondrial oxidative phosphorylation proteins in BALB/cByJ or BALB/cJ. These results suggest that alterations in the mitochondrial proteome due to increased reactive dicarbonyls, particularly mitochondrial oxidative phosphorylation proteins, could underlie sensory neuron dysfunction and have a role in the development of hyperglycemia-induced axonopathy in diabetic neuropathy.

2. Introduction

Mitochondria function in wide range of critical cellular pathways including fatty acid breakdown, calcium homeostasis, oxidative phosphorylation, and energy production, all of which are required for proper neuronal function (Mattson, Gleichmann et al. 2008; Luce, Weil et al. 2010; Pickrell and Moraes 2010). Consequently, neurons are especially sensitive and vulnerable to alterations of normal mitochondrial function (Han, Tomizawa

et al. 2011). Mitochondrial dysfunction has been recognized in numerous neurological disorders (Mattson, Gleichmann et al. 2008). It has also become an increasingly recognized and clinically important mechanism in the development of peripheral neuropathies, which suggests diabetic neuropathy could also result from mitochondrial damage in sensory neurons (Mattson, Gleichmann et al. 2008; Feely, Laura et al. 2011; Lehmann, Chen et al. 2011). Oxidative phosphorylation defects have been recognized in secondary complications of diabetes mellitus, such as nephropathy and cardiomyopathy, however, investigation into alterations of the mitochondrial proteome in diabetic neuropathy has severely lagged behind.

Several studies have shown reactive dicarbonyls target and modify mitochondrial proteins including oxidative phosphorylation proteins and can result in reduced expression of these complexes (Rosca, Mustata et al. 2005; Morcos, Du et al. 2008; Brouwers, Niessen et al. 2010). Indeed, in Chapter 4, our results revealed that mitochondrial oxidative phosphorylation protein expression was blunted in DRG from diabetic BALB/cJ mice that have low levels of GLO1 and develop increased mechanical thresholds. On the other hand, diabetic BALB/cByJ mice, which have higher levels of GLO1, were protected from sensory neuron dysfunction and perturbations of mitochondrial oxidative phosphorylation complexes. In support of these findings, this study set out to determine if cultured sensory neurons were vulnerable to methylglyoxal-induced reductions of mitochondrial oxidative phosphorylation complexes.

3. Experimental Procedures

Animals

All experiments were approved by the University of Kansas Medical Center Institutional Animal Care and Use Committee in accordance with NIH guidelines and Animal Care and Use Protocol. Male C57BL/6 (Charles River, Wilmington, MA), BALB/cByJ, and BALB/cJ (Jackson Laboratories, Bar Harbor MA) were purchased at 8 weeks of age. Animals were house in 12/12-h light/dark cycle under pathogen free conditions.

Adult DRG Culture

Mice were anesthetized with avertin (1.25% v/v tribromoethanol, 2.5% tert-amyl alcohol, dH_2O; 200 mg/kg body weight) and transcardially perfused with ice-cold Hank's Buffered Salt Solution (HBSS; Sigma Aldrich). DRG were harvested and transferred to HBSS without Ca^{2+}/Mg^{2+}. Culture conditions were performed in accordance with previously published protocols (Malin, Davis et al. 2007). DRG were partially digested with papain (Worthington; Lakewood, NJ) solution followed by digestion with collagenase type II (Worthington, Lakewood, NJ)/dispase (Roche; Basel, Switzerland) solution. Sensory neurons were titurated with a fire-polished glass Pasteur pipette to dissociate neuronal cell bodies. Neurons were grown on Laminin/poly-D-lysine coated coverslips (BD Biosciences; Bedford, MA) placed in 24 well culture plates (Sigma Aldrich) for viability studies. For western blot analysis, neurons were grown in

Laminin/poly-D-lysine coated 6-well plates (BD Biosciences; Bedford, MA). F12 culture medium (Invitrogen; Carlsbad, CA) was supplemented with 1X B27 minus antioxidant supplement (Invitrogen) and 1,000 U/ml penicillin/streptomycin antibiotics. Cultures were maintained at 37^{o}C and 5% CO_2.

Methylglyoxal Treatment

Methylglyoxal (Sigma Aldrich) was diluted to 100 mM in sterile H_2O and maintained at 4^{o}C. For low dose culture treatments, F12 media supplemented with 1X B27 minus antioxidants and antibiotics was prepared with methylglyoxal diluted to the working concentration (5, 10, 15, 20, of 25 μM). For high dose culture treatments, F12 media with antibiotics only was prepared with methylglyoxal diluted to 100 μM. Control wells received media only. Media was replaced with medium containing methylglyoxal 12-18 hours after initial culturing. Cultures were treated for 24 hours total with the media being replaced after 12 hours of treatment to maintain methylglyoxal concentrations.

LIVE/DEAD Assay

The LIVE/DEAD Viability/Cytotoxicity Kit (Invitrogen) was used to determine neuronal viability following methylglyoxal treatment. After 24 hour methylglyoxal treatment, coverslips were washed with D-PBS (Sigma Aldrich). Coverslips were then covered with LIVE/DEAD solution containing 2 mM EthD-1 and 4 mM calcein AM for 30 minutes. Coverslips were mounted on slides and imaged. Live (green) and dead (red)

neurons were counted in six frames from each coverslip. Three coverslips per treatment were counted.

Western Blot

Cultures were washed three times with D-PBS before harvesting protein. Cell Extraction Buffer (Invitrogen) containing protease inhibitor cocktail (Sigma, St. Louis, MO), 200 mM NaF, and 200 mM Na_3VO_4 was added to the wells and cells were harvested using a cell scraper. Samples were then incubated on ice for 30 minutes with light vortexing every 5 minutes followed by centrifugation at 7000 rpm for 10 minutes at 4^{o}C. Amicon Ultra-0.5 mL Centrigugal Filters (Millipore; Billerica, MA) were used to concentrate protein samples. Following concentration, protein concentrations were determined with a Bradford assay (Bio-Rad; Hercules, CA). 10 µg of protein were separated by electrophoresis (150 V, 2 h, 4^{o}C) on a 10-20% Tris-Glycine SDS-PAGE gels (Invitrogen, Carlsbad, CA) and transferred onto nitrocellulose paper (150 mA, 2 h, 4^{o}C).

For fluorescent Western blot detection, immunoblots were blocked in Odyssey Blocking Buffer (LI-COR Biosciences; Lincoln, NE) for 1 h at RT followed by overnight incubation with a rabbit anti-actin (Millipore; 1:1000) primary antibody at 4^{o}C in blocking buffer. The IR Dye 800 anti-rabbit antibody (Rockland; 1:1000) and Odyssey infrared imaging system (LI-COR) were used to detect the fluorescence signal.

To detect mitochondrial oxidative phosphorylation proteins, membranes were then blocked in 5% non-fat milk and 0.05% Tween-20 in phosphate buffered saline for 3 hours at RT. An antibody cocktail against mitochondrial electron transport proteins (MS601, MitoSciences, Eugene, OR) was diluted 208X in 1% milk and incubated at RT for 3 h.. The donkey anti-mouse IgG-HRP (Santa Cruz, Santa Cruz, CA) secondary antibody was used diluted 1:1000 in blocking buffer at RT for 2 h. Membranes were also incubated with either rabbit anti-Akt (Cell Signaling; Danvers, MA; 1:000) or rabbit anti-neurofilament L (Cell Signaling; 1:1000) for 1 h at RT. The donkey anti-rabbit IgG-HRP (Santa Cruz) secondary antibody was used diluted 1:1000 in 1% milk at RT for 1 h. The chemiluminescence signal was acquired using Supersignal West Femto Maximum Sensitivity Substrate (Pierce, Rockford, IL) and a CCD camera (BioSpectrum Imaging System, UVP, Upland, CA). LabWorks Analysis Software (UVP, Upland, CA) was used to quantify densitometry readings. All measurements were normalized to a housekeeping gene.

Statistics

Data are expressed as mean ± SEM. Differences were analyzed using Student's T-test or ANOVA followed by Bonferroni's test, as appropriate. Significance was defined as $p \leq 0.05$.

4. Results and Figures

Viability of Cultured Sensory Neurons After Low Dose Methylglyoxal Treatment

To determine if methylglyoxal was significantly toxic to cells, neuronal survival was measured following methylglyoxal treatment. Primary cultures of adult sensory neurons from nondiabetic C57BL/6 mice were treated with 0, 5, 10, 15, 20, or 25 µM methylglyoxal. The viability of neurons following methylglyoxal treatment was not significantly impaired (Figure 1a and 1b). Sensory neurons had a survival of 98% ± 1 following treatment with the highest concentration of methylglyoxal (25 µM).

Expression of Mitochondrial Oxidative Phosphorylation Proteins Following Low Dose Methylglyoxal Treatment of Sensory Neurons from C57BL/6 Mice

To determine if methylglyoxal has an effect on the expression of oxidative phosphorylation proteins, DRG sensory neurons were treated with low dose methylglyoxal. Following 24-hour methylglyoxal treatment, the expression of mitochondrial oxidative phosphorylation proteins was determined in C57BL/6 sensory neurons by Western blot. The expression of structural components of Complex V, III, II, and I were not altered following low dose methylglyoxal treatment (Figure 2).

Figure 1: Sensory neurons survival methylglyoxal treatment

Cultured C57BL/6 sensory neuron viability was accessed following treatment with (a) 0, 5, 10, 15, 20, and 25 µM methylglyoxal for 24 hours. Live (green) and dead (red) cells were counted as shown in the photomicrographs and the percent viability was calculated. (b) Quantification of the percent viability for each treatment. Scale bar; 50 µM.

Figure 1

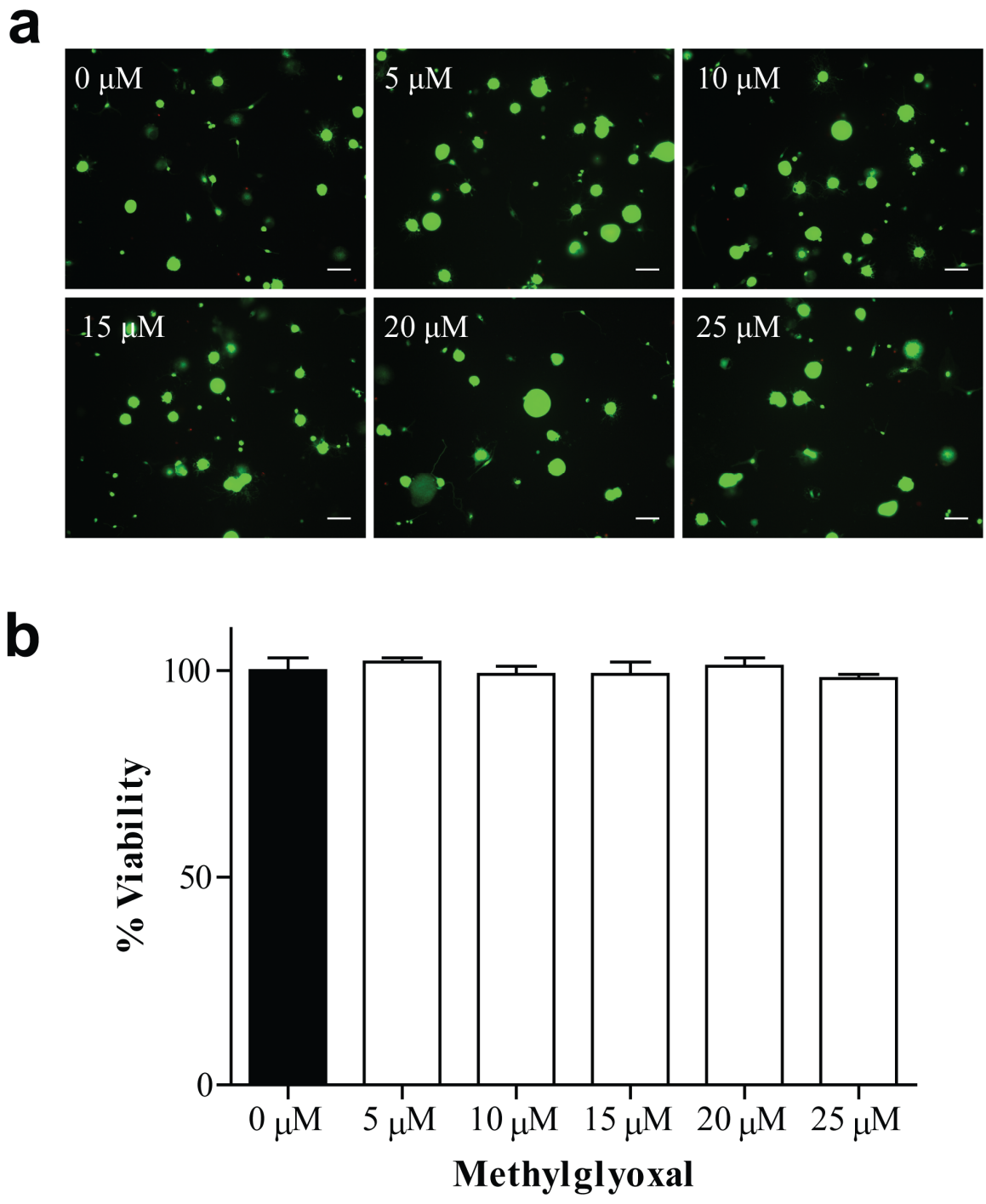
a
0 μM
5 μM
10 μM
15 μM
20 μM
25 μM
b
100
50
0
% Viability
0 μM
5 μM
10 μM
15 μM
20 μM
25 μM
Methylglyoxal

Figure 2: Mitochondrial oxidative phosphorylation protein expression following 24 hours with low dose methylglyoxal treatment

Cultured sensory neurons from C57BL/6 mice were treated with 0, 5, 10, 15, 20, and 25 µM methylglyoxal for 24 hours. Mitochondrial oxidative phosphorylation proteins were measured by Western blot. (a) Complex V, (b) Complex III, (c) Complex II, and (d) Complex I intensities were normalized to Akt.

Figure 2

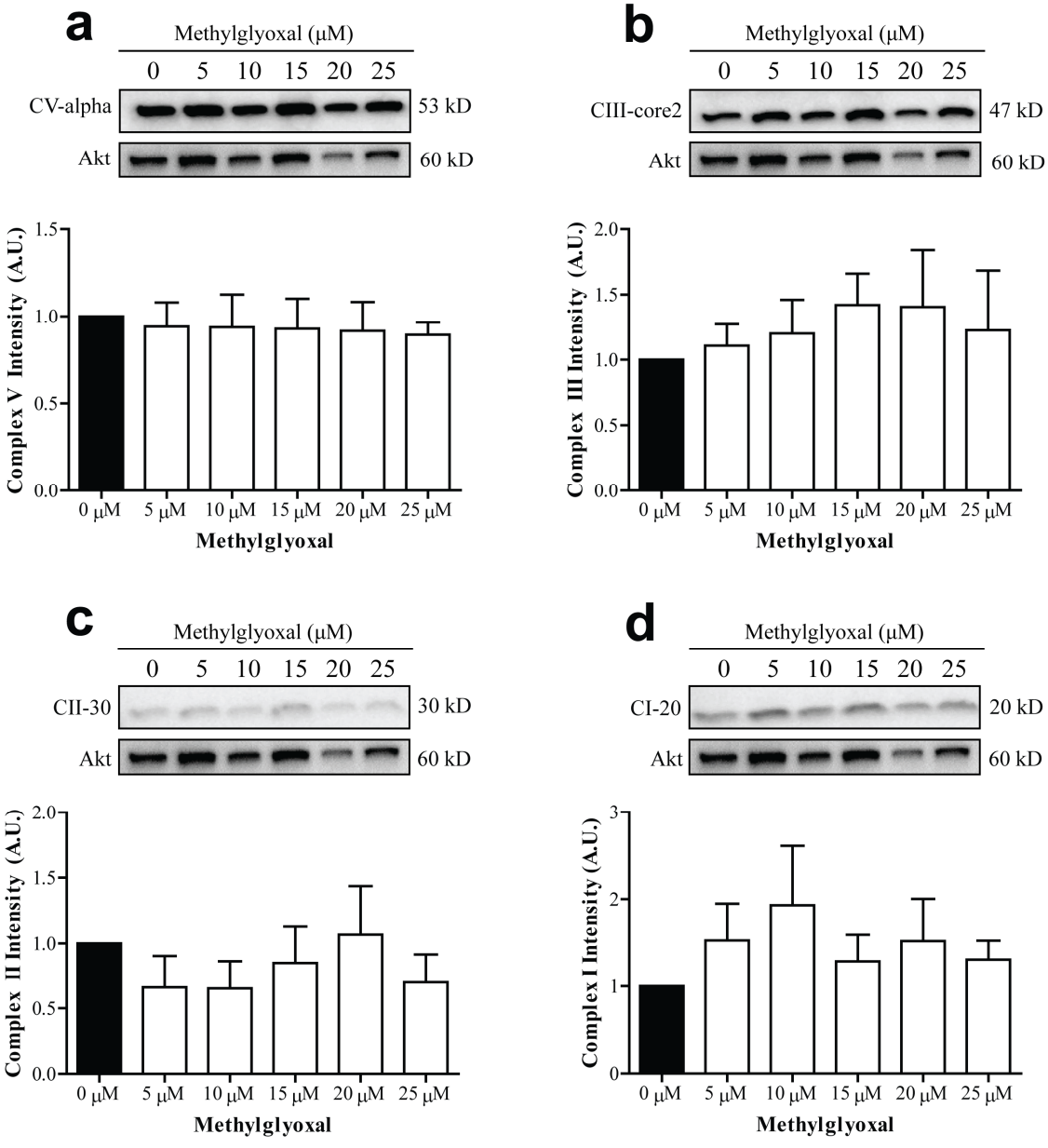
a
Methylglyoxal (μM)
0 5 10 15 20 25
CV-alpha
53 kD
Akt
60 kD
Complex V Intensity (A.U.)
0 μM 5 μM 10 μM 15 μM 20 μM 25 μM
Methylglyoxal
b
Methylglyoxal (μM)
0 5 10 15 20 25
CIII-core2
47 kD
Akt
60 kD
Complex III Intensity (A.U.)
0 μM 5 μM 10 μM 15 μM 20 μM 25 μM
Methylglyoxal
c
Methylglyoxal (μM)
0 5 10 15 20 25
CII-30
30 kD
Akt
60 kD
Complex II Intensity (A.U.)
0 μM 5 μM 10 μM 15 μM 20 μM 25 μM
Methylglyoxal
d
Methylglyoxal (μM)
0 5 10 15 20 25
CI-20
20 kD
Akt
60 kD
Complex I Intensity (A.U.)
0 μM 5 μM 10 μM 15 μM 20 μM 25 μM
Methylglyoxal

High Dose Methylglyoxal Treatment of Sensory Neurons from C57BL/6 Mice

Since low dose methylglyoxal treatment did not show changes in the expression of oxidative phosphorylation proteins, the concentration of methylglyoxal was increased to 100 µM and oxidative phosphorylation proteins were measured. Following 4-hour treatment with high dose methylglyoxal, Complex I, II, and III showed modest reductions (Figure 3). Consequently, cultured sensory neurons were then treated with higher dose methylglyoxal for 24 hours. After 24 hours, sensory neurons from C57BL/6 mice treated with 100 µM methylglyoxal showed significant reductions in the expression of Complex V, III, and II structural proteins (Figure 4). Complex V, III, and II were reduced by 13%, 31%, and 42%, respectively. Importantly, viability was not different in the high dose treated DRG sensory neurons compared to control (Figure 5).

High Dose Methylglyoxal Treatment of Sensory Neurons from BALB/cByJ and BALB/cJ Mice

Since BALB/cByJ and BALB/cJ express different amounts of GLO1, we used cultured sensory neurons from these two strains to determine if elevated levels of GLO1 would protect against methylglyoxal-induced reductions in the expression of oxidative phosphorylation proteins. Following 24 hour treatment with 100 µM methylglyoxal, neither BALB/cByJ nor BALB/cJ mice displayed altered expression of structural proteins from oxidative phosphorylation complexes (Figure 6).

Figure 3: Mitochondrial oxidative phosphorylation protein expression following 4 hours with high dose methylglyoxal treatment

Cultured sensory neurons from C57BL/6 mice were treated with 0 or 100 µM methylglyoxal for 4 hours in supplement free media. Mitochondrial oxidative phosphorylation proteins were measured by Western blot. (a) Complex V, (b) Complex III, (c) Complex II, and (d) Complex I intensities were normalized to neurofilament L. Actin was used to confirm neurofilament L as a loading control.

Figure 3

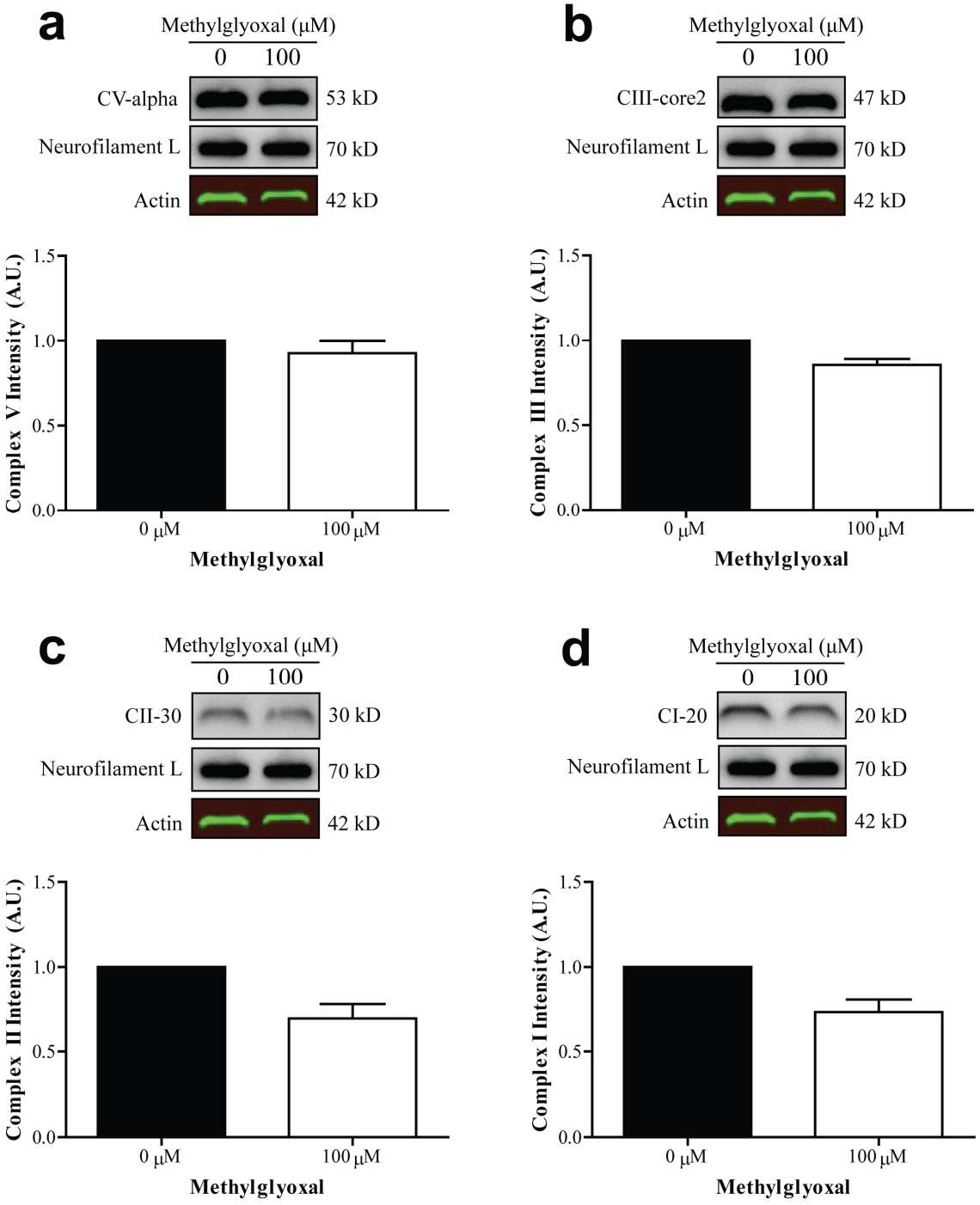
a
Methylglyoxal (μM)
0
100
CV-alpha
53 kD
Neurofilament L
70 kD
Actin
42 kD
Complex V Intensity (A.U.)
1.5
1.0
0.5
0.0
0 μM
100 μM
Methylglyoxal
b
Methylglyoxal (μM)
0
100
CIII-core2
47 kD
Neurofilament L
70 kD
Actin
42 kD
Complex III Intensity (A.U.)
1.5
1.0
0.5
0.0
0 μM
100 μM
Methylglyoxal
c
Methylglyoxal (μM)
0
100
CII-30
30 kD
Neurofilament L
70 kD
Actin
42 kD
Complex II Intensity (A.U.)
1.5
1.0
0.5
0.0
0 μM
100 μM
Methylglyoxal
d
Methylglyoxal (μM)
0
100
CI-20
20 kD
Neurofilament L
70 kD
Actin
42 kD
Complex I Intensity (A.U.)
1.5
1.0
0.5
0.0
0 μM
100 μM
Methylglyoxal

Figure 4: Mitochondrial oxidative phosphorylation protein expression following 24 hours with high dose methylglyoxal treatment

Cultured sensory neurons from C57BL/6 mice were treated with 0 or 100 µM methylglyoxal for 24 hours. Mitochondrial oxidative phosphorylation proteins were measured by Western blot. (a) Complex V, (b) Complex III, (c) Complex II, and (d) Complex I intensities were normalized to neurofilament L.

Figure 4

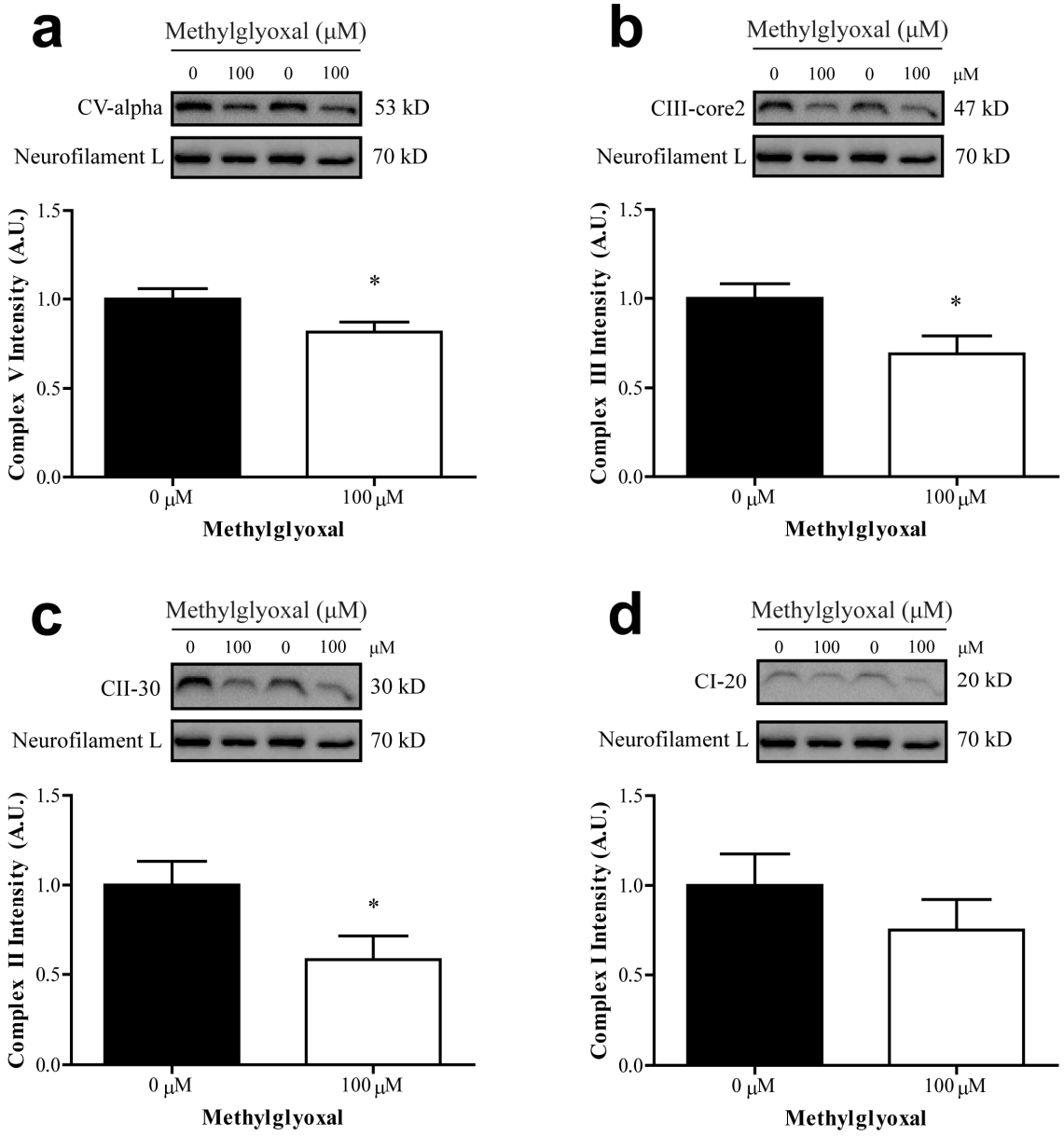
a
Methylglyoxal (μM)
0 100 0 100
CV-alpha
53 kD
Neurofilament L
70 kD
Complex V Intensity (A.U.)
1.5
1.0
0.5
0.0
*
0 μM
100 μM
Methylglyoxal
b
Methylglyoxal (μM)
0 100 0 100 μM
CIII-core2
47 kD
Neurofilament L
70 kD
Complex III Intensity (A.U.)
1.5
1.0
0.5
0.0
*
0 μM
100 μM
Methylglyoxal
c
Methylglyoxal (μM)
0 100 0 100 μM
CII-30
30 kD
Neurofilament L
70 kD
Complex II Intensity (A.U.)
1.5
1.0
0.5
0.0
*
0 μM
100 μM
Methylglyoxal
d
Methylglyoxal (μM)
0 100 0 100 μM
CI-20
20 kD
Neurofilament L
70 kD
Complex I Intensity (A.U.)
1.5
1.0
0.5
0.0
0 μM
100 μM
Methylglyoxal

Figure 5: Sensory neuron survival following 24 hour treatment with high dose methylglyoxal

Cultured sensory neurons from C57BL/6 mice were treated with 0 or 100 µM methylglyoxal for 24 hours. (a) Representative photomicrographs of live (green) and dead (red) cells. (b) Quantification of cultured sensory neuron viability following 24 hour treatment with 100 µM methylglyoxal.

Figure 5

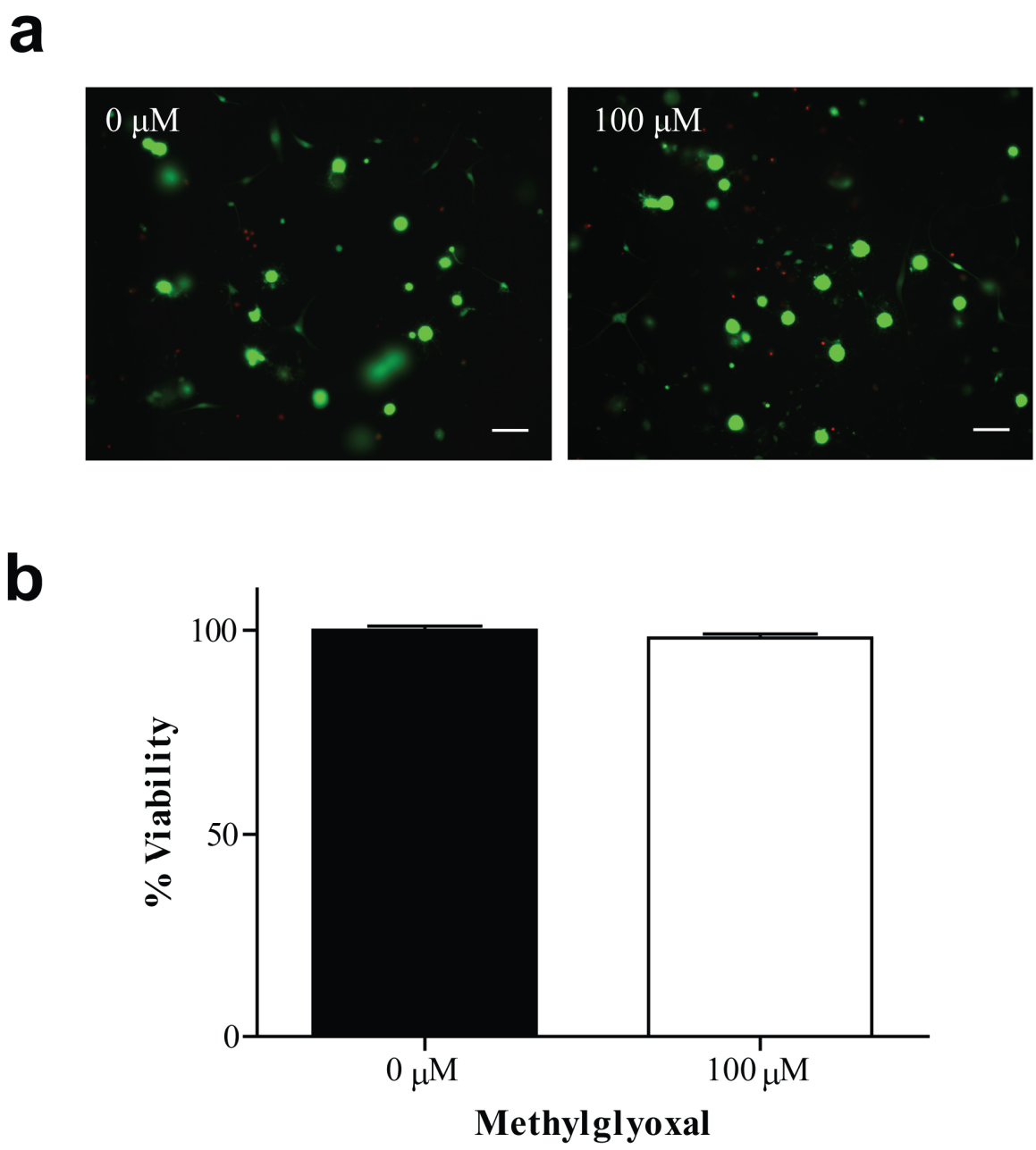

Figure 6: Mitochondrial oxidative phosphorylation protein expression in sensory neuron cultures from BALB/cByJ and BALB/cJ mice following 24 hours with high dose methylglyoxal treatment

Cultured sensory neurons from BALB/cByJ (black bars) and BALB/cJ (white bars) mice were treated with 0 or 100 µM methylglyoxal for 24 hours. Mitochondrial oxidative phosphorylation proteins were measured by Western blot. (a) Complex V, (b) Complex III, (c) Complex II, and (d) Complex I intensities were normalized to neurofilament L.

Figure 6

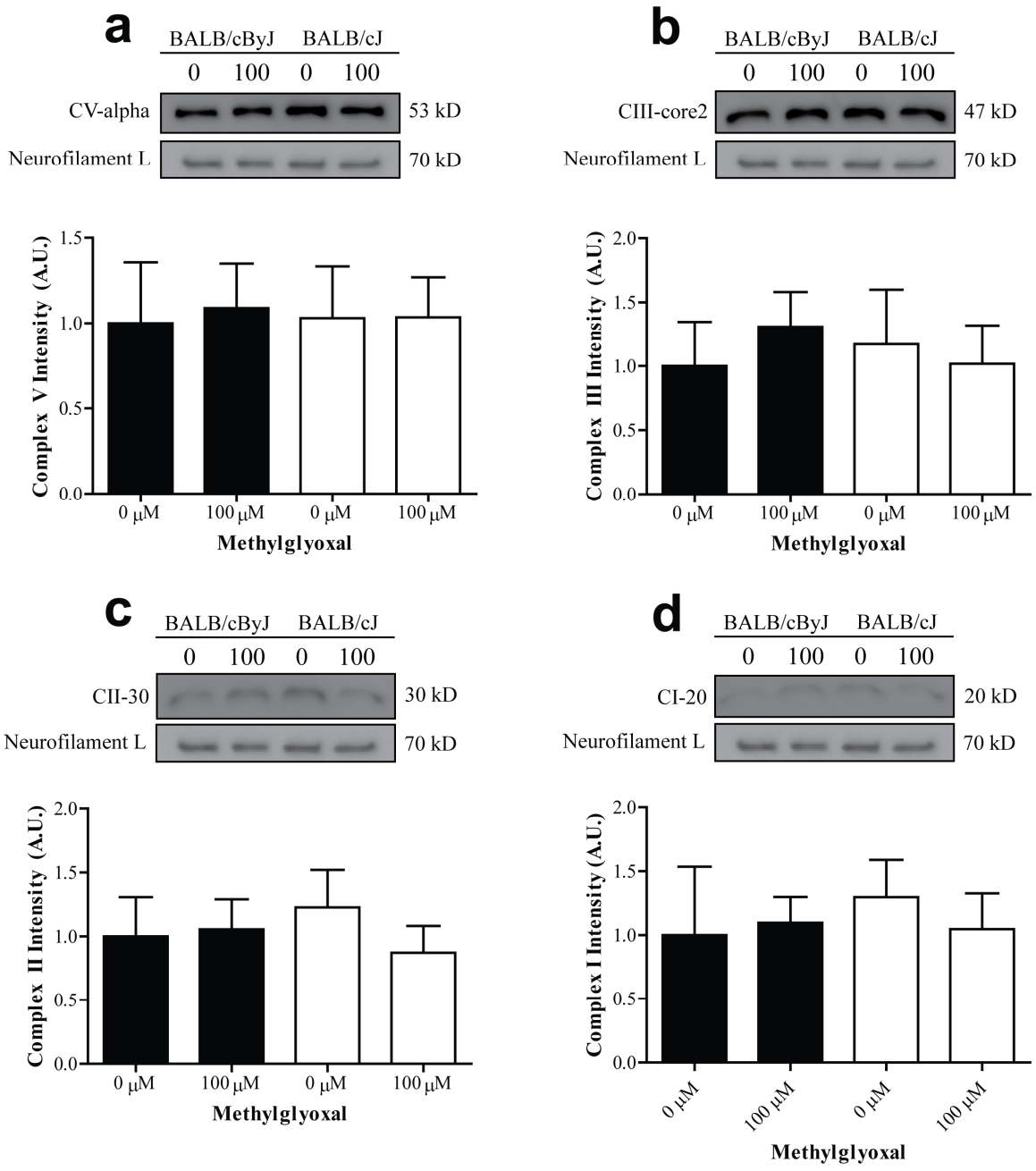
a
BALB/cByJ
BALB/cJ
0
100
0
100
CV-alpha
53 kD
Neurofilament L
70 kD
Complex V Intensity (A.U.)
0 μM
100 μM
0 μM
100 μM
Methylglyoxal
b
BALB/cByJ
BALB/cJ
0
100
0
100
CIII-core2
47 kD
Neurofilament L
70 kD
Complex III Intensity (A.U.)
0 μM
100 μM
0 μM
100 μM
Methylglyoxal
c
BALB/cByJ
BALB/cJ
0
100
0
100
CII-30
30 kD
Neurofilament L
70 kD
Complex II Intensity (A.U.)
0 μM
100 μM
0 μM
100 μM
Methylglyoxal
d
BALB/cByJ
BALB/cJ
0
100
0
100
CI-20
20 kD
Neurofilament L
70 kD
Complex I Intensity (A.U.)
0 μM
100 μM
0 μM
100 μM
Methylglyoxal

5. Discussion

Reactive dicarbonyls, such as methylglyoxal, have been show to target and impair components of the mitochondrial oxidative phosphorylation pathway (Rosca, Mustata et al. 2005; Morcos, Du et al. 2008; Schlotterer, Kukudov et al. 2009). In our previous study in Chapter 5, reduced expression of GLO1 correlated with the development of mechanical insensitivity, loss of epidermal innervation, and reduced expression of structural proteins from Complex V and I of the mitochondrial oxidative phosphorylation cascade. This study suggested that increased levels of reactive dicarbonyls due to STZ-induced diabetes, presumably due to reduced GLO1 expression, may modify components of these complexes, alter the expression levels, and subsequently lead to mitochondrial dysfunction and altered neuronal function.

In this study, methylglyoxal treatment of cultured sensory neurons from nondiabetic C57BL/6 mice was used to assess the vulnerability of mitochondrial oxidative phosphorylation proteins to methylglyoxal. Initial studies using low levels of methylglyoxal had no effect on the expression of mitochondrial proteins. This low dose treatment included B27 minus antioxidants in the medium to negate the influence of high levels of glutathione while still providing neurons with necessary nutrients. However, this supplement also contains high levels of protein, including bovine serum albumin. Consequently, negative results could be attributed to the high reactivity of methylglyoxal and the probability of reacting with the elevated levels of exogenous protein. Similarly, it is important to note that majority of *in vitro* studies that treat different cell types with

reactive dicarbonyls typically do so at much higher doses including micromolar concentrations (Rosca, Monnier et al. 2002; de Arriba, Stuchbury et al. 2007; Huang, Chuang et al. 2008; Mukohda, Yamawaki et al. 2009).

Subsequent investigation utilized higher dose methylglyoxal and supplement free media. Again, the concentration of methylglyoxal utilized in these studies was still far less than other studies. However, DRG neurons cultured from C57BL/6 mice resulted in reduced oxidative phosphorylation protein abundance. Importantly, the higher dose of methylglyoxal did not impair the viability of DRG sensory neurons. Previous *in vitro* studies on embryonic DRG neurons under hyperglycemic conditions suggested a key feature of neuronal degeneration included apoptosis (Vincent, Stevens et al. 2005; Zherebitskaya, Akude et al. 2009). Apoptosis was then erroneously characterized as a key feature underlying fiber loss in diabetic neuropathy, which was subsequently disproven using adult DRG neurons (Zherebitskaya, Akude et al. 2009). Similarly, treatment of neuroblastoma cells with methylglyoxal or inhibition of GLO1 resulted in apoptosis (Kuhla, Luth et al. 2006; de Arriba, Stuchbury et al. 2007); however, in our study, methylglyoxal impairs the mitochondrial proteome but it does not result in neuronal death.

Finally, we cultured sensory neurons from two strains of mice that have different levels of GLO1 expression, as characterized in Chapter 4. Due to lower GLO1 expression, we anticipated BALB/cJ mice would be more vulnerable to methylglyoxal treatment and have reduced oxidative phosphorylation protein expression, while

BALB/cByJ mice would be protected. However, this study showed methylglyoxal treatment did not impair mitochondrial proteins in DRG neurons from the BALB/cJ substrain. It is plausible that differences in glutathione levels between BALB/cJ and C57BL/6 mice could explain the divergent results. Also, the threshold at which methylglyoxal treatment results in altered mitochondrial proteins could be different between the two strains.

CHAPTER 6

Conclusions

Diabetes-induced hyperglycemia causes metabolic derangement of the peripheral nervous system resulting in diabetic peripheral neuropathy. Sensory neuron damage manifests as cutaneous fiber loss, altered nerve conduction, and altered sensation to various stimuli. Diabetic neuropathy can lead to debilitating pain or the loss of protective sensation; however, some diabetic patients do not experience altered sensation or nervous system complications. An understanding of why certain symptoms, either painful or painless, develop in patients and why others are protected from damage to the peripheral nervous system remains elusive.

The purpose of this study was to elucidate the relationship between differential GLO1 expression in the peripheral nervous system, the development and/or progression of diabetic neuropathy, and pathological mechanisms that may underlie hyperglycemia-induced sensory neuron dysfunction with reduced protective mechanisms in diabetes mellitus. In pursuit, studies in this dissertation characterized the pattern of expression of GLO1 in the peripheral nervous system, utilized numerous inbred strains of mice that vary in their GLO1 expression due to a known copy number variant to assess various sensory modalities following diabetes induction, and investigated alterations of the mitochondrial oxidative phosphorylation complexes as a mechanism of sensory neuron dysfunction.

Chapter 2: Characterization of glyoxalase I in the peripheral nervous system

While all accounts in the literature characterize GLO1 as having a ubiquitous presence in all cells of the body, our findings suggest that GLO1 has a much more

restricted pattern in the nervous system. Immunohistochemical studies revealed GLO1 was primarily expressed in small peptidergic neurons that function in thermal, mechanical, and pain transmission from the periphery. Investigation of different inbred strains of mice also revealed GLO1 expression was quite variable in the DRG and other tissues of the peripheral and central nervous system, which is a consequence of either duplication or loss of the region of the genome encompassing GLO1.

While these results have clear functional relevance in the peptidergic subpopulation of nociceptive C-fibers, the seeming lack of GLO1 in other populations of sensory neurons is also intriguing. This seems to suggest one of two concepts: either these other populations of sensory neurons rely on other mechanisms to detoxify reactive dicarbonyls besides the glyoxalase system or these fiber types are particularly vulnerable to elevated intracellular glucose and reactive dicarbonyl-mediated damage. As discussed in this dissertation, other minor pathways have been recognized that have the ability to recognize and breakdown reactive dicarbonyls, but do not have as much specificity for reactive dicarbonyls or the efficiency as GLO1 does. It is likely these populations rely on other detoxification systems given the clear deleterious nature of reactive dicarbonyl and AGE accumulation. However, what these systems are, how efficient these are, and how they are affected in diabetes is entirely unknown. Clearly, further understanding these differences in sensory neurons would lead to a better understanding of the secondary mechanisms of hyperglycemia-induced damage that target specific fiber types and reveal novel therapeutic targets based on the signs and symptoms of a patient, i.e. fiber types affected.

As emphasized throughout this dissertation, majority of diabetic patients will develop signs and symptoms of diabetic neuropathy throughout the course of the disease. However, a minority of patients, between 30-40%, do not develop sensory complications. The interesting question is what makes these patients different. With regards to this dissertation, it is plausible these patients have an abundance of protective mechanisms, such as GLO1, that can limit the toxic effects of hyperglycemia. The recent study highlighting the Joslin 50-year medalists is a clear example of a patient population that is enriched in these protective mechanisms and investigating the genetics underlying this protection could lead to improved screening techniques and biomarkers that predict the development of diabetic neuropathy (Sun, Keenan et al. 2011).

Another important aspect that could benefit patients clinically is determining CNV, SNPs, regulatory factors, and genetic alterations that lead to reduced expression or activity of GLO1 in human patients. Recently, two studies have highlighted the importance of conducting these studies by showing that both SNPs in the coding region and in the promotor region of GLO1 reduced the activity in patients with autism and type II diabetic patients with retinopathy and nephropathy, respectively (Barua, Jenkins et al. 2011; Wu, Li et al. 2011). As previously mentioned, GLO1 was recognized as a CNV in a large screen of the human genome. However, to date, no investigation into the nature or abundance of this genetic finding in healthy patient populations or diabetic patients with or without neuropathy has occurred. Again, studying both of these aspects of protection likely would improve our understanding of diabetic neuropathy, improve screening in patients, and develop novel drug targets for improved treatments.

While we have characterized GLO1 expression in the nervous system of inbred strains of mice and type I diabetic models, GLO1 has only been characterized in the kidney of type II diabetic rodents. Since type II diabetes is far more prevalent than type I diabetes, it would be interesting to measure the expression level, expression pattern, and activity in the peripheral nervous system of type II diabetic animals, including ob/ob and db/db mice. While both of these strains are on a C57BL/6 background, alterations in GLO1 expression or activity following insulin resistance and development of diabetes is particularly interesting given these two strains develop different signs of diabetic neuropathy.

Chapter 3: Characterization of Glyoxalase I in Mouse Models of Painful and Insensate Diabetic Neuropathy

Since peptidergic neurons are known to have a role in pain transmission and previous work in our laboratory recognized the onset of mechanical and thermal insensitivity correlated with the loss of peptidergic neurons, the exclusive expression of GLO1 in this population of dorsal root ganglion neurons suggested it may have a role in protecting this subpopulation from reactive dicarbonyl-mediated damage depending on the strain and the level of GLO1 expression. In this study, we characterized both the development of sensory deficits in diabetic A/J and C57BL/6 mice and GLO1 expression in these strains. The development of reduced mechanical and thermal sensitivity correlated with reduced GLO1 expression in diabetic C57BL/6 mice. Surprisingly, diabetic A/J mice that have high levels of GLO1 developed reduced mechanical

thresholds indicative of painful neuropathy. These results suggest that an imbalance of fiber types may underlie the development of dichotomous signs and symptoms of diabetic neuropathy.

Future studies investigating a correlation between loss of specific fiber types and development of either increased or decreased sensory thresholds would be beneficial. The MrgD mice are a beneficial tool for accomplishing this study. By developing A/J mice that express GFP in nonpeptidergic C-fibers would enable improved detection of specific fiber types that are lost in painful diabetic neuropathy. This would determine if an imbalance of fiber types underlies the development of insensate and/or painful neuropathy.

Chapter 4: Elevated Glyoxalase I Expression Provides Protection From Diabetes-Induced Peripheral Neuropathy

To determine the role of GLO1 in the presentation and/or progression of sensory deficits and hyperglycemia-induced damage, two BALB/c substrains that have similar genetic backgrounds but maintain differential expression of GLO1 were utilized. In this study, diabetic BALB/cByJ mice that have highest expression of GLO1 were protected from alterations of mechanical thresholds, loss of epidermal innervation, and changes in the expression of mitochondrial electron transport chain proteins. Oppositely, diabetic BALB/cJ mice with reduced expression of GLO1 showed increased mechanical thresholds, loss of epidermal fibers, and reduced expression of certain mitochondrial oxidative phosphorylation proteins. Our findings nicely support previous data from

diabetic rats showing similar reductions of the mitochondrial proteome without an increase in oxidative stress (Akude, Zherebitskaya et al. 2011).

Our studies using BALB/c substrains investigated mechanism of neuronal damage shortly after the onset of behavior changes in mechanical sensitivity. Thus, at least after six weeks of diabetes, BALB/cByJ mice were protected from developing changes in mechanical sensation since the mechanical thresholds of these mice were not different from nondiabetic animals. Future studies should follow the same experimental design, but extend the studies to longer time points to determine if BALB/cByJ mice are only protected in the early stages of diabetes or all together resistant against developing diabetic neuropathy.

While these two BALB/c substrains are very similar, they do have documented differences. To confirm our findings, a conditional knockout of GLO1 in peptidergic neurons on a BALB/cByJ background or overexpression in BALB/cJ mice would be beneficial. Other experiments could use an *in vivo* lentivirial shRNA knockdown in the dorsal root ganglia of diabetic BALB/cByJ mice to determine if indeed elevated levels of reactive dicarbonyls in this strain would produce similar sensory deficits and hallmarks of diabetic neuropathy that we measured in diabetic BALB/cJ mice.

While hyperglycemia has a clear role in the pathogenesis of diabetic neuropathy, environmental factors likely also have a role in modulating or exacerbating signs and symptoms of diabetic neuropathy. Thus, examining both GLO1 levels and reactive dicarbonyl concentrations in the peripheral nervous system following exercise or high fat

diet administration in a type I diabetic model would determine if outside factors have an influence on this pathway implicated in the development of diabetic neuropathy. These studies would have direct clinical relevance in advising patients with diabetes which factors may increase or decrease their risk for developing diabetic neuropathy.

It also remains to be determined if the increased physiological expression of GLO1 is capable at preventing increased concentrations of reactive dicarbonyls and accumulation of AGEs in the setting of diabetes mellitus. Thus, measuring reactive dicarbonyls, such as methylglyoxal, glyoxal, and 3-deoxyglucose, and AGEs would be beneficial to determine if the increased levels of GLO1 are indeed protective. Similarly, characterizing proteins that are modified by methylglyoxal and other reactive dicarbonyls, particularly mitochondrial proteins, would be advantageous. While a number of proteins have been identified as targets for reactive dicarbonyls and explain various aspects of cellular dysfunction, proteins modified in diabetic sensory neurons have yet to be determined. Therefore, experiments using proteomic techniques and designed to measure proteins modified by methylglyoxal would provide better understanding of the pathogenesis of diabetic neuropathy.

It would also be interesting to determine if reduced expression of mitochondrial oxidative phosphorylation protein in the BALB/cJ model results in oxidative stress in sensory neurons. Though questions are arising in the field where precisely oxidative damage occurs in the neuron and what mechanism produces these reactive oxygen species, sensory neurons from diabetic rats show reduced activity of mitochondria that do

not produce increased reactive oxygen species. This is contrary to a number of findings in other diabetic tissues suggesting the pathogenic mechanisms believed to occur in all tissues that are prone to secondary complications may indeed not be the case and tissue specificity may be important at elucidating these mechanisms.

Also, sensory neurons from type II diabetic mouse models have displayed altered biogenesis, fission, and morphology of mitochondria indicating hyperglycemia triggers physiological changes of cellular energy production. It would be interesting to determine if any of these parameters were different between the two substrains. This would suggest that reactive dicarbonyl damage may result in other measures of mitochondrial dysfunction and GLO1 may protect against more global damage to these organelles. Similarly, isolating mitochondria from the cell body and the peripheral terminals of sensory neurons from these two strains would determine if reduced GLO1 expression makes mitochondria in the periphery more susceptible to damage as compared to those in the cell body.

Finally, our findings from this study suggest elevated GLO1 may be protective in the peripheral nervous system. Consequently, the development of small molecules that target GLO1 and increase its activity could have therapeutic benefit in diabetic neuropathy. Unfortunately, drug discovery has mainly focused on inhibitors of GLO1 due to its necessary role in cancer cells and in the development of multi-drug resistance. A recent study using Akita mice, a spontaneous type I diabetic model, found fisetin, a rare flavone, increased GLO1 levels and activity and increased the synthesis of

glutathione (Maher, Dargusch et al. 2011). Treatment reduced methylglyoxal modification of proteins and protected against kidney damage in these mice (Maher, Dargusch et al. 2011). This compound appears to be a promising target of the glyoxalase pathway. Treatment of BALB/cJ mice with this compound could determine if elevated GLO1 could protect against the development of insensate neuropathy.

Chapter 5: Mitochondrial Oxidative Phosphorylation Proteins Are Reduced Following *In Vitro* Methylglyoxal Treatment of Sensory Neurons

In the final study, cultured sensory neurons were treated with various concentrations of methylglyoxal to determine if oxidative phosphorylation complexes were targets of protein modification. Cultured DRG neurons from C57BL/6 mice treated with 100 µM methylglyoxal showed significant reductions in three of four complexes measured. However, sensory neurons from BALB/cByJ and BALB/cJ mice did not display alterations in protein expression following *in vitro* treatment with methylglyoxal. These differences could be attributable to a number of variables that need further investigation.

Since sensory neurons from C57BL/6 mice showed mitochondrial alterations, this model could be used to determine precisely the pathogenic and mechanistic consequences of mitochondrial dysfunction that is occurring in methylglyoxal treated cells. In neuroblastoma cell lines, ATP production has been shown to be significantly reduced following methylglyoxal treatment that is probably a direct consequence of reduced electron transport chain proteins, although these lines also showed increased cell death.

However, as previously discussed, reduced expression of oxidative phosphorylation proteins often results in a compensatory increase in reactive oxygen species and oxidative stress in certain tissue under hyperglycemic conditions. Consequently, determining the precise mechanism by which altered mitochondrial proteins produce neuronal dysfunction is clearly worth studying.

Future experiments may also utilize primary sensory neuron cultures from both type I and type II diabetic mouse models to better understand the effects of methylglyoxal treatment. Utilizing diabetic sensory neurons that have inherent metabolic deficits could show more dramatic reductions in the expression of oxidative phosphorylation proteins following methylglyoxal treatment than nondiabetic sensory neurons. Consequently, due to these inherent baseline differences, diabetic sensory neuron cultures may be more sensitive to reactive dicarbonyl treatment and near physiologic concentrations of methylglyoxal may be sufficient to alter the mitochondrial proteome.

New research suggests mitochondria are highly dynamic organelles that localize in sites of high energy demand in the sensory neuron including the cell body and in the axon, particularly in free nerve endings of the skin. *In vitro* studies could isolate mitochondria from the perikyma and distal nerves to compare the expression of mitochondrial oxidative phosphorylation proteins, mitochondrial morphology, and ATP levels to determine if the axonal mitochondria are even more susceptible to protein alterations and energy depletion indicative of length-dependent damage following methylglyoxal treatment. While mitochondria from the cell body are damaged, the

periphery may be more dependent on normal mitochondrial function and thus more susceptible to mitochondrial dysfunction as a result of high reactive dicarbonyls.

While *in vitro* methylglyoxal treatment provides insight into key pathogenic mechanisms, *in vivo* methylglyoxal treatment of nondiabetic and diabetic BALB/c mice would also be valuable. Lumbar intrathecal injections of methylglyoxal would target the compound to the DRG that supply sensory innervation to the hindpaw. This treatment would determine if alterations in mechanical thresholds can be achieved in treated nondiabetic mice and if treated diabetic mice have exacerbated signs of diabetic neuropathy.

CHAPTER 7

References

Ahmed, N. (2005). "Advanced glycation endproducts--role in pathology of diabetic complications." Diabetes Res Clin Pract **67**(1): 3-21.

Ahmed, N., R. Babaei-Jadidi, et al. (2005). "Degradation products of proteins damaged by glycation, oxidation and nitration in clinical type 1 diabetes." Diabetologia **48**(8): 1590-1603.

Ahmed, N. and P. J. Thornalley (2007). "Advanced glycation endproducts: what is their relevance to diabetic complications?" Diabetes Obes Metab **9**(3): 233-245.

Ahmed, U., D. Dobler, et al. (2008). "Reversal of hyperglycemia-induced angiogenesis deficit of human endothelial cells by overexpression of glyoxalase 1 in vitro." Ann N Y Acad Sci **1126**: 262-264.

Akude, E., E. Zherebitskaya, et al. (2011). "Diminished superoxide generation is associated with respiratory chain dysfunction and changes in the mitochondrial proteome of sensory neurons from diabetic rats." Diabetes **60**(1): 288-297.

Almeida, T. F., S. Roizenblatt, et al. (2004). "Afferent pain pathways: a neuroanatomical review." Brain Res **1000**(1-2): 40-56.

Araszkiewicz, A., D. Naskret, et al. (2011). "Increased Accumulation of Skin Advanced Glycation End Products Is Associated with Microvascular Complications in Type 1 Diabetes." Diabetes Technol Ther.

Arezzo, J. C. and E. Zotova (2002). "Electrophysiologic measures of diabetic neuropathy: mechanism and meaning." Int Rev Neurobiol **50**: 229-255.

Bailey, D. W. (1978). Sources of subline divergence and their relative importance for sublines of six major inbred strains of mice. Origins of inbred mice. H. C. M. III. New York, Academic Press**:** 197-213.

Barua, M., E. C. Jenkins, et al. (2011). "Glyoxalase I polymorphism rs2736654 causing the Ala111Glu substitution modulates enzyme activity-implications for autism." Autism Res.

Beisswenger, P. J., K. S. Drummond, et al. (2005). "Susceptibility to diabetic nephropathy is related to dicarbonyl and oxidative stress." Diabetes **54**(11): 3274-3281.

Beisswenger, P. J., S. K. Howell, et al. (2003). "Alpha-oxoaldehyde metabolism and diabetic complications." Biochem Soc Trans **31**(Pt 6): 1358-1363.

Beisswenger, P. J., S. K. Howell, et al. (2003). "Glyceraldehyde-3-phosphate dehydrogenase activity as an independent modifier of methylglyoxal levels in diabetes." Biochim Biophys Acta **1637**(1): 98-106.

Bento, C. F., F. Marques, et al. (2010). "Methylglyoxal alters the function and stability of critical components of the protein quality control." PLoS One **5**(9): e13007.

Bierhaus, A., K. M. Haslbeck, et al. (2004). "Loss of pain perception in diabetes is dependent on a receptor of the immunoglobulin superfamily." J Clin Invest **114**(12): 1741-1751.

Bohlender, J. M., S. Franke, et al. (2005). "Advanced glycation end products and the kidney." Am J Physiol Renal Physiol **289**(4): F645-659.

Braz, J. M., M. A. Nassar, et al. (2005). "Parallel "pain" pathways arise from subpopulations of primary afferent nociceptor." Neuron **47**(6): 787-793.

Brouwers, O., P. M. Niessen, et al. (2010). "Overexpression of glyoxalase-I reduces hyperglycemia-induced levels of advanced glycation endproducts and oxidative stress in diabetic rats." J Biol Chem.

Brouwers, O., P. M. Niessen, et al. (2010). "Hyperglycaemia-induced impairment of endothelium-dependent vasorelaxation in rat mesenteric arteries is mediated by intracellular methylglyoxal levels in a pathway dependent on oxidative stress." Diabetologia **53**(5): 989-1000.

Brownlee, M. (2001). "Biochemistry and molecular cell biology of diabetic complications." Nature **414**(6865): 813-820.

Brownlee, M. (2005). "The pathobiology of diabetic complications: a unifying mechanism." Diabetes **54**(6): 1615-1625.

Calcutt, N. A. (2004). "Experimental models of painful diabetic neuropathy." J Neurol Sci **220**(1-2): 137-139.

Calcutt, N. A. and M. M. Backonja (2007). "Pathogenesis of pain in peripheral diabetic neuropathy." Curr Diab Rep **7**(6): 429-434.

Casey, G. (2011). "The sugar disease--understanding type 2 diabetes mellitus." Nurs N Z **17**(2): 16-21.

Centers for Disease Control and Prevention (2011). National diabetes fact sheet: national estimates and general information on diabetes and prediabetes in the United States. Atlanta, GA, U.S. Department of Health and Human Services, Centers for Disease Control and Prevention.

Chabroux, S., F. Canoui-Poitrine, et al. "Advanced glycation end products assessed by skin autofluorescence in type 1 diabetics are associated with nephropathy, but not retinopathy." Diabetes Metab **36**(2): 152-157.

Chaplan, S. R., F. W. Bach, et al. (1994). "Quantitative assessment of tactile allodynia in the rat paw." J Neurosci Methods **53**(1): 55-63.

Chougale, A. D., S. P. Bhat, et al. (2011). "Proteomic Analysis of Glycated Proteins from Streptozotocin-Induced Diabetic Rat Kidney." Mol Biotechnol.

Chowdhury, S. K., E. Zherebitskaya, et al. (2010). "Mitochondrial respiratory chain dysfunction in dorsal root ganglia of streptozotocin-induced diabetic rats and its correction by insulin treatment." Diabetes **59**(4): 1082-1091.

Choy, K. W., S. R. Setlur, et al. "The impact of human copy number variation on a new era of genetic testing." BJOG **117**(4): 391-398.

Christianson, J. A., J. M. Ryals, et al. (2007). "Neurotrophic modulation of myelinated cutaneous innervation and mechanical sensory loss in diabetic mice." Neuroscience **145**(1): 303-313.

Christianson, J. A., J. M. Ryals, et al. (2003). "Beneficial actions of neurotrophin treatment on diabetes-induced hypoalgesia in mice." J Pain **4**(9): 493-504.

Courteix, C., A. Eschalier, et al. (1993). "Streptozocin-induced diabetic rats: behavioural evidence for a model of chronic pain." Pain **53**(1): 81-88.

Das Evcimen, N. and G. L. King (2007). "The role of protein kinase C activation and the vascular complications of diabetes." Pharmacol Res **55**(6): 498-510.

DCCT (1993). "The effect of intensive treatment of diabetes on the development and progression of long-term complications in insulin-dependent diabetes mellitus. The Diabetes Control and Complications Trial Research Group." N Engl J Med **329**(14): 977-986.

de Arriba, S. G., G. Stuchbury, et al. (2007). "Methylglyoxal impairs glucose metabolism and leads to energy depletion in neuronal cells--protection by carbonyl scavengers." Neurobiol Aging **28**(7): 1044-1050.

Dixon, W. J. (1980). "Efficient analysis of experimental observations." Annu Rev Pharmacol Toxicol **20**: 441-462.

Duby, J. J., R. K. Campbell, et al. (2004). "Diabetic neuropathy: an intensive review." Am J Health Syst Pharm **61**(2): 160-173; quiz 175-166.

Duran-Jimenez, B., D. Dobler, et al. (2009). "Advanced glycation end products in extracellular matrix proteins contribute to the failure of sensory nerve regeneration in diabetes." Diabetes **58**(12): 2893-2903.

Edwards, J. L., A. M. Vincent, et al. (2008). "Diabetic neuropathy: mechanisms to management." Pharmacol Ther **120**(1): 1-34.

Engelen, L., I. Ferreira, et al. (2009). "Polymorphisms in glyoxalase 1 gene are not associated with vascular complications: the Hoorn and CoDAM studies." J Hypertens **27**(7): 1399-1403.

England, J. D., G. S. Gronseth, et al. (2005). "Distal symmetric polyneuropathy: a definition for clinical research: report of the American Academy of Neurology, the American Association of Electrodiagnostic Medicine, and the American Academy of Physical Medicine and Rehabilitation." Neurology **64**(2): 199-207.

Feely, S. M., M. Laura, et al. (2011). "MFN2 mutations cause severe phenotypes in most patients with CMT2A." Neurology **76**(20): 1690-1696.

Figueroa-Romero, C., M. Sadidi, et al. (2008). "Mechanisms of disease: the oxidative stress theory of diabetic neuropathy." Rev Endocr Metab Disord **9**(4): 301-314.

Fleming, T. H., P. M. Humpert, et al. (2010). "Reactive Metabolites and AGE/RAGE-Mediated Cellular Dysfunction Affect the Aging Process - A Mini-Review." Gerontology.

Fujimoto, M., S. Uchida, et al. (2008). "Reduced expression of glyoxalase-1 mRNA in mood disorder patients." Neurosci Lett **438**(2): 196-199.

Gale, C. P., T. S. Futers, et al. (2004). "Common polymorphisms in the glyoxalase-1 gene and their association with pro-thrombotic factors." Diab Vasc Dis Res **1**(1): 34-39.

Gale, C. P. and P. J. Grant (2004). "The characterisation and functional analysis of the human glyoxalase-1 gene using methods of bioinformatics." Gene **340**(2): 251-260.

Gangadhariah, M. H., M. Mailankot, et al. (2010). "Inhibition of methylglyoxal-mediated protein modification in glyoxalase I overexpressing mouse lenses." J Ophthalmol **2010**: 274317.

Genuth, S., W. Sun, et al. (2005). "Glycation and carboxymethyllysine levels in skin collagen predict the risk of future 10-year progression of diabetic retinopathy and nephropathy in the diabetes control and complications trial and epidemiology of

diabetes interventions and complications participants with type 1 diabetes." Diabetes **54**(11): 3103-3111.

Geraldes, P. and G. L. King (2010). "Activation of protein kinase C isoforms and its impact on diabetic complications." Circ Res **106**(8): 1319-1331.

Gibbons, C. and R. Freeman (2004). "The evaluation of small fiber function-autonomic and quantitative sensory testing." Neurol Clin **22**(3): 683-702, vii.

Graubert, T. A., P. Cahan, et al. (2007). "A high-resolution map of segmental DNA copy number variation in the mouse genome." PLoS Genet **3**(1): e3.

Han, X. J., K. Tomizawa, et al. (2011). "Regulation of mitochondrial dynamics and neurodegenerative diseases." Acta Med Okayama **65**(1): 1-10.

Han, Y., E. Randell, et al. (2009). "Plasma advanced glycation endproduct, methylglyoxal-derived hydroimidazolone is elevated in young, complication-free patients with Type 1 diabetes." Clin Biochem **42**(7-8): 562-569.

Haslbeck, K. M., E. D. Schleicher, et al. (2002). "N(epsilon)-Carboxymethyllysine in diabetic and non-diabetic polyneuropathies." Acta Neuropathol **104**(1): 45-52.

Huang, S. M., H. C. Chuang, et al. (2008). "Cytoprotective effects of phenolic acids on methylglyoxal-induced apoptosis in Neuro-2A cells." Mol Nutr Food Res **52**(8): 940-949.

Huijberts, M. S., N. C. Schaper, et al. (2008). "Advanced glycation end products and diabetic foot disease." Diabetes Metab Res Rev **24**(S1): S19-S24.

Hwang, J. S., C. H. Shin, et al. (2005). "Clinical implications of N epsilon-(carboxymethyl)lysine, advanced glycation end product, in children and adolescents with type 1 diabetes." Diabetes Obes Metab **7**(3): 263-267.

Jack, M. M., J. M. Ryals, et al. (2011). "Characterisation of glyoxalase I in a streptozocin-induced mouse model of diabetes with painful and insensate neuropathy." Diabetologia.

Johnson, M. S., J. M. Ryals, et al. (2008). "Early loss of peptidergic intraepidermal nerve fibers in an STZ-induced mouse model of insensate diabetic neuropathy." Pain **140**(1): 35-47.

Kankova, K. (2008). "Diabetic threesome (hyperglycaemia, renal function and nutrition) and advanced glycation end products: evidence for the multiple-hit agent?" Proc Nutr Soc **67**(1): 60-74.

Karachalias, N., R. Babaei-Jadidi, et al. (2003). "Accumulation of fructosyl-lysine and advanced glycation end products in the kidney, retina and peripheral nerve of streptozotocin-induced diabetic rats." Biochem Soc Trans **31**(Pt 6): 1423-1425.

Kennedy, J. M. and D. W. Zochodne (2000). "The regenerative deficit of peripheral nerves in experimental diabetes: its extent, timing and possible mechanisms." Brain **123 (Pt 10)**: 2118-2129.

Kennedy, J. M. and D. W. Zochodne (2005). "Impaired peripheral nerve regeneration in diabetes mellitus." J Peripher Nerv Syst **10**(2): 144-157.

Kles, K. A. and V. Bril (2006). "Diagnostic tools for diabetic sensorimotor polyneuropathy." Curr Diabetes Rev **2**(3): 353-361.

Koenig, R. J., C. M. Peterson, et al. (1976). "Correlation of glucose regulation and hemoglobin AIc in diabetes mellitus." N Engl J Med **295**(8): 417-420.

Kuhla, B., K. Boeck, et al. (2006). "Age-dependent changes of glyoxalase I expression in human brain." Neurobiol Aging **27**(6): 815-822.

Kuhla, B., H. J. Luth, et al. (2006). "Pathological effects of glyoxalase I inhibition in SH-SY5Y neuroblastoma cells." J Neurosci Res **83**(8): 1591-1600.

Lee, H. J., S. K. Howell, et al. (2005). "Methylglyoxal can modify GAPDH activity and structure." Ann N Y Acad Sci **1043**: 135-145.

Lehmann, H. C., W. Chen, et al. (2011). "Mitochondrial dysfunction in distal axons contributes to human immunodeficiency virus sensory neuropathy." Ann Neurol **69**(1): 100-110.

Lindfors, P. H., V. Voikar, et al. (2006). "Deficient nonpeptidergic epidermis innervation and reduced inflammatory pain in glial cell line-derived neurotrophic factor family receptor alpha2 knock-out mice." J Neurosci **26**(7): 1953-1960.

Little, A. A., J. L. Edwards, et al. (2007). "Diabetic neuropathies." Pract Neurol **7**(2): 82-92.

Lu, B. (2009). "Mitochondrial dynamics and neurodegeneration." Curr Neurol Neurosci Rep **9**(3): 212-219.

Luce, K., A. C. Weil, et al. (2010). "Mitochondrial protein quality control systems in aging and disease." Adv Exp Med Biol **694**: 108-125.

Lukic, I. K., P. M. Humpert, et al. (2008). "The RAGE pathway: activation and perpetuation in the pathogenesis of diabetic neuropathy." Ann N Y Acad Sci **1126**: 76-80.

Madonna, R. and R. De Caterina (2011). "Cellular and molecular mechanisms of vascular injury in diabetes - Part I: Pathways of vascular disease in diabetes." Vascul Pharmacol **54**(3-6): 68-74.

Maher, P., R. Dargusch, et al. (2011). "Fisetin lowers methylglyoxal dependent protein glycation and limits the complications of diabetes." PLoS One **6**(6): e21226.

Malik, R. A., S. Tesfaye, et al. (2005). "Sural nerve pathology in diabetic patients with minimal but progressive neuropathy." Diabetologia **48**(3): 578-585.

Malik, R. A., A. Veves, et al. (2001). "Sural nerve fibre pathology in diabetic patients with mild neuropathy: relationship to pain, quantitative sensory testing and peripheral nerve electrophysiology." Acta Neuropathol **101**(4): 367-374.

Malin, S. A., B. M. Davis, et al. (2007). "Production of dissociated sensory neuron cultures and considerations for their use in studying neuronal function and plasticity." Nat Protoc **2**(1): 152-160.

Mannervik, B. (2008). "Molecular enzymology of the glyoxalase system." Drug Metabol Drug Interact **23**(1-2): 13-27.

Mattson, M. P., M. Gleichmann, et al. (2008). "Mitochondria in neuroplasticity and neurological disorders." Neuron **60**(5): 748-766.

McHugh, J. M. and W. B. McHugh (2004). "Diabetes and peripheral sensory neurons: what we don't know and how it can hurt us." AACN Clin Issues **15**(1): 136-149.

Meerwaldt, R., T. P. Links, et al. (2005). "Increased accumulation of skin advanced glycation end-products precedes and correlates with clinical manifestation of diabetic neuropathy." Diabetologia **48**(8): 1637-1644.

Mendez, J. D., J. Xie, et al. "Molecular susceptibility to glycation and its implication in diabetes mellitus and related diseases." Mol Cell Biochem **344**(1-2): 185-193.

Mendez, J. D., J. Xie, et al. (2010). "Molecular susceptibility to glycation and its implication in diabetes mellitus and related diseases." Mol Cell Biochem **344**(1-2): 185-193.

Meyer, R. A. and M. Ringkamp (2008). "A role for uninjured afferents in neuropathic pain." Sheng Li Xue Bao **60**(5): 605-609.

Miller, A. G., D. G. Smith, et al. (2006). "Glyoxalase I is critical for human retinal capillary pericyte survival under hyperglycemic conditions." J Biol Chem **281**(17): 11864-11871.

Mirza, M. A., A. J. Kandhro, et al. (2007). "Determination of glyoxal and methylglyoxal in the serum of diabetic patients by MEKC using stilbenediamine as derivatizing reagent." Electrophoresis **28**(21): 3940-3947.

Misur, I., K. Zarkovic, et al. (2004). "Advanced glycation endproducts in peripheral nerve in type 2 diabetes with neuropathy." Acta Diabetol **41**(4): 158-166.

Morcos, M., X. Du, et al. (2008). "Glyoxalase-1 prevents mitochondrial protein modification and enhances lifespan in Caenorhabditis elegans." Aging Cell **7**(2): 260-269.

Mukohda, M., H. Yamawaki, et al. (2009). "Methylglyoxal inhibits smooth muscle contraction in isolated blood vessels." J Pharmacol Sci **109**(2): 305-310.

Muller, K. A., J. M. Ryals, et al. (2008). "Abnormal muscle spindle innervation and large-fiber neuropathy in diabetic mice." Diabetes **57**(6): 1693-1701.

Munch, G., B. Westcott, et al. (2010). "Advanced glycation endproducts and their pathogenic roles in neurological disorders." Amino Acids.

Nass, N., B. Bartling, et al. (2007). "Advanced glycation end products, diabetes and ageing." Z Gerontol Geriatr **40**(5): 349-356.

Nemet, I., L. Varga-Defterdarovic, et al. (2006). "Methylglyoxal in food and living organisms." Mol Nutr Food Res **50**(12): 1105-1117.

Obrosova, I. G. (2009). "Diabetic painful and insensate neuropathy: pathogenesis and potential treatments." Neurotherapeutics **6**(4): 638-647.

Oya, T., N. Hattori, et al. (1999). "Methylglyoxal modification of protein. Chemical and immunochemical characterization of methylglyoxal-arginine adducts." J Biol Chem **274**(26): 18492-18502.

Pambianco, G., T. Costacou, et al. (2011). "The assessment of clinical distal symmetric polyneuropathy in type 1 diabetes: A comparison of methodologies from the Pittsburgh Epidemiology of Diabetes Complications Cohort." Diabetes Res Clin Pract.

Peppa, M., P. Stavroulakis, et al. (2009). "Advanced glycoxidation products and impaired diabetic wound healing." Wound Repair Regen **17**(4): 461-472.

Perry, G. H., F. Yang, et al. (2008). "Copy number variation and evolution in humans and chimpanzees." Genome Res **18**(11): 1698-1710.

Pfaffl, M. W., G. W. Horgan, et al. (2002). "Relative expression software tool (REST) for group-wise comparison and statistical analysis of relative expression results in real-time PCR." Nucleic Acids Res **30**(9): e36.

Phillips, S. A., D. Mirrlees, et al. (1993). "Modification of the glyoxalase system in streptozotocin-induced diabetic rats. Effect of the aldose reductase inhibitor Statil." Biochem Pharmacol **46**(5): 805-811.

Phillips, S. A. and P. J. Thornalley (1993). "The formation of methylglyoxal from triose phosphates. Investigation using a specific assay for methylglyoxal." Eur J Biochem **212**(1): 101-105.

Pickrell, A. M. and C. T. Moraes (2010). "What role does mitochondrial stress play in neurodegenerative diseases?" Methods Mol Biol **648**: 63-78.

Portha, B., O. Blondel, et al. (1989). "The rat models of non-insulin dependent diabetes induced by neonatal streptozotocin." Diabete Metab **15**(2): 61-75.

Powell, H. C., R. S. Garrett, et al. (1991). "Fine-structural localization of aldose reductase and ouabain-sensitive, K(+)-dependent p-nitro-phenylphosphatase in rat peripheral nerve." Acta Neuropathol **81**(5): 529-539.

Quattrini, C. and S. Tesfaye (2003). "Understanding the impact of painful diabetic neuropathy." Diabetes Metab Res Rev **19 Suppl 1**: S2-8.

Queisser, M. A., D. Yao, et al. (2010). "Hyperglycemia impairs proteasome function by methylglyoxal." Diabetes **59**(3): 670-678.

Rabbani, N. and P. J. Thornalley (2008). "Dicarbonyls linked to damage in the powerhouse: glycation of mitochondrial proteins and oxidative stress." Biochem Soc Trans **36**(Pt 5): 1045-1050.

Rabbani, N. and P. J. Thornalley (2010). "Methylglyoxal, glyoxalase 1 and the dicarbonyl proteome." Amino Acids.

Rabbani, N. and P. J. Thornalley (2011). "Glyoxalase in diabetes, obesity and related disorders." Semin Cell Dev Biol.

Racker, E. (1951). "The mechanism of action of glyoxalase." J Biol Chem **190**(2): 685-696.

Ramasamy, R., S. J. Vannucci, et al. (2005). "Advanced glycation end products and RAGE: a common thread in aging, diabetes, neurodegeneration, and inflammation." Glycobiology **15**(7): 16R-28R.

Ramasamy, R., S. F. Yan, et al. (2008). "Receptor for advanced glycation end products: fundamental roles in the inflammatory response: winding the way to the pathogenesis of endothelial dysfunction and atherosclerosis." Ann N Y Acad Sci **1126**: 7-13.

Ranganathan, S., P. J. Ciaccio, et al. (1999). "Genomic sequence of human glyoxalase-I: analysis of promoter activity and its regulation." Gene **240**(1): 149-155.

Rau, K. K., S. L. McIlwrath, et al. (2009). "Mrgprd enhances excitability in specific populations of cutaneous murine polymodal nociceptors." J Neurosci **29**(26): 8612-8619.

Redon, R., S. Ishikawa, et al. (2006). "Global variation in copy number in the human genome." Nature **444**(7118): 444-454.

Riboulet-Chavey, A., A. Pierron, et al. (2006). "Methylglyoxal impairs the insulin signaling pathways independently of the formation of intracellular reactive oxygen species." Diabetes **55**(5): 1289-1299.

Ringkamp, M. and R. A. Meyer (2005). "Injured versus uninjured afferents: Who is to blame for neuropathic pain?" Anesthesiology **103**(2): 221-223.

Rosca, M. G., V. M. Monnier, et al. (2002). "Alterations in renal mitochondrial respiration in response to the reactive oxoaldehyde methylglyoxal." Am J Physiol Renal Physiol **283**(1): F52-59.

Rosca, M. G., T. G. Mustata, et al. (2005). "Glycation of mitochondrial proteins from diabetic rat kidney is associated with excess superoxide formation." Am J Physiol Renal Physiol **289**(2): F420-430.

Rossini, A. A., A. A. Like, et al. (1977). "Studies of streptozotocin-induced insulitis and diabetes." Proc Natl Acad Sci U S A **74**(6): 2485-2489.

Ryle, C. and M. Donaghy (1995). "Non-enzymatic glycation of peripheral nerve proteins in human diabetics." J Neurol Sci **129**(1): 62-68.

Said, G. (2007). "Diabetic neuropathy--a review." Nat Clin Pract Neurol **3**(6): 331-340.

Said, G., G. Slama, et al. (1983). "Progressive centripetal degeneration of axons in small fibre diabetic polyneuropathy." Brain **106 (Pt 4)**: 791-807.

Schalkwijk, C. G., O. Brouwers, et al. (2008). "Modulation of insulin action by advanced glycation endproducts: a new player in the field." Horm Metab Res **40**(9): 614-619.

Schalkwijk, C. G., J. van Bezu, et al. (2006). "Heat-shock protein 27 is a major methylglyoxal-modified protein in endothelial cells." FEBS Lett **580**(6): 1565-1570.

Scheffler, I. E. (2001). "Mitochondria make a come back." Adv Drug Deliv Rev **49**(1-2): 3-26.

Schlotterer, A., G. Kukudov, et al. (2009). "C. elegans as model for the study of high glucose- mediated life span reduction." Diabetes **58**(11): 2450-2456.

Sheetz, M. J. and G. L. King (2002). "Molecular understanding of hyperglycemia's adverse effects for diabetic complications." JAMA **288**(20): 2579-2588.

Shields, S. D., D. J. Cavanaugh, et al. (2010). "Pain behavior in the formalin test persists after ablation of the great majority of C-fiber nociceptors." Pain **151**(2): 422-429.

Shinohara, M., P. J. Thornalley, et al. (1998). "Overexpression of glyoxalase-I in bovine endothelial cells inhibits intracellular advanced glycation endproduct formation and prevents hyperglycemia-induced increases in macromolecular endocytosis." J Clin Invest **101**(5): 1142-1147.

Sima, A. A., V. Nathaniel, et al. (1988). "Histopathological heterogeneity of neuropathy in insulin-dependent and non-insulin-dependent diabetes, and demonstration of axo-glial dysjunction in human diabetic neuropathy." J Clin Invest **81**(2): 349-364.

Sima, A. A. and K. Sugimoto (1999). "Experimental diabetic neuropathy: an update." Diabetologia **42**(7): 773-788.

Sinnreich, M., B. V. Taylor, et al. (2005). "Diabetic neuropathies. Classification, clinical features, and pathophysiological basis." Neurologist **11**(2): 63-79.

Sorensen, L., L. Molyneaux, et al. (2002). "Insensate versus painful diabetic neuropathy: the effects of height, gender, ethnicity and glycaemic control." Diabetes Res Clin Pract **57**(1): 45-51.

Sparkes, R. S., M. C. Sparkes, et al. (1983). "Glyoxalase I "null" allele in a new family: identification by abnormal segregation pattern and quantitative assay." Hum Genet **64**(2): 146-147.

Stevens, M. J., I. Obrosova, et al. (2000). "Effects of DL-alpha-lipoic acid on peripheral nerve conduction, blood flow, energy metabolism, and oxidative stress in experimental diabetic neuropathy." Diabetes **49**(6): 1006-1015.

Stitt, A. W. (2010). "AGEs and diabetic retinopathy." Invest Ophthalmol Vis Sci **51**(10): 4867-4874.

Sugimoto, K., Y. Murakawa, et al. (2000). "Diabetic neuropathy--a continuing enigma." Diabetes Metab Res Rev **16**(6): 408-433.

Sugimoto, K., Y. Nishizawa, et al. (1997). "Localization in human diabetic peripheral nerve of N(epsilon)-carboxymethyllysine-protein adducts, an advanced glycation endproduct." Diabetologia **40**(12): 1380-1387.

Sun, J. K., H. A. Keenan, et al. (2011). "Protection from retinopathy and other complications in patients with type 1 diabetes of extreme duration: the joslin 50-year medalist study." Diabetes Care **34**(4): 968-974.

Szkudelski, T. (2001). "The mechanism of alloxan and streptozotocin action in B cells of the rat pancreas." Physiol Res **50**(6): 537-546.

Tavakoli, M. and R. A. Malik (2008). "Management of painful diabetic neuropathy." Expert Opin Pharmacother **9**(17): 2969-2978.

Tavee, J. and L. Zhou (2009). "Small fiber neuropathy: A burning problem." Cleve Clin J Med **76**(5): 297-305.

Tesfaye, S. and P. Kempler (2005). "Painful diabetic neuropathy." Diabetologia **48**(5): 805-807.

Thornalley, P. J. (1990). "The glyoxalase system: new developments towards functional characterization of a metabolic pathway fundamental to biological life." Biochem J **269**(1): 1-11.

Thornalley, P. J. (1996). "Pharmacology of methylglyoxal: formation, modification of proteins and nucleic acids, and enzymatic detoxification--a role in pathogenesis and antiproliferative chemotherapy." Gen Pharmacol **27**(4): 565-573.

Thornalley, P. J. (1998). "Glutathione-dependent detoxification of alpha-oxoaldehydes by the glyoxalase system: involvement in disease mechanisms and antiproliferative activity of glyoxalase I inhibitors." Chem Biol Interact **111-112**: 137-151.

Thornalley, P. J. (2002). "Glycation in diabetic neuropathy: characteristics, consequences, causes, and therapeutic options." Int Rev Neurobiol **50**: 37-57.

Thornalley, P. J. (2003). "Glyoxalase I--structure, function and a critical role in the enzymatic defence against glycation." Biochem Soc Trans **31**(Pt 6): 1343-1348.

Thornalley, P. J. (2005). "Dicarbonyl intermediates in the maillard reaction." Ann N Y Acad Sci **1043**: 111-117.

Thornalley, P. J. (2008). "Protein and nucleotide damage by glyoxal and methylglyoxal in physiological systems--role in ageing and disease." Drug Metabol Drug Interact **23**(1-2): 125-150.

Tomlinson, D. R. and N. J. Gardiner (2008). "Diabetic neuropathies: components of etiology." J Peripher Nerv Syst **13**(2): 112-121.

Tomlinson, D. R. and N. J. Gardiner (2008). "Glucose neurotoxicity." Nat Rev Neurosci **9**(1): 36-45.

Toth, C., J. Martinez, et al. (2007). "RAGE, diabetes, and the nervous system." Curr Mol Med **7**(8): 766-776.

Toth, C., L. L. Rong, et al. (2008). "Receptor for advanced glycation end products (RAGEs) and experimental diabetic neuropathy." Diabetes **57**(4): 1002-1017.

Turk, Z. (2010). "Glycotoxines, carbonyl stress and relevance to diabetes and its complications." Physiol Res **59**(2): 147-156.

Ulrich, P. and A. Cerami (2001). "Protein glycation, diabetes, and aging." Recent Prog Horm Res **56**: 1-21.

van Belle, T. L., K. T. Coppieters, et al. (2011). "Type 1 diabetes: etiology, immunology, and therapeutic strategies." Physiol Rev **91**(1): 79-118.

Velez, L., G. Sokoloff, et al. (2010). "Differences in aggressive behavior and DNA copy number variants between BALB/cJ and BALB/cByJ substrains." Behav Genet **40**(2): 201-210.

Veves, A., M. Backonja, et al. (2008). "Painful diabetic neuropathy: epidemiology, natural history, early diagnosis, and treatment options." Pain Med **9**(6): 660-674.

Vincent, A. M., L. Perrone, et al. (2007). "Receptor for advanced glycation end products activation injures primary sensory neurons via oxidative stress." Endocrinology **148**(2): 548-558.

Vincent, A. M., J. W. Russell, et al. (2004). "Oxidative stress in the pathogenesis of diabetic neuropathy." Endocr Rev **25**(4): 612-628.

Vincent, A. M., M. J. Stevens, et al. (2005). "Cell culture modeling to test therapies against hyperglycemia-mediated oxidative stress and injury." Antioxid Redox Signal **7**(11-12): 1494-1506.

Vinik, A. I., T. S. Park, et al. (2000). "Diabetic neuropathies." Diabetologia **43**(8): 957-973.

Walwyn, W. M., Y. Matsuka, et al. (2006). "HSV-1-mediated NGF delivery delays nociceptive deficits in a genetic model of diabetic neuropathy." Exp Neurol **198**(1): 260-270.

Wautier, J. L. and A. M. Schmidt (2004). "Protein glycation: a firm link to endothelial cell dysfunction." Circ Res **95**(3): 233-238.

Williams, R. t., J. E. Lim, et al. (2009). "A common and unstable copy number variant is associated with differences in Glo1 expression and anxiety-like behavior." PLoS One **4**(3): e4649.

Williams, S. K., N. L. Howarth, et al. (1982). "Structural and functional consequences of increased tubulin glycosylation in diabetes mellitus." Proc Natl Acad Sci U S A **79**(21): 6546-6550.

Wu, G., M. Ringkamp, et al. (2002). "Degeneration of myelinated efferent fibers induces spontaneous activity in uninjured C-fiber afferents." J Neurosci **22**(17): 7746-7753.

Wu, J. C., X. H. Li, et al. (2011). "Association of Two Glyoxalase 1 Gene Polymorphisms with Nephropathy and Retinopathy in Type 2 Diabetes." J Endocrinol Invest.

Xue, M., N. Rabbani, et al. (2011). "Glyoxalase in ageing." Semin Cell Dev Biol **22**(3): 293-301.

Yagihashi, S., S. Yamagishi, et al. (2007). "Pathology and pathogenetic mechanisms of diabetic neuropathy: correlation with clinical signs and symptoms." Diabetes Res Clin Pract **77 Suppl 1**: S184-189.

Yu, Y., S. R. Thorpe, et al. (2006). "Advanced glycation end-products and methionine sulphoxide in skin collagen of patients with type 1 diabetes." Diabetologia **49**(10): 2488-2498.

Zherebitskaya, E., E. Akude, et al. (2009). "Development of selective axonopathy in adult sensory neurons isolated from diabetic rats: role of glucose-induced oxidative stress." Diabetes **58**(6): 1356-1364.

Zochodne, D. W. (1999). "Diabetic neuropathies: features and mechanisms." Brain Pathol **9**(2): 369-391.

Zochodne, D. W. (2007). "Diabetes mellitus and the peripheral nervous system: manifestations and mechanisms." Muscle Nerve **36**(2): 144-166.

Zochodne, D. W., N. Ramji, et al. (2008). "Neuronal targeting in diabetes mellitus: a story of sensory neurons and motor neurons." Neuroscientist **14**(4): 311-318.

Zylka, M. J. (2005). "Nonpeptidergic circuits feel your pain." Neuron **47**(6): 771-772.

Zylka, M. J., F. L. Rice, et al. (2005). "Topographically distinct epidermal nociceptive circuits revealed by axonal tracers targeted to Mrgprd." Neuron **45**(1): 17-25.